UiT
THE ARCTIC
UNIVERSITY
OF NORWAY

Department of Electrical Engineering

HVDC Transmission and Energy Storage for Wind Power Plant

Torgeir Moe

Master's thesis in Electrical Engineering Spring 2019

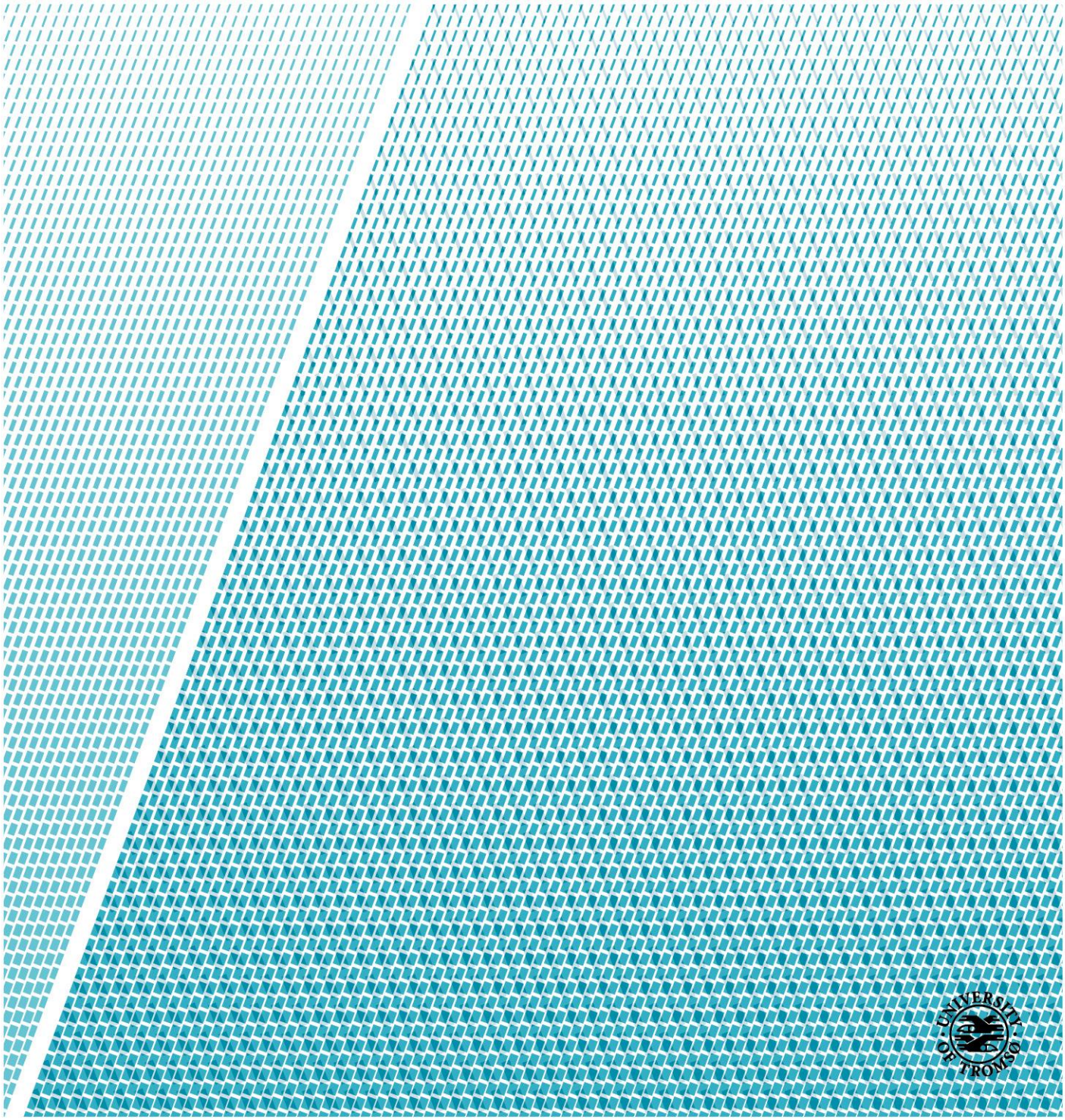

UiT

NORGES
ARKTISKE
UNIVERSITET

Title: **HVDC Transmission and Energy Storage for Wind Power Plant**

Date: 11 juni 2019

Classification: Open

Author: **Torgeir Moe**

Pages:

Attachments:

Department: Department of Electrical Engineering

Line of study: Electrical Engineering

Supervisor: Umer Sohail, Trond Østrem

Principal: UiT The Artic University of Norway, Campus Narvik

Principal contact: **Trond Østrem**

Key words: MMC, hybrid energy storage system, supercapacitor, wind power, VSC control, P-Q control, HVDC, grid.

Abstract

This thesis will investigate the effects of an energy storage system incorporated into the submodules of a modular multilevel converter connected to a HVDC line. A simulation has been made to see the effects of energy storage on the transmission of power from a generator connected to the grid via a HVDC line with two MMCs connected in each end, one of which incorporates the energy storage system.

The simulation has been run in several different scenarios with different levels of contribution from the energy storage and the generator, which will allow an insight into the effects of submodule-based energy storage. The goal is verifying the benefits of energy storage in MMCs and their effect on the output into the grid.

Table of Contents

1 List of notations

1.1 Abbreviations

MMC	Modular Multilevel Converter
SM	Submodule
BESS	Battery Energy Storage System
SC	Super Capacitor
CESS	Capacitor Energy Storage System
SOH	State of Health
HESS	Hybrid Energy Storage System
SOC	State Of Charge
ROD	Rate Of Discharge
AC	Alternating Current
DC	Direct Current
HVAC	High Voltage AC
HVDC	High Voltage DC
FB	Full Bridge
HB	Half Bridge
DoD	Depth of Discharge
EP	Energy Power ratio
PWM	Pulse Width Modulation
PDPWM	Phase disposition PWM
APODPWM	Alternate phase opposition PWM
PODPWM	Phase opposition disposition PWM

1.2 Symbols

i_{u_j}	Upper leg current in phase j
i_{l_j}	Lower leg current in phase j
i_{dc}	DC current
V_{dc}	DC voltage
R_o	Arm resistance
L_o	Arm inductance
P_{l_j}	Power lower leg phase j
W_{u_j}	Energy in capacitors of upper leg of phase j
n_{u_j}	number of active submodules in upper leg of phase j
n_{l_j}	number of active submodules in lower leg of phase j
N	Number of submodules in a leg
$V_{c_{u_j}}$	Capacitor voltage of upper leg phase j
i_j	AC current of phase j
i_{cir_j}	circulating current of phase j
V_C	Capacitor voltage
V_{l_j}	Lower leg voltage of phase j
P_{u_j}	Power lower leg phase j
P_{loss}	Power lost
V_{cm}	Common mode voltage
$V_{c\_l_j}$	Capacitor voltage of lower leg phase j
Csm	Capacitance of a submodule
K	Polarization constant/polarization resistance
I	Battery current.
I*	Low frequency current dynamics
It	Extracted capacity in Ah.
Q	Max battery capacity, given in Ah.

A	Exponential voltage, V.
B	Exponential capacity, Ah^{-1}.
E_0	Constant voltage, V.
Exp(s)	Exponential zone dynamics, in V.
$I_{measured}$	Measured current in Buck/Boost converter [B/B]
I_{ref}	Reference current in B/B
$I_{missing}$	Difference between I_{ref} and $I_{measured}$
$V_{measured}$	Measured voltage in B/B
$P_{Brequested}$	Requested power in B/B
$P_{mod\ n}$	Modifier for power output in battery or SC
SOC_{nsc}	SC state of charge for SM n
P_{SCarm}	Power expected of the SCs in an MMC arm.
$P_{requestedarm}$	Total power requested by MMC arm
$P_{batteryarm}$	Power covered by batteries in MMC arm
$P_{SC\ n}$	Power requested of SC n
$P_{Battery\ n}$	Power provided by battery n
$P_{Battery\ nom}$	Nominal battery power
R	Slew rate for batteries
SOC_a	SOC of battery a
SOC_n	Average SOC in batteries of the arm
I_{dref}	Reference d current (dq0)
V_{DCref}	Reference DC voltage
$V_{DCmeasured}$	measured DC voltage
L	Line inductance
I_d	Measured d current VSC (dq0)
I_q	Measured q current VSC (dq0)
$L_{tot_{pu}}$	Total pu value inductance
L_{choke}	Choke inductance VSC
L_{xfo}	Feedforward inductance
$R_{tot_{pu}}$	Total pu value resistance
R_{xfo}	Feedforward resistance
R_{choke}	Choke resistance

V_{q_conv}	Conversion voltage value for reference voltage q
V_{d_conv}	Conversion voltage value for reference voltage d
V_j	Voltage phase j
V_0	0-vector voltage
$I_{L_{on}}$	Coil current B/B on
$I_{L_{off}}$	Coil current B/B off
V_o	Output voltage
V_i	Input voltage
D	Duty cycle
T	Commutation period
I_0	Output current
W	Energy SC
C	Capacitance (SC)
R_i	Internal voltage
V_{end}	End of cycle voltage SC
V_{init}	initial cycle voltage SC
P_{max}	Maximum power
V_{SC}	SC voltage
N_S	number of series capacitors
Q_T	electric charge
d	molecular radius
N_p	number of parallel capacitors
N_e	number of layers of electrodes
ε	permittivity of SC material
ε_0	permittivity of free space
A_i	interfacial area between electrodes and electrolytes
R	ideal gas constant
T	operating temperature (K)
F	faraday constant
c	molar concentration SC
R_{SC}	total SC resistance
i_{SC}	

$$Q_T = \int i_{SC} dt$$

$$Q_T = \int i_{dis}^{self} dt$$

$$i_{dis}^{self} = \frac{C_T \alpha_z}{1 + sR_{SC}C_T}$$

2 Introduction

Why is this needed, what am I doing… limit the thesis to a clear area of research.

In short: grab attention and explain what this is about.

With the current issues and debate around global warming and the causes human society is responsible for, it is tempting to turn to energy sources which do not contribute to greenhouse gas emissions during operation. Wind power is a well-established alternative to fossil fuels and one alternative that is very effective if placed out on the ocean, where the wind is not hindered by cliffs, valleys or other obstacles which reduce windspeed, and therefore energy potential.

One prevalent issue with the increase of renewable energy sources today is that several of them are not controllable to a high enough degree, they cannot contribute to grid stability and inertia, they can in fact be a liability. In the case of wind power, the blades are usually not synced to the grid frequency and can't contribute energy to the grid in deficit situations in the same way an AC generator can, by acting as a flywheel. The exception to this is the direct online wind turbines, but they are limited in capacity by a rapid increase in generator weight and size as the power increases and are also built with rare and expensive earth-magnet materials.[1]

By adding an energy storage element into the converter, it is possible to use these energy-sources to contribute more energy when the grid is in a deficit situation or charge its batteries instead of loading energy onto a grid in a surplus situation. Thus, the windfarm can participate in increasing grid inertia and alleviate one of the common critiques against renewable energy-sources like wind.

2.1 Windfarm – HVDC – MMC – Grid

This thesis will focus on the MMC [Modular Multilevel Converter], but it is important to know why energy storage is needed and how the energy is transported to the MMC and onwards to the grid.

In this case the power generator is a generic off-shore windfarm which produces AC power which then needs to be transported by subsea cables to the mainland. To make this transfer more efficient it is feasible to convert the AC power to HVDC for transportation to reduce losses and then convert it back to HVAC on-shore. The cost-efficiency of this conversion depends on losses over distance vs the increased cost of a HVDC rectifier/inverter as opposed to the cost of transforming the voltage to HVAC with increased losses per distance.

2.2 Motivation and objective

The point of integrating energy storage in wind power transmission is to make an increased portion of generated power make eco-friendly. If eco-friendly power is more available, more profitable and contributes to grid stability. It can aid in supplementing or replacing undesirable sources of energy.

The modularity of the MMC increases reliability, adaptability and ease of repair, so making this converter able to contribute to grid stability as well will further increase its utility, which can make the MMC and ESS [Energy Storage System].

3 Modular multilevel converter

The modular multilevel converter is an up and coming form of solid-state AC/DC converter. MMCs are scalable and easily repaired due to their modularity, mechanically simple to construct and they are reliable.

MMCs were first introduced in 2003 [2] and are currently enjoying increased attention, likely due to HVDC becoming more popular and mature. MMCs enjoy many advantages over several other AC/DC converters, such as lower switching frequency, lower losses and they only need small L-filters on the AC side. One particularly interesting possibility is being able to incorporate energy storage into MMCs so that renewable energy sources like wind and solar power can contribute to grid inertia instead of being a liability, due to the way the energy production they contribute to the grid is dependent on uncontrollable factors such as windspeed, sunlight, clouds etc.

MMCs are made of one leg per phase, with each leg consisting of 2 arms with N identical submodules [SM] each. Each submodule can output the capacitor voltage (FB SMs can output both positive and negative voltage) or 0V, but each arm is either positively charged or negatively charged. This allows an inverter MMC to turn on submodules in an arm to build the output voltage stepwise, which then creates a sinewave that can be output to an AC grid through a small inductor-filter. It is important to keep capacitor voltages balanced, and a control scheme must be implemented to create the sinewave as well as ensure that the capacitors, and the energy storage elements if they are implemented, are evenly charged and that the submodules are turned on to build the AC voltages as smoothly as possibly.

3.1 Submodule topologies

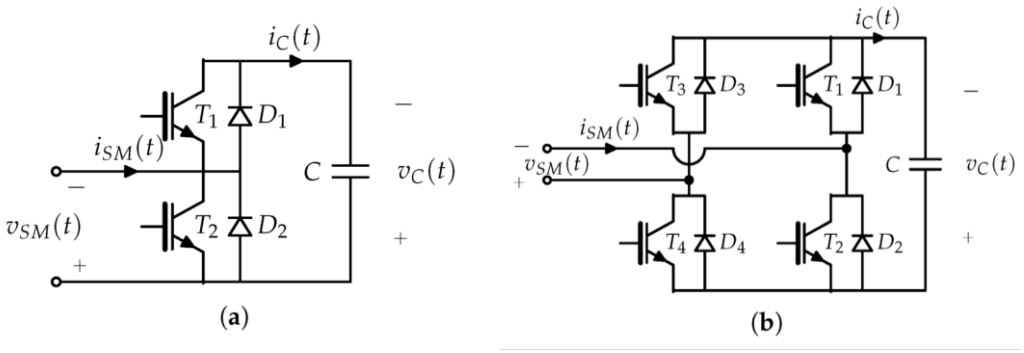

A: half-bridge submodule *B: full-bridge submodule*

Figure 3.1. The most common submodule topologies [3]

There are several ways to design the submodules of an MMC. The varying SM topologies have different levels of complexity, losses, switches and need to be handled differently regarding voltage balancing [4].

The most commonly used one is the Half Bridge [HB] SMs which has lower losses because of fewer semiconductors, and the voltage balancing is relatively simple. The voltage levels each SM can output are either 0V or V_C. An MMC will have a circulating current which will increase losses and reduce capacity if it is not limited through SM topologies, voltage balancing or an inductor. HB SMs do not suppress the circulating current, so an inductor is needed. The inductor has the added benefit of reducing an eventual DC fault current as well.

Full bridge [FB] SMs are more complex. They have more switches, which lead to higher losses, but they can output three voltage levels: $-V_C$, 0V or V_C, which also makes an MMC with FB SMs capable of working as an AC/AC converter [5]. The FB submodules have the added advantage of being able to block DC fault currents and limit the circulating current that flows between SMs.

For the simulation the HB SM is used. Since the thesis focuses on integrating energy storage into the SMs the HB cover the simulations needs, and it is more commonly used, so it is presumably more relevant.

The HB SM topology has some advantages and disadvantages over the FB SM topology:

Advantages:

- The fewest number of components.

Disadvantages:

- No capability of suppressing fault currents.

For the FB SM:

Advantages:

- SM output voltage can be of either polarity.
- Can hinder DC side current faults without triggering the AC side breakers.

Disadvantages:

- More expensive.
- Higher losses due to more switches.

3.2 Design

3.2.1 Number of Submodules

The number N of SMs in the simulation is 4 per arm, whereas more SMs would mean more computing, which the simulation is already quite intense on. The controls would not change much if the simulation were to be expanded with more SMs, just expanding voltage balancing and SM activation in the modulators to include the additional SMs as well as expanding the controls for the hybrid energy storage system [HESS] included in the SMs.

Physical MMC stations have a much higher number of SMs in each arm than the simulation, where the number of SMs can be in the hundreds. The reason for this is mainly standardising submodules, but a higher number of SMs also gives more accurate control of the output AC voltage.[6]

3.2.2 Submodule capacitance

SM capacitor capacitance are chosen to limit the voltage ripple in the SM. The capacitors need to contain enough energy to discharge onto the grid without a significant voltage drop. This means the capacitance must be rated to contain enough energy that the difference in voltage during a charge/discharge cycle is beneath a set percentage.

The equations for voltage ripples are included in the mathematical model for the MMC.

We want a ripple under 5%, the SM capacitances are 2mC and simulations show a ripple of +/- 50V in a 2500V capacitor, which falls well within our parameter of a 5% ripple in either direction.

.

3.3 MMC advantages and disadvantages

3.3.1 Advantages

MMCs have several advantages over similar converters. The most notable advantages are based on the modularity and increased adaptability and reliability that comes with it.

The notable advantages of MMCs include:[6, 7]

- increased reliability.
- no need for a large AC side filter.
- scalability in both power and voltage levels due to its modularity.
- lower losses compared to similarly sized converters, mainly due to lower switching frequency.
- Most components in the MMC are smaller as they are divided between the SMs. This makes them cheaper and more readily available.

3.3.2 Disadvantages

MMCs have several problems that need to be kept in mind when designing them. The circulating current and the voltage ripple needs to be suppressed and this must be done without raising the costs and losses of the MMC beyond reasonable levels.

More overall disadvantages include:

- an increased number of semiconductors.
- more advanced control.
- Less compact. The converter needs more space than certain other multilevel converters.

The Circulating current is created by an imbalance between the capacitor voltages of the upper and lower arms, which creates the current and increases losses, but does not affect the DC and AC current. In a HB MMC this circulating current needs to be limited by inductors on each arm, in addition to balancing capacitor voltage between SMs to prevent any current from circulating in the first place.

The voltage ripples are the difference in voltage in the SM capacitors before and after the submodule is turned on. The capacitors charge and discharge themselves and will have different voltage levels. This affects the output voltage amplitude as well as the circulating current.

3.4 Mathematical model

To get an understanding of how an MMC works it is helpful to have a mathematical model to see how the MMC operates during the steady state and dynamic conditions.

3.4.1 Inverter

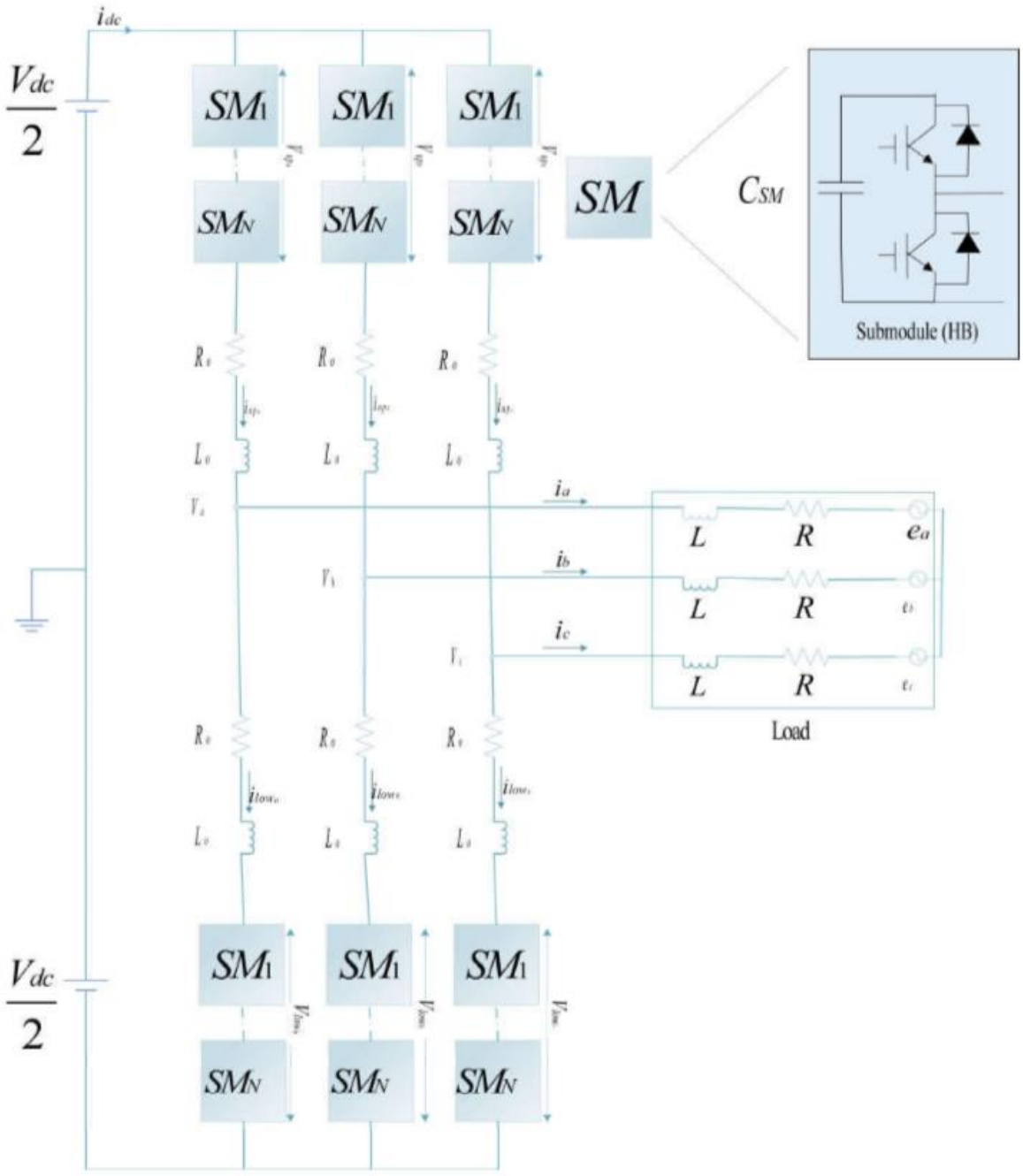

Figure 3-2. Schematic diagram for MMC

As shown in figure 3-2 the DC voltage is split in two between upper and lower sets of legs. The upper and lower leg phase current i_{u_j} and i_{l_j} of phase j is the defined by the DC current i_{dc}, the phase AC current i_j and the circulating current i_{cir_j} in formula () and ()

$$i_{u_j} = \frac{1}{3} i_{dc} + \frac{1}{2} i_j + i_{cir_j} \tag{3.1}$$

$$i_{l_j} = \frac{1}{3} i_{dc} - \frac{1}{2} i_j + i_{cir_j} \tag{3.2}$$

Solving these for i_{cir_j} gives the circulating current.

$$i_{cir_j} = \frac{1}{2}\left(i_{u_j} + i_{l_j}\right) - \frac{1}{3} i_{dc} \tag{3.3}$$

The difference between the DC voltage V_{dc} and the upper and lower arm phase voltages $V_{u_j}$and V_{l_j} are found by summing the losses in the arm resistor R_o and arm inductance L_o with the common mode voltage V_{cm} and the phase voltage V_j.

$$\frac{1}{2} V_{dc} - V_{u_j} = R_o i_{u_j} + L_o \frac{di_{u_j}}{dt} + V_j + V_{cm} \tag{3.4}$$

$$\frac{1}{2} V_{dc} - V_{l_j} = R_o i_{l_j} + L_o \frac{di_{l_j}}{dt} + V_j - V_{cm} \tag{3.5}$$

Incorporating the formulas for upper and lower phase current and voltage into each other to find the fundamental phase voltage and common mode voltage gives:

$$V_j + V_{cm} = \frac{1}{2}(V_{l_j} - V_{u_j} - \frac{R_o}{2} i_j + L_o \frac{di_j}{dt}) \tag{3.6}$$

Using the circulating current

$$L_o \frac{di_{cir_j}}{dt} = \frac{1}{2}\left(V_{dc} - V_{l_j} + V_{u_j}\right) - \frac{R_o}{3} i_{dc} \tag{3.7}$$

Considering that leg voltages are determined by how many SMs are active at the time we can define the leg voltages as:

$$V_{u_j} = n_{u_j} V_{c\_u_j} \tag{3.8}$$

$$V_{l_j} = n_{l_j} V_{c\_l_j} \tag{3.9}$$

Where n_{u_j} and n_{l_j} are the number of active SMs in the upper and lower arm respectively and $V_{c\_u_j}$ and $V_{c_l_j}$are the capacitor voltages of the individual SMs in the upper and lower arms of phase j. Inserting the newly defined arm voltages into () and () we get:

$$V_j + V_{cm} = \frac{1}{2}(n_{u_j} V_{c_{u_j}} - n_{l_j} V_{c\_l_j} - \frac{R_o}{2} i_j + L_o \frac{di_{l_j}}{dt}) \quad (3.10)$$

$$L_o \frac{di_{cir_j}}{dt} + R_o i_{cir_j} = \frac{1}{2} V_{dc} - n_{u_j} V_{c_{u_j}} - n_{l_j} V_{c_{l_j}}) - \frac{R_o}{3} i_{dc} \quad (3.11)$$

The power from the DC line is equal to the AC output and the losses in the MMC:

$$V_{dc} i_{dc} = P_{loss} + V_a i_a + V_b i_b + V_c i_c \quad (3.12)$$

This gives the equations for phase power based on active SMs:

$$P_{u_j} = n_{u_j} V_{c_{u_j}} i_{u_j} \quad (3.13)$$

$$P_{l_j} = n_{l_j} V_{c_{l_j}} i_{l_j} \quad (3.14)$$

An alternative would be to take the derivative of the capacitor energy to get the power from the capacitors in the arm in question.

$$W_{u_j} = N \frac{1}{2} Csm {V_{c_{u_j}}}^2 \quad (3.15)$$

$$P_{u_j} = \frac{dW_{u_j}}{dt} = \frac{d(N\frac{1}{2} Csm {V_{c_{u_j}}}^2)}{dt} = NCsm V_{c_{u_j}} \frac{dV_{c_{u_j}}}{dt} \quad (3.16)$$

And for the lower arms:

$$P_{l_j} = NCsm V_{c_{l_j}} \frac{dV_{c_{l_j}}}{dt} \quad (3.17)$$

With this we can express the ripples in the capacitors as:

$$\frac{dV_{c_{u_j}}}{dt} = \frac{1}{NCsm}(\frac{1}{3} i_{dc} + \frac{1}{2} i_j + i_{cir_j}) n_{u_j} \quad (3.18)$$

Which in turn can be expressed as:

$$\frac{dV_{c_{l_j}}}{dt} = \frac{1}{NCsm}(\frac{1}{3} i_{dc} - \frac{1}{2} i_j + i_{cir_j}) n_{l_j} \quad (3.19)$$

Through our previously established equations.

The equations for current, common mode voltage, DC side to AC side voltage and current and the derivative of capacitor voltages form the complete dynamical model for the MMC inverter.[4]

3.4.2 Rectifier

For the rectifier the mathematical model equations are restructured to express the DC power, voltage and current.

The current equations for upper and lower phase currents are restructured with respect to the DC current. The circulating current would ideally be zero.

$$i_{dc} = 3 \times \left(i_{u_j} + i_{l_j} + i_{cir_j}\right) \tag{3.20}$$

The DC voltage is expressed as:

$$V_{dc} = 2 \times \left(L_o \frac{di_{cir_j}}{dt} + \frac{R_o}{3} i_{dc}\right) + V_{l_j} - V_{u_j} \tag{3.21}$$

And the DC power is expressed as the sum of the phase powers and P_{loss}.

$$P_{dc} = P_{loss} + V_a i_a + V_b i_b + V_c i_c = \sum P_{u_j} + \sum P_{l_j} + P_{loss} \tag{3.22}$$

4 Energy Storage Systems

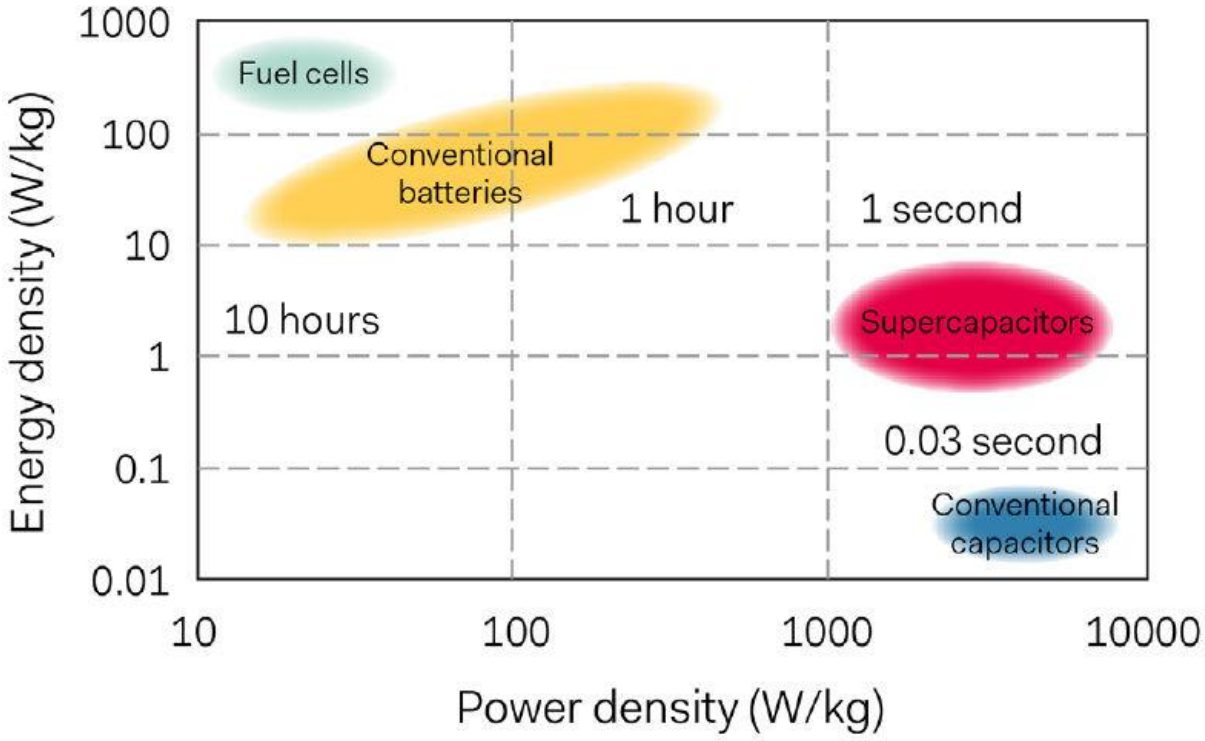

Figure 4.1. A chart showing the difference in power and energy density between different storage devices.[8]

Energy storage systems are, like the name describes, systems where energy is stored. This is done electrochemically through batteries, electrostatically through capacitors, hydropower with damns and/or pumps, tidal powerplants, spinning masses in generators, pressurized air, heated salt or heated oil to name a few.

In this thesis the focus will be on lithium-ion batteries and supercapacitors integrated into the SMs of an MMC.

The collective size of the batteries and supercapacitors [SC] should be collectively approximately 5% of the total capacity of the wind farm to make the converter able to contribute inertia to the grid like a similarly sized synchronous generator as suggested by this article [9].

4.1 Battery Energy Storage System

A pure battery energy storage system [BESS] would have high energy-density, but low power-density, and the State of Health [SOH] of the batteries would deteriorate significantly faster if they had to output high currents than if they could keep within their nominal ratings. The same can be said for charging/discharging the batteries completely as well, since the final top percentages of a battery take much longer to charge, while the final bottom percentages of a battery cause more stress due to a higher current. Put simply, the final top and bottom percentages cause a higher amount of stress on the battery (even within the safe limits to avoid deep discharges). One way to limit the degradation of batteries is to only use the battery at a low depth of discharge (DoD). This means that the battery is only charged and discharged between set levels of charge, for an example 20% and 80% (DoD of 60%), to avoid the increased stress of full charge and discharge cycles, this can prolong battery life by an order of magnitude. [10]

The reason using Li-Ion batteries reduces their SOH is because as the battery is used, the carbon in the anode reacts with the electrolyte which creates a solid layer called Solid Electrolyte Interface (SEI) which consumes some of the lithium. This layer cracks open when the battery is used, which frees up more carbon to convert more lithium. On the cathode there is a build-up of a layer of oxidation from the electrolyte. Both these effects change the voltage of anode and cathode and these layers start building up faster as the battery ages, especially with high cell-voltages.

Deep discharges and overcharges cause the cathode and anode respectively to create dendrites of copper and lithium, which eventually cause short circuits. These two states are highly unwanted, and modern batteries usually are made so that they are disconnected before this can happen. [11] [12] [13]

4.1.1 Li-Ion battery model

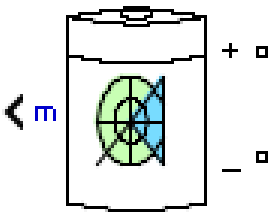

Figure 4.2 image of the battery used in the simulation.

The battery is set in the lithium-ion setting, taking on the characteristics of a lithium ion energy for the simulation.

The batteries have a discharge model and a charge model, both of which will be described here.

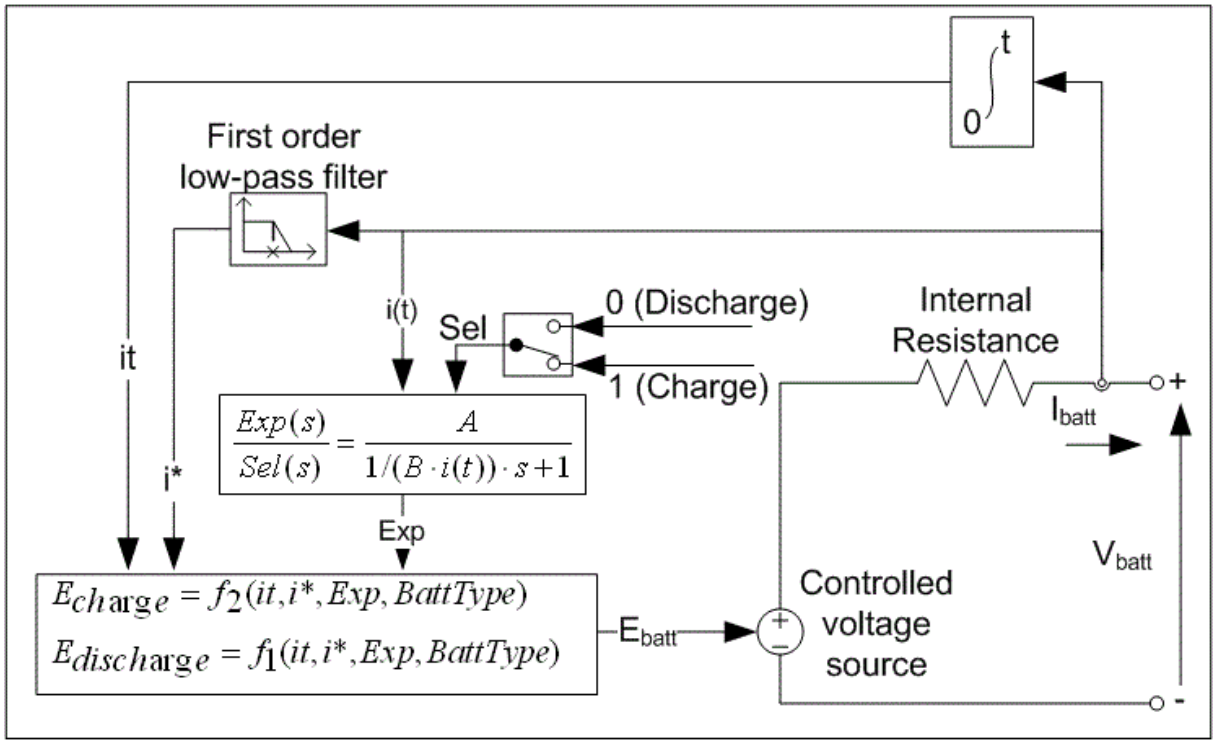

Figure 4.3 equivalent circuit modelled by the battery block.

The charge or discharge models are used based on the direction of the current.

The discharge model (i<0) is described by:

$$f_1(It, I*, I) = E_0 - K \times \frac{Q}{Q-It} \times I* - K\frac{Q}{Q-It} \times It + A \times \exp(-B \times It) \quad (4.1)$$

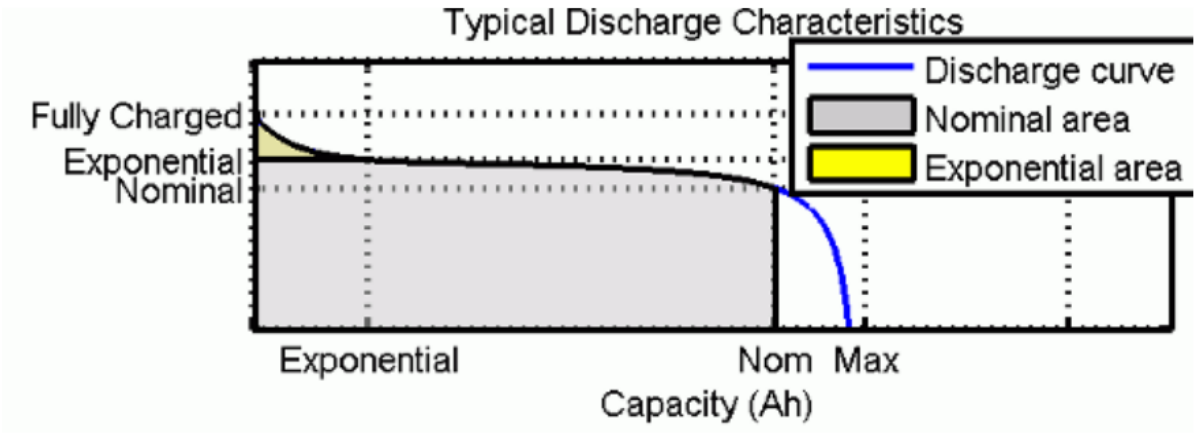

Figure 4.4. Battery discharge characteristics.

Here is a graphical representation of the discharge characteristics. Note the stable output voltage after the exponential area and the sudden drop once nominal capacity has been reached.

The charge model (i>0) is described by:

$$f_2(it, i*, i) = E_0 - K \times \frac{Q}{it+0.1\times Q} \times i* - K\frac{Q}{Q-it} \times it + A \times \exp(-B \times it) \quad (4.2)$$

Where:

- K is a polarization constant or polarization resistance in V/Ah or Ohms.
- I is battery current.
- I* is low frequency current dynamics, given in A.
- It is extracted capacity in Ah.
- Q is max battery capacity, given in Ah.
- A is exponential voltage, V.
- B is exponential capacity, Ah^{-1}.
- $E_0$is the constant voltage, V.
- Exp(s) is exponential zone dynamics, in V.

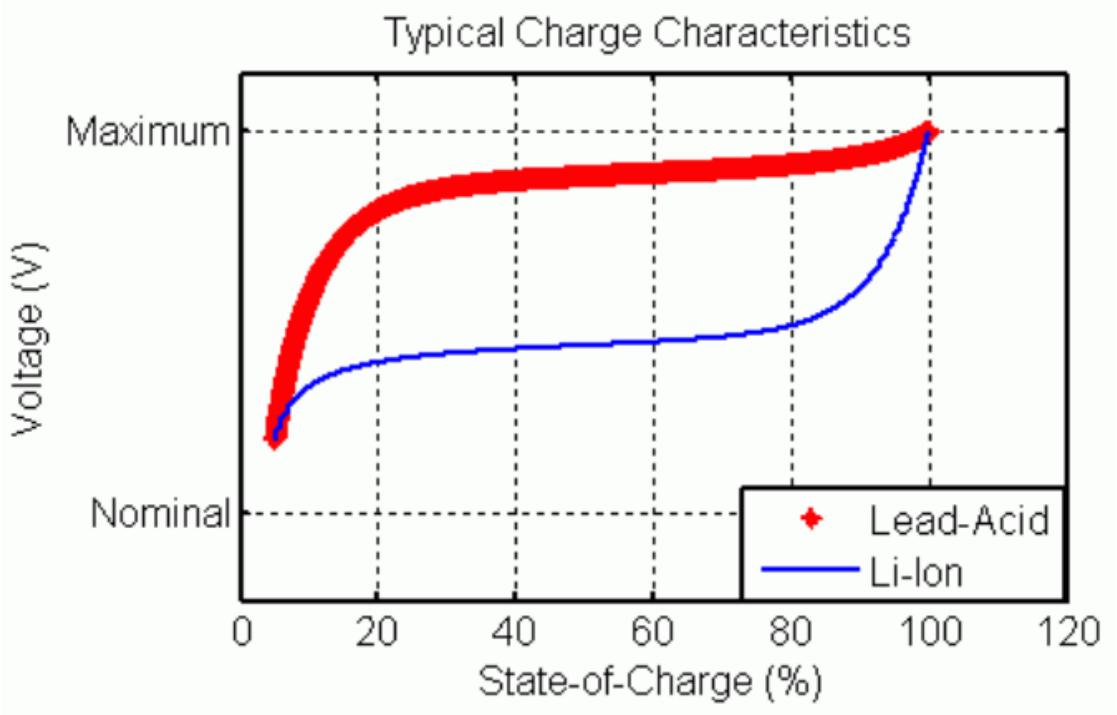

Figure 4.5. charge characteristics of a lithium ion battery compared to a lead-acid battery.

As shown in figure 4.5 the charging voltage is even apart from the final ~20% to full or empty capacity. Also, of note is the lower relative voltage compared to a lead-acid battery. [14]

4.2 Supercapacitor Energy Storage System

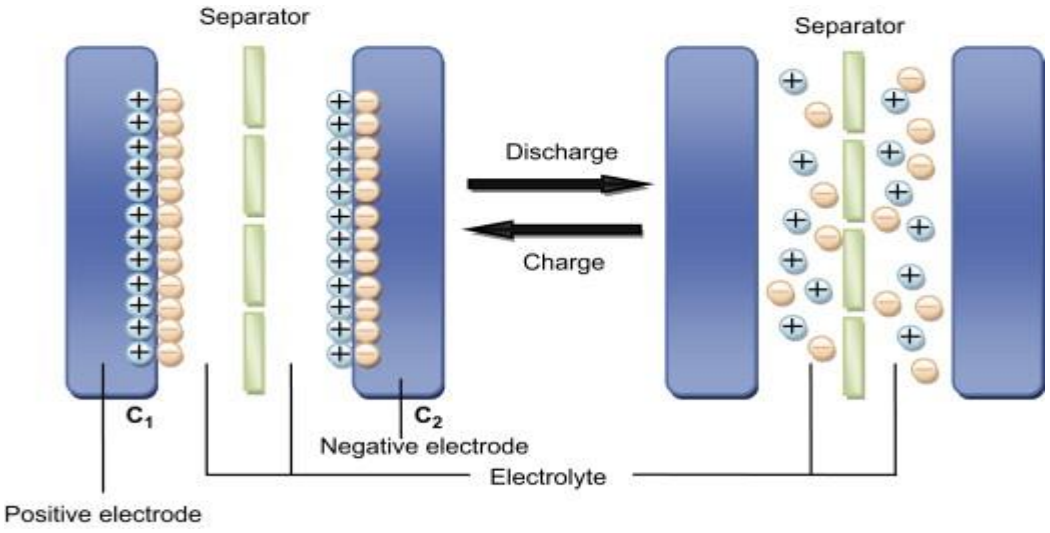

Figure 4.6 graphic representation of a supercapacitor

As previously mentioned a capacitor stores energy in a static charge between two conductive plates isolated by a dielectric. A pure SC energy storage system would have a high power-density, but a low energy-density. This means that the SC would be able to contribute to the grid in terms of short-term inertia, but eventually the capacitors would run out of surplus energy and the MMC would need to run according to power-production like a normal MMC until the SCs can be recharged by surplus production compared to demand.

An MMC has capacitors in the SMs already, but these are used as voltage sources, not as an energy storage system of any significance. Normal capacitors are unsuited for energy storage due to their low energy density. With SCs the energy density is higher than capacitors, but the low energy-density and resulting high price per Ah compared to a BESS makes a pure SCESS less viable for supplying any significant amounts of energy to the grid.

One of the more important benefits of SCs over batteries is that since they do not have any electrochemical reactions going on, they retain their functionality and capacity despite both DoDs as high as 80% or as low as 5% with very little difference in performance between the two scenarios. SCs are less susceptible to wear and tear from charging and discharging [15] than batteries, and they have a wide range of effective temperatures that go below temperatures where batteries cannot be used without external warmup.

An issue with using SCs for long term storage of energy is the fact that they self-discharge significantly faster than a battery does. A SC can lose up to 50% of its charge during the course of a month in contrast to a Li-Ion battery with a loss of 5% [16]. This potentially be circumvented by not storing the energy for long periods of time, or by using SCs in a hybrid energy storage system where the SCs and batteries can be used to reduce the amount of energy lost this way while still having the rapid response of an SC.

4.2.1 Supercapacitor Model

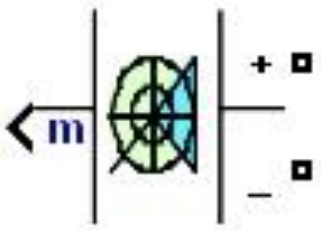

Figure 4.7 Supercapacitor block

The supercapacitor block is described by the following equivalent circuit and equations:

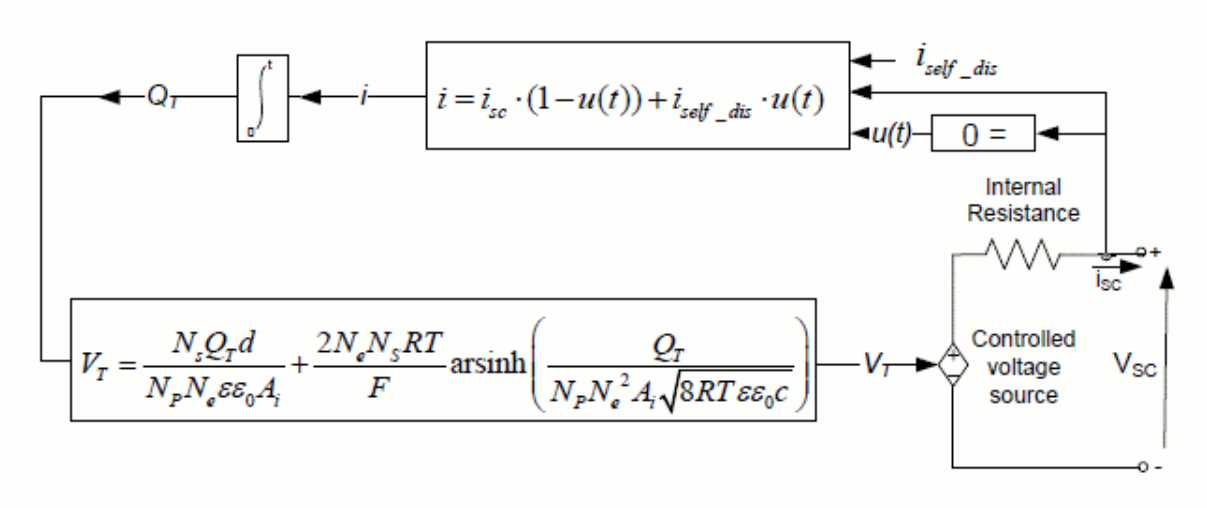

Figure 4.8 equivalent circuit for the supercapacitor block.

$$V_{SC} = \frac{N_S Q_T d}{N_p N_e \varepsilon \varepsilon_0 A_i} + \frac{2 N_e N_S R T}{F} sinh^{-1}\left(\frac{Q_T}{N_p N_e^2 A_i \sqrt{8 R T \varepsilon \varepsilon_0 c}}\right) - R_{SC} \times i_{SC} \tag{4.3}$$

Where

$$Q_T = \int i_{SC} dt \tag{4.4}$$

It is a possibility to include a self-discharge representation

$$Q_T = \int i_{dis}^{self} dt \tag{4.5}$$

Where i_{dis}^{self} is represented by:

$$i_{dis}^{self} = \frac{C_T \alpha_z}{1 + s R_{SC} C_T} \tag{4.6}$$

Where α_z is a constant determined by the time that has passed and represents the rate at which the supercapacitors voltage changes.[17]

4.2.2 Power and energy in a supercapacitor

The Energy in a SC is determined by its capacitance and its voltage.

$$W = 0.5 \times C \times V^2 \tag{4.7}$$

And the delivered energy is decided by the change in voltage.

$$W = 0.5 \times C \times ({V_{init}}^2 - {V_{end}}^2) \quad (4.8)$$

The maximum power is limited by internal resistance R_i.[18]

$$P_{max} = \frac{1}{4} \times \frac{V^2}{R_i} \quad (4.9)$$

Which is set at 8.9mΩ in the simulation. [19]

4.3 DC/DC Buck/Boost converter mathematical model

The battery and SC need DC/DC converters to be able to charge or discharge themselves at the capacitor voltage. The buck/boost converters are the connections between the battery, SC and the SM capacitor.

The output voltage is dependent on the input voltage and the duty cycle D as shown in the following equation:

$$V_o = \frac{-D \times V_i}{1-D} \quad (4.9)$$

Assuming the converter is in continuous mode. V_o is the SM capacitor voltage and $V_i$is the supercapacitor voltage. [20]

The output current is decided by an inductor. The current at the beginning, $I_{L_{on}}$, and end, $I_{L_{off}}$, of a cycle will be the same in continuous mode. The output current in onmode is described as:

$$I_{L_{on}} = \frac{V_i DT}{L} \quad (4.11)$$

While in offmode it is:

$$I_{L_{off}} = \frac{V_o(1-D)T}{L} \quad (4.12)$$

The discontinuous output voltage is described below:

$$V_o = \frac{-D^2 \times V_i^2}{2LI_0} \quad (4.13)$$

Where L is the coil inductance and I_0 is the output current: The output current is described as:

$$I_o = \frac{-V_i^2 D^2 T}{2LV_o} \tag{4.14}$$

4.4 Hybrid Energy Storage system

A Hybrid energy storage system is made with both batteries and supercapacitors [SC] to utilize both their respective strengths and to counter their weaknesses. The high power-density of SCs makes up for the low power density of batteries, while the batteries makes up for the low energy density of SCs. Because they make up for each other's weaknesses the combination of SCs and batteries is not uncommon.

While batteries work by using electrochemical reactions to store and release energy, capacitors store energy as a static charge between conductive plates. The difference between the static charge and electrochemical reactions is how much time is needed to release the energy versus how much energy can be stored in a static charge as well as the reduced wear and tear from the lack of electrochemical processes.

The difference in energy density between batteries and SCs is 10:1 in a best-case scenario according to [16] with SCs having 4-10 Wh/kg to lithium ion batteries 100-265 Wh/kg. This means that any HESS incorporating both these types of energy storage should divide their intended storage capacity thereafter to avoid spending more money and room than necessary for the intended capacity while keeping the SC benefits relevant.

Considering the system of this thesis transmits 1.12 MVA, the batteries and SCs need to cover 55 KVA of power across 24 batteries and 24 SCs where the batteries will cover a greater part of the energy storage due to their higher energy density, but the power capabilities on the other hand will be determined to let the SCs cover a majority of the power for a short amount of time. The energy capacity of an SC is at best 10% of the capacity of a similarly sized Li-ion battery, thus the share of energy between them should be scaled accordingly to reduce cost per AH while keeping cost down per Ah and the SCs advantages relevant.[16]

4.4.1 HESS design

The HESS should be able to supply the inverter MMC with 55kw at any moment, but also be able to supply this amount of power over a reasonable amount of time. This means that the SCs and batteries need to have a capacity of several times 50000j as a system. This change will be in capacity for the batteries and both capacitance and rated voltage for the SCs.

The SCs and batteries chosen ratings are noted on this table:

Table 4.1. HESS ratings.

	Battery	Supercapacitor
Rated voltage (V)	200	82
Capacity (Ah)	13	-
Capacitance (F)	0	6.82
Nominal power (W)	1130	2300
Power over 24 SM (KW)	27.12	55.2
Energy	9.36MJ	22.91667KJ
Energy over 24 SM	224.464MJ	550KJ

This table gives a suggestion for a HESS where the SCs can supply full power of 55KW for 10 seconds and the batteries can supply a decent amount of the 5% goal of power for an hour at approximately nominal values.

The nominal discharge current of the batteries is 0.8695A.

5 Control Strategies.

In this thesis there are several devices which need a control strategy; The battery output and SOC, the SC output and SOC and the MMCs all need different controls.

The goal of any of these control strategies is to make the converter and energy storage facilities effective and reduce wear and tear as well as any risks for faults and uneven outputs.

The batteries and SCs can only be controlled through their current with regards to the output from the submodule, the voltage is determined by the SM capacitor. The buck/boost and boost converters in the submodules are controlled by a power input, which then increases the current drawn from the storage device into the converter. The converters then output the power at capacitor voltage to contribute power to the MMC arm.

5.1 MMC control

5.1.1 PWM

Pulse Width Modulation (PWM) is a common way of controlling MMCs. The PWM controls of the simulation are already in place. The PWM control is located in the modulators and compares the voltage reference signal to the 4 PWM signals before sending the control signal through the sorting algorithm which decides which SMs have the highest/lowest charge depending on the direction of the arm current.

PWM has several variants shortly described below, common for all is that the converter switches between a discrete number of levels of the DC voltage depending on which PWM carriers the sine wave is higher and lower than. When the reference voltage is at either the highest or the lowest level of the sinewave above/beneath all carrier signals the output voltage is set at Vdc/2 and 0V, with the remaining steps indicating that the sinewave is below some carrier waves, while above others, which determines the number of active SMs and the output voltage for the arm.[21]

5.1.1.1 Phase disposition PWM (PDPWM)

All the carriers in this method are in the same phase, regardless of being above or below zero reference line. PDPWM is a widely used strategy for MMCs and conventional multilevel inverters because it provides load voltage and current with lower harmonic distortion. [21]

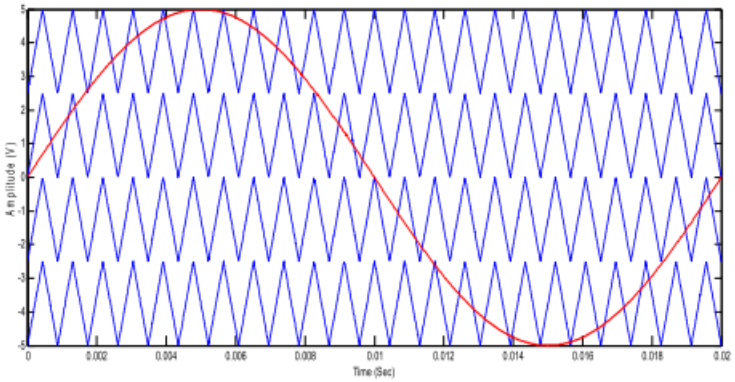

Figure 5.1 Carrier arrangement example for PDPWM

This is the method used in the simulation.

5.1.1.2 Phase opposition disposition PWM (PODPWM)

The carriers in PODPWM have the same frequency and an adjustable amplitude. All the carriers above the zero-value reference are in phase, but phase shifted 180 degrees to those below the zero-value reference.[21]

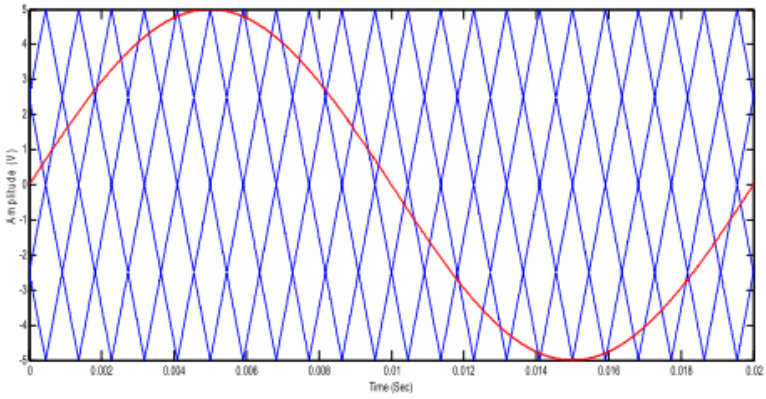

Figure 5.2 Carrier arrangement example for PODPWM

5.1.1.3 Alternate phase opposition PWM (APODPWM)

Here the carriers have the same frequency and their amplitudes are adjustable. All carriers are phase shifted 180 degrees between each other.[21]

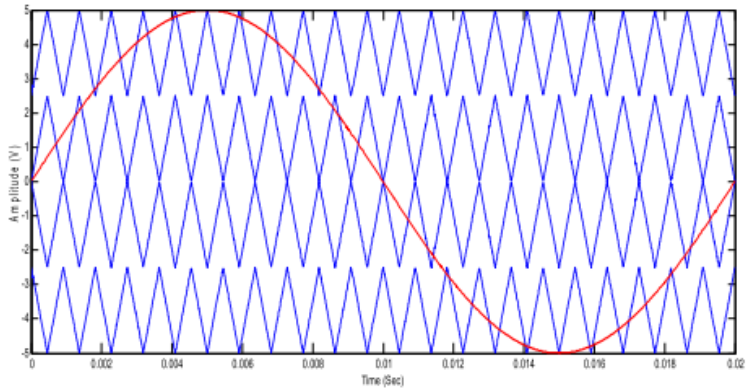

Figure 5.3 Carrier arrangement example for APODPWM

5.1.1.4 Phase shift PWM (PSPWM)

Phase shift multicarrier PWM is a multicarrier PWM strategy and is close to PDPWM. IT uses four carrier signals with the same amplitude and frequency but shifted 90 degrees to one another.[21]

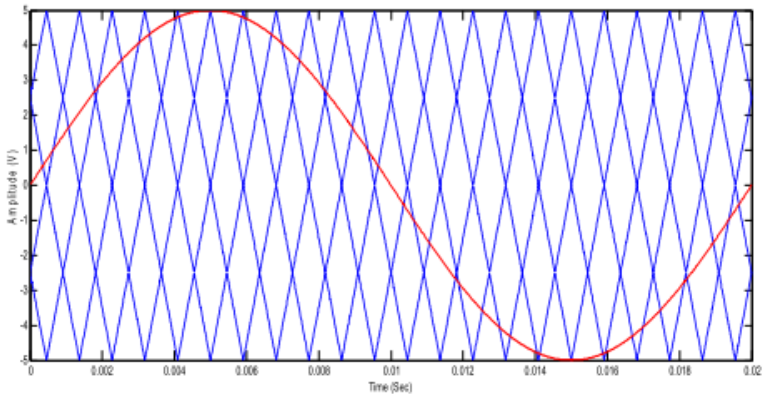

Figure 5.4 Carrier arrangement example for PSPWM

5.2 P-Q control (instantaneous power theory)

Used in the inverter. P-Q control was proposed in 1984. The control strategy focuses on having the same active and reactive power before and after the converter. P-Q relies on the park transformation to calculate the active and reactive power. [22] The instantaneous powers P and Q are compensated for by the controller so that output power equals input power and converter losses: [23]

5.2.1 P-Q control mathematical model

The grid side control has the following mathematical model:

The dq0 transform yields the following equations:

$$V_d = \frac{2}{3} \times (V_a \times \sin(\omega t) + V_b \times \sin\left(\omega t - \frac{2\pi}{3}\right) + V_c \times \sin(\omega t + \frac{2\pi}{3})) \quad (5.1)$$

$$V_q = \frac{2}{3} \times (V_a \times \cos(\omega t) + V_b \times \cos\left(\omega t - \frac{2\pi}{3}\right) + V_c \times \cos(\omega t + \frac{2\pi}{3})) \quad (5.2)$$

$$V_0 = \frac{V_a + V_b + V_c}{3} \quad (5.3)$$

$$I_d = \frac{2}{3} \times (I_a \times \sin(\omega t) + I_b \times \sin\left(\omega t - \frac{2\pi}{3}\right) + I_c \times \sin(\omega t + \frac{2\pi}{3})) \quad (5.4)$$

$$I_q = \frac{2}{3} \times (I_a \times \cos(\omega t) + I_b \times \cos\left(\omega t - \frac{2\pi}{3}\right) + I_c \times \cos(\omega t + \frac{2\pi}{3})) \quad (5.5)$$

V_d and V_q are sent onwards to P-Q calculation where they are used in the following equations to find a reference value for I_d and I_q.

$$I_{qref} = \frac{2}{3} \times \frac{V_q \times P_{ref} - V_d \times Q_{ref}}{V_q^2 + V_d^2} \quad (5.6)$$

$$I_{dref} = \frac{2}{3} \times \frac{V_d \times P_{ref} + V_q \times Q_{ref}}{V_q^2 + V_d^2} \quad (5.7)$$

The reference currents (5.6) and (5.7) are subtracted the measured currents from (5.5) and (5.4), respectively, and the difference is sent through PI controllers. The PI control output is sent as a voltage reference signal for reverse dq0 transformation and sent to the modulators.

The final voltage reference signal reverse dq0 transform is shown below:

$$V_a = V_d \times \sin(\omega t) + V_q \times \cos(\omega t) + V_0 \quad (5.8)$$

$$V_b = V_d \times \sin\left(\omega t - \frac{2\pi}{3}\right) + V_q \times \cos\left(\omega t - \frac{2\pi}{3}\right) + V_0 \quad (5.9)$$

$$V_c = V_d \times \cos(\omega t + \frac{2\pi}{3}) + V_q \times \cos(\omega t + \frac{2\pi}{3}) + V_0 \quad (5.10)$$

5.3 VSC control

Used in the rectifier.

Voltage Source Converters work as both inverters and rectifiers and are therefore well suited to back-to-back converter set-ups. The VSC control is capable of independent control of both active and reactive power, which makes it versatile and

VSC controller send a voltage reference signal to the modulators which sort the SMs and turn on the number of SMs indicated by the voltage reference signal compared to the PWM signal.

5.3.1 VSC control model

The VSC control is divided into several parts: Measurements. the Vdc regulator, the current regulator followed by a reverse dq0 transform. The measurements is mainly the dq0 transform of the pu voltage and current.

5.3.1.1 Vdc regulator:

The DC voltage regulator simply compares the DC voltage with the desired reference voltage. The difference is then divided by the line inductance and sent to a current PI controller. The output signal is sent to the current controller as the reference current I_{dref}

$$I_{dref} = \frac{V_{DCmeasured} - V_{DCref}}{L} \quad (5.11)$$

The measured $I_q$and I_d is subtracted from the reference I_{dref} and I_{qref}, where I_{qref} is set as zero in the model, and putting it through another PI controller. This gives us the derivative currents $\frac{dI_d}{dt}$ and $\frac{dI_q}{dt}$.

The result from the PI controller is summed with the feedforward voltage signal, which requires the use of line impedances found below to find the dq feedforward values:

:

$$L_{tot_{pu}} = L_{xfo} + L_{choke} \tag{5.12}$$

$$R_{tot_{pu}} = R_{xfo} + R_{choke} \tag{5.13}$$

$$V_{d\_conv} = V_{d\_mes} + I_d \times R_{tot_{pu}} - I_q \times L + \frac{dI_d}{dt} \times L_{tot_{pu}} \tag{5.14}$$

$$V_{q\_conv} = V_{q\_mes} + I_d \times L_{tot_{pu}} + I_q \times R_{tot_{pu}} + \frac{dI_d}{dt} \times L_{tot_{pu}} \tag{5.15}$$

$V_{d\_conv} + V_{q\_conv}$ are sent onwards to a reverse dq0 converter to create the phase voltage reference value.

The feed forward is used to decouple the active and reactive power, so they can be changed independently and simultaneously.

5.4 Balancing SOC in the HESS

5.4.1 Batteries

The balancing strategy that was decided upon was discharging the batteries according to their SOC. The SOC of a battery in the positive/negative part of the arm will be divided by the average SOC in the positive or negative SMs of the arm. This is then used to increase or decrease the input signal to the converter for the battery, which will adjust the output for that battery according to its relative SOC.

The SOC modifier for each SM in an arm is determined by:

$$P_{mod\ n} = \frac{SOC_1+SOC_2+SOC_3+SOC_4}{N} \times SOC_n \tag{5.16}$$

Where SOC_n is the average SOC in the arm amongst the batteries.

The SOC modifier is then multiplied with the power which the SM is expected to supply, which is inserted as a control signal in the battery converter.

$$P_{Battery\ n} = P_{mod\ n} \times \frac{P_{requested}}{k} \tag{5.17}$$

However, the batteries have a maximum output associated with each battery and we want to hinder any sudden changes in output. This is implemented with saturation and slew rate limiters in the controls and serves to keep the batteries within nominal operating conditions to extend the lifespan of the batteries.

$$P_{Battery\ n} \leq P_{Battery\ nom} \tag{5.18}$$

$$\frac{dP_{Battery\ n}}{dt} \leq R \tag{5.19}$$

Where R is a chosen slew rate.

5.4.2 SC control

The SCs are controlled by the same method as the batteries. The SOC of the SC is compared to the average SOC of the positive or negative arm and the output modifier is multiplied by the power expected of the SM. The power expected of the SM is found by subtracting the battery output of the arm from the energy expected by the arm. This makes the arm HESS output respond to any sudden changes by discharging from the SCs since the batteries have a slew rate limiter in the controls which reduces any sudden changes in power output.

The SC output is determined by:

$$P_{mod\ n} = \frac{SOC_{1sc}+SOC_{2sc}+SOC_{3sc}+SOC_{4sc}}{N} \times SOC_n \tag{5.20}$$

$$P_{SCarm} = P_{requestedarm} - P_{batteryarm} \quad (5.21)$$

$$P_{SC\ n} = \frac{P_{SCarm}}{N} \times P_{mod\ n} \quad (5.22)$$

Where $P_{SC\ n}$is limited to a value slightly above $P_{SC\ nominal}$.

5.4.3 Buck/boost DC/DC converter

The SCs and batteries rely on Buck/boost converters to be able to supply the MMC with energy as well as getting recharged. The converter is controlled by giving it a power reference which is eventually used to create the gating-signal.

The buck/boost converter has slightly different controls depending on if the power reference is positive or negative, but the initial part is the same for both.

The requested power is divided by the voltage to get the needed current. The needed current is then compared to the measured current and the result is sent to a PID regulator, which then sends the result to compare to a PWM signal which goes from 1 to -1. When the control reference signal is not greater than the PWM signal the MOSFET is sent a on signal, effectively creating a D value depending on the difference between needed and measured current. A converter which outputs exactly as much power as is requested would have a D-value of 0.5 as the PWM would sink below 0 50% of the time.

Negative power (charging):

When the converter is charging the battery or SC the active MOSFET is placed in series with the output terminals. In the current comparison the measured current is the positive, while the requested current is subtracted to get the required derivative current to even out input power and the available power for charging (as stated by the power reference).

Positive power (discharging):

When the converter is discharging into the SM the active MOSFET is placed in parallel with the output terminals. In the current comparison the requested current is the positive, while the measured current is subtracted to get the required derivative current to even out output power and requested power from the control.

$$\frac{P_{Brequested}}{V_{measured}} = I_{requested} \quad (5.23)$$

For discharge mode:

$$I_{ref} - I_{measured} = I_{missing} = \frac{dI}{dt} \quad (5.24)$$

For charge mode:

$$I_{measured} - I_{ref} = I_{missing} = \frac{dI}{dt} \quad (5.25)$$

$I_{missing}$ is put into a PID controller and compared to the PWM signal to get a duty cycle.

6 Simulation and results

The simulation is a modified MMC with an integrated HESS in the submodules which works as an inverter and an MMC controlled by a VSC that works as a rectifier. The original control system for the inverter was also a VSC controller, but eventually it was replaced by a P-Q controller in the inverter MMC, mostly for ease, but with the added advantage of testing how it works with the HESS.

The simulation starts with a three-phase voltage source representing the wind farm, which feeds into a rectifier MMC which is controlled by a VSC controller. This rectifier feeds into the modified MMC which transforms the DC voltage into AC voltage and contains the energy storage elements. The MMC feeds into a filter, then it goes to the grid, represented by another three-phase voltage source representing the grid.

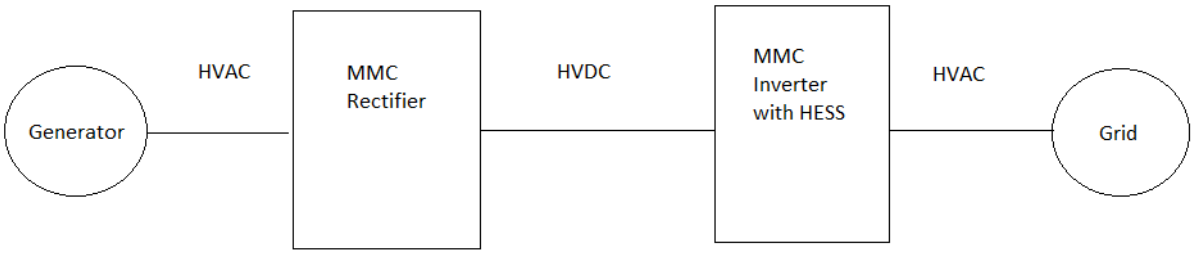

Figure 6.1. simplified overview of simulation

6.1 Results

Simulation results are shown and discussed in this chapter. The difference between power generation, output, HESS participation and their effect on how quickly the system reaches steady state, if ever, will be compared and a conclusion will be drawn for chapter 7.

6.1.1 MMC output with 0 KW output from batteries, no deficiency

Running the simulation without any modifications like HESS contributions, surplus power or deficit in power yields an output AC phase voltage and current shown in figure 6.1. with a close-up of the phase voltage and current in steady state is shown in figure 6.2

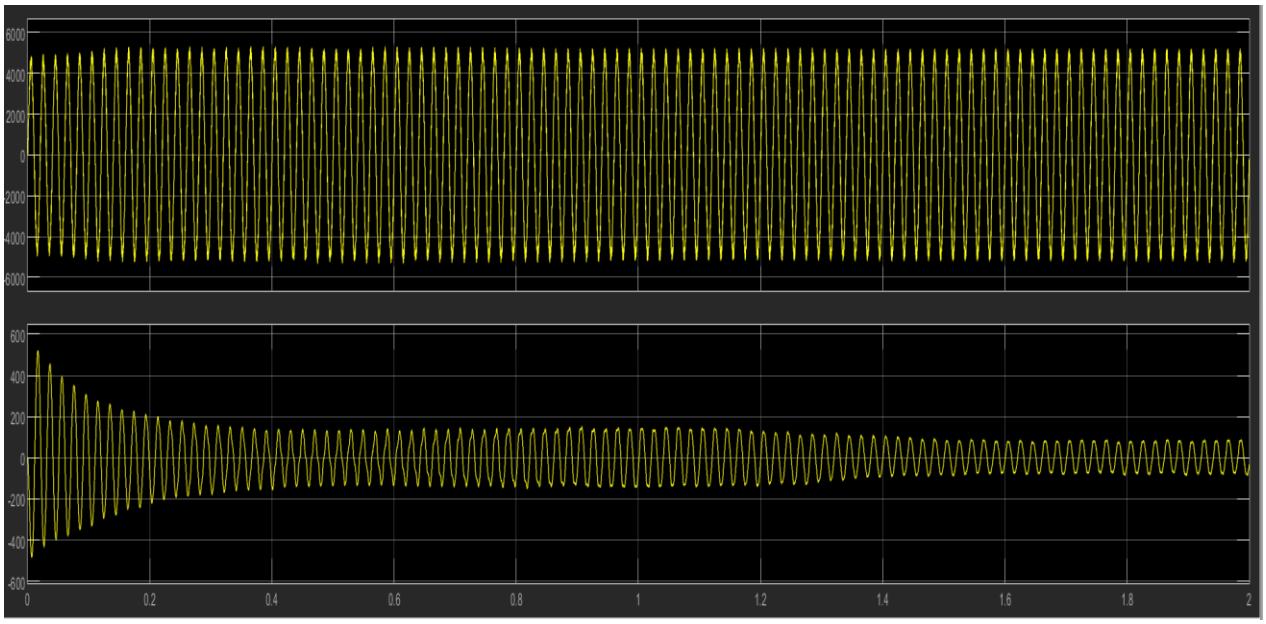

Figure 6.1. Phase A AC current and voltage.

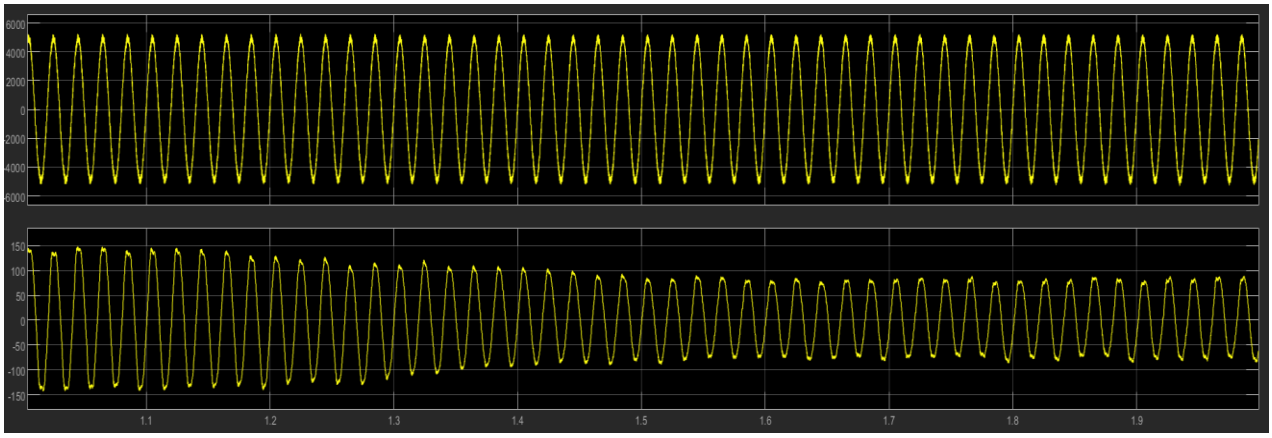

Figure 6.2 phase A AC current and voltage close-up after 1s.

As we can see the AC current is still settling after 1.2 seconds. The voltage is even as expected considering it is connected to the grid. We can also see the current and voltage are in phase after 0.5 seconds, so power is being delivered to the grid.

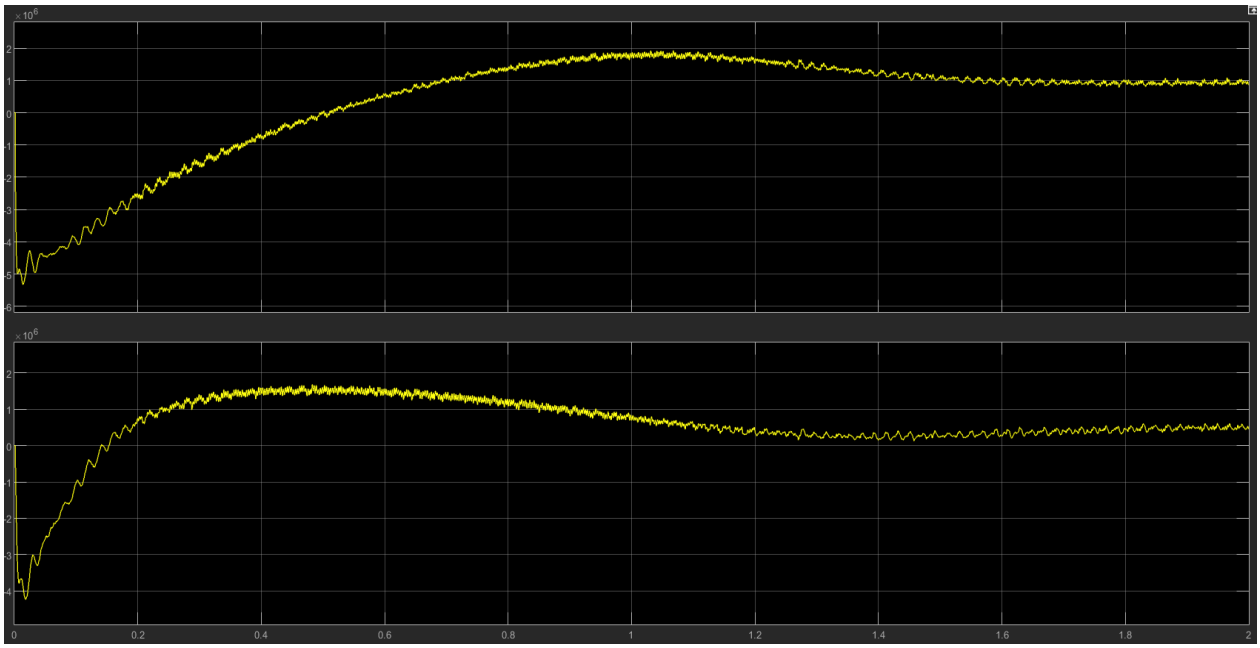

figure 6.3 active and reactive power from the inverter.

Figure 6.3 shows the power delivered by the system to the grid. The desired output power is determined by the P-Q control and the end power output is correct, though slow. We also see the delivery of active power to the grid after 0.5s. While the system is

The DC current and voltage is shown in figure 6.3.

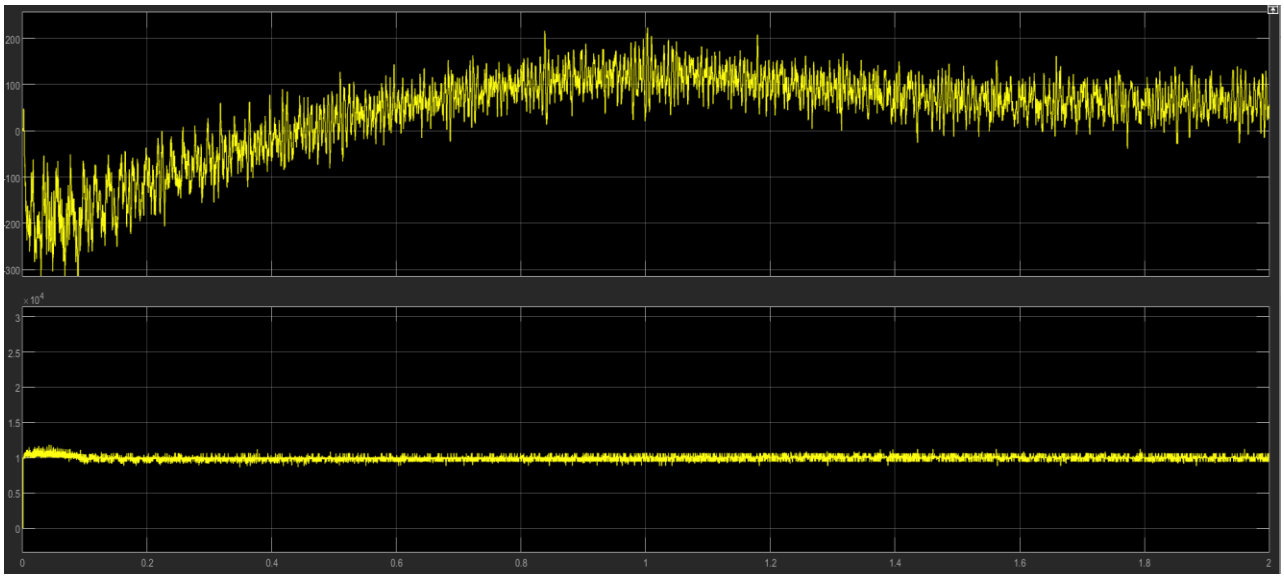

Figure 6.4 DC voltage and current.

As shown the voltage settles within 0.2s, while the current takes about 1.2 to 1.4 seconds to settle. This results in the overshoot for both P and Q in figure 6.3.

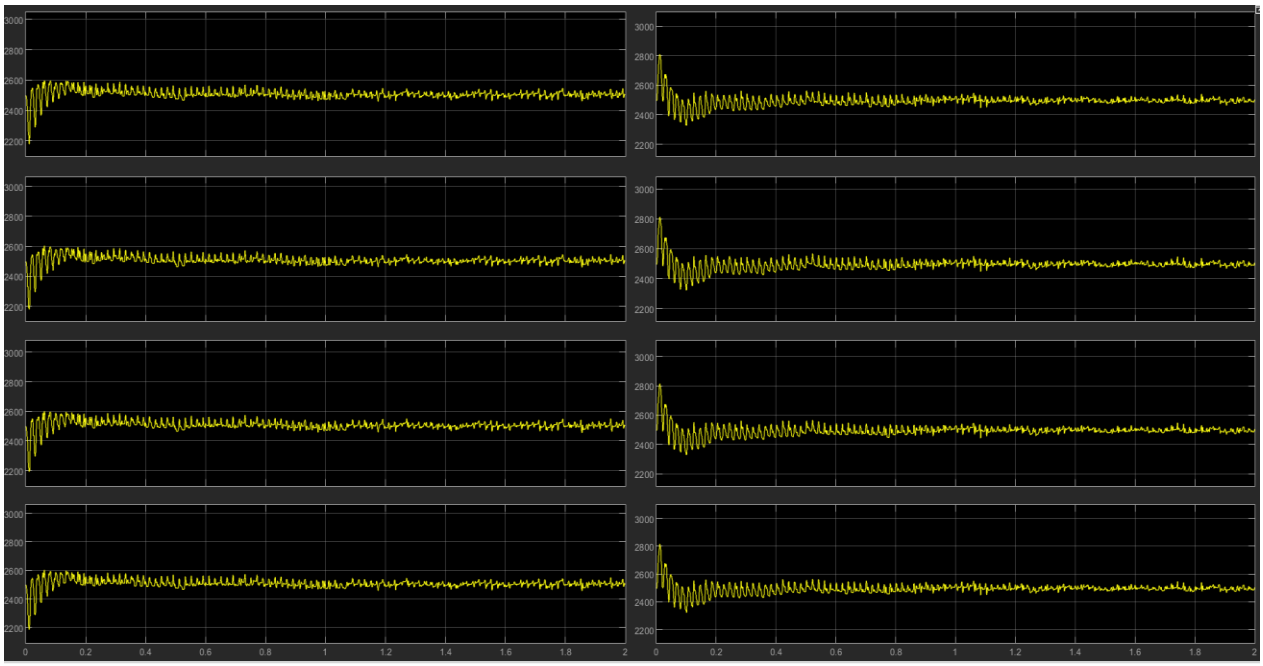

Figure 6.5. Capacitor voltages

The capacitor voltages however settle quickly at ~2500V and stay stable with a ripple of about +/-50V, which is acceptable. The quick settling of the capacitor voltages contributes directly to the HVDC voltage settling so quickly.

As seen from the images of the system test without ESS contributions the system is slow to settle, but stable. The important subject is how the system responds to injected power from the ESS. The results found here will be the basis the other tests will be compared to.

6.1.2 inverter output with 48KW output from batteries

Running the simulation with a 48kw output from the HESS. The Instantaneous power control should include this input in its calculation of the voltage reference signal and take less from the DC line. The figure 6.6 shows phase voltage and current on the AC line, with a close-up on the steady state is shown in figure 6.7

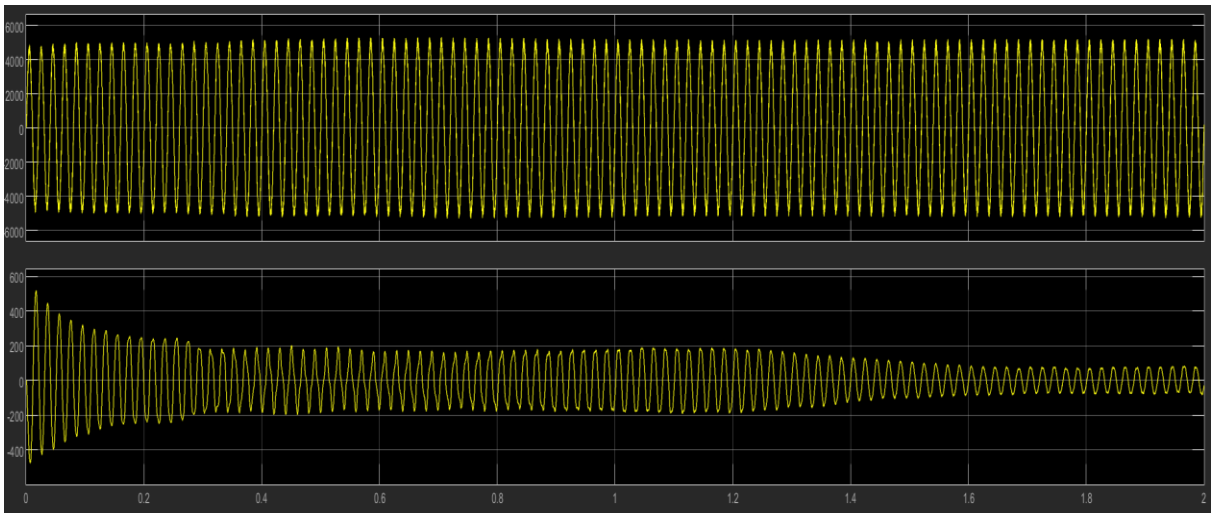

Figure 6.6 phase AC current and voltage.

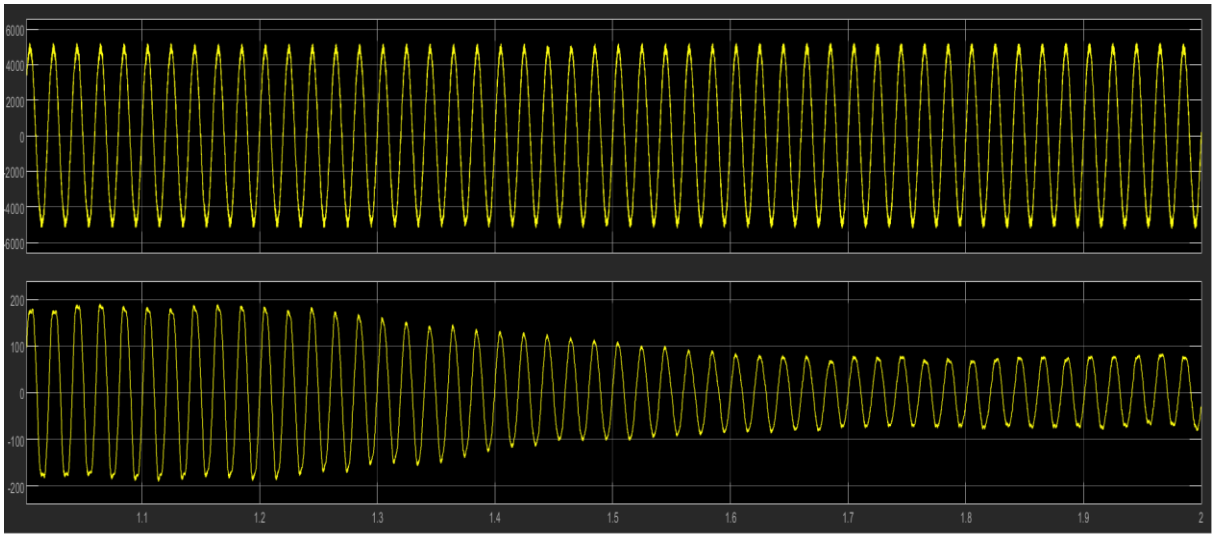

Figure 6.7 phase AC current and voltage close-up of last 1s.

The phase current changes like in the previous simulation. The current amplitude is predictably higher than before, and it settles a bit slower than without the surplus.

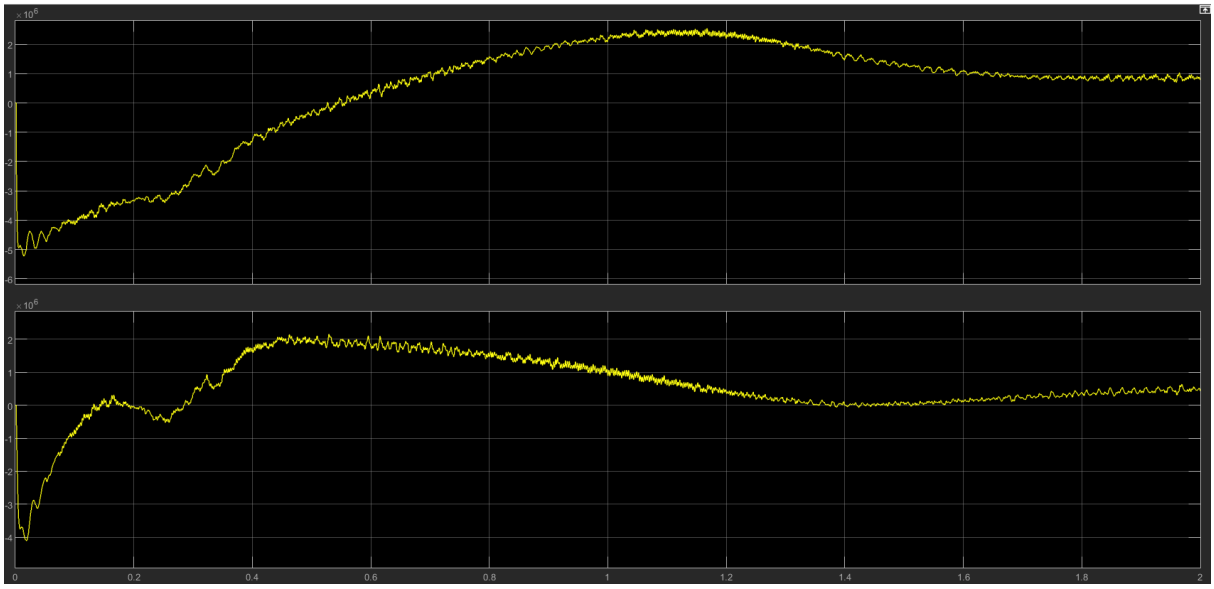

figure 6.8 Active and reactive power from the inverter

The power output, both active and reactive, directly from the inverter is shown in figure 6.8. The curves are less stable and take longer to settle, this can be attributed to the surplus power delivered to the converter. The overshoot is also greater.

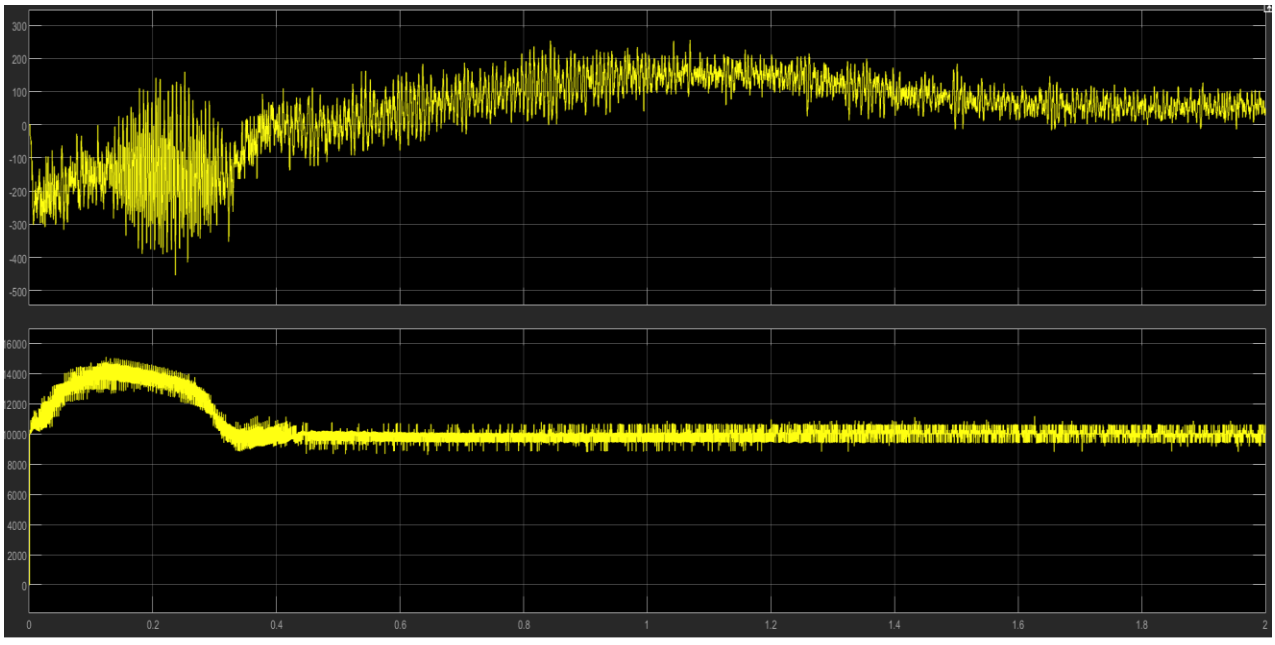

Figure 6.9 DC voltage and current

The DC current and voltage is shown in figure 6.9. The voltage uses noticeably more time to settle than the previous simulation and has a greater overshoot in current amplitude. The current settles in roughly the same time.

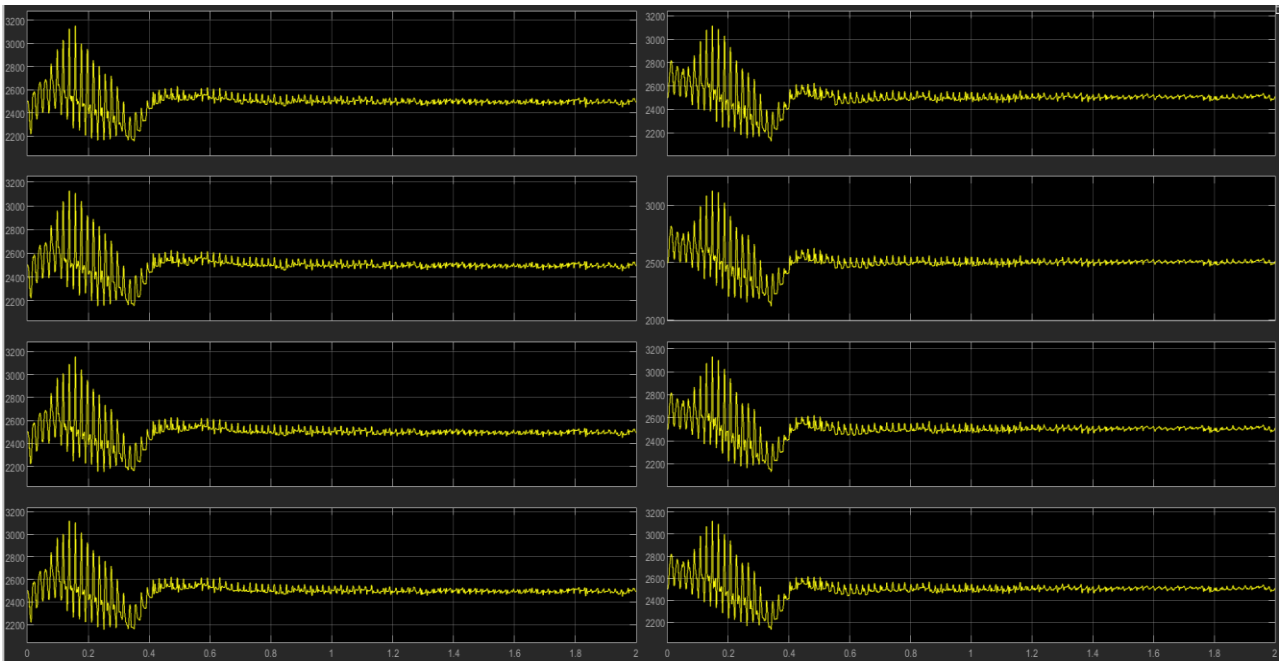

Figure 6.10 Capacitor voltages

With exception to the first 0.4 seconds the capacitor voltages are as stable as in figure 6.5. the initial instability is possibly due to the overactivity of the batteries in the first 0.3 seconds.

As for the HESS we can see the SOC, voltage and the current of a submodule's battery and SC in figure 6.11 and 6.12.

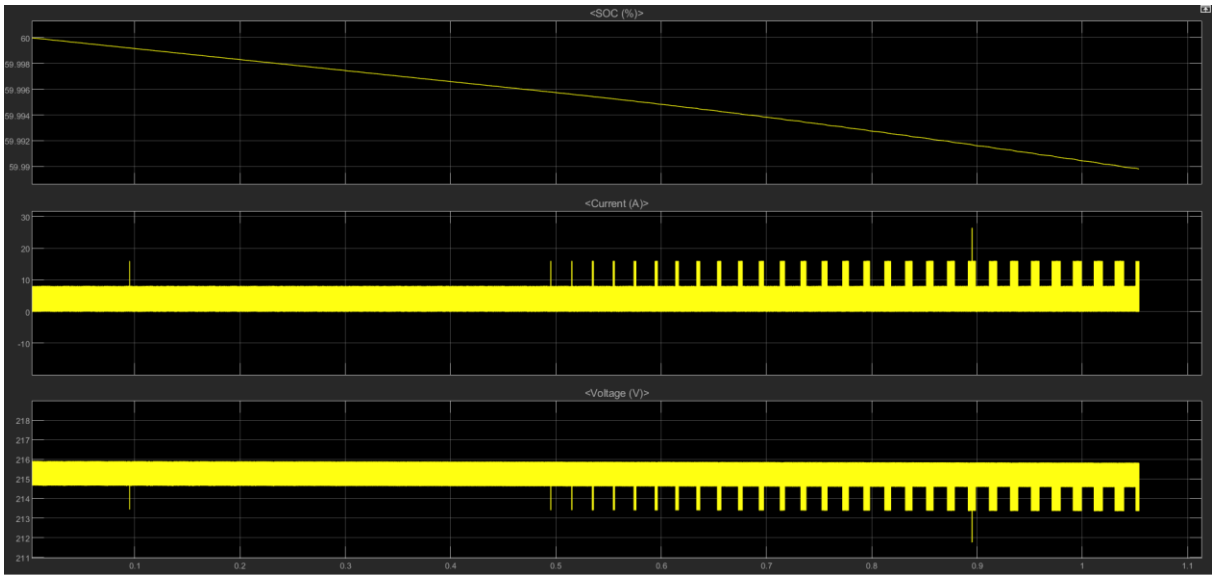

Figure 6.11. Battery SOC, voltage and current.

As shown in figure 6.11 the current is even, though it increases as the power demand for the battery increases. The current is somewhat higher than nominal, and the latter values are markedly higher than nominal.

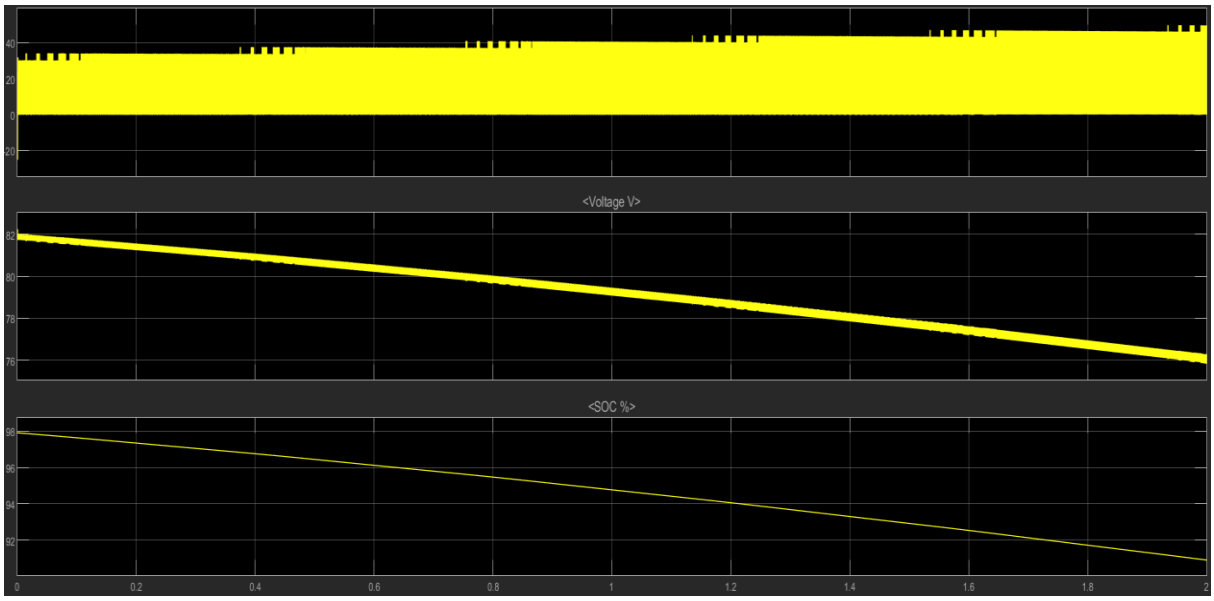

Figure 6.12 supercapacitor current, voltage and SOC.

We see the current rise as the voltage drops steadily along the SOC, this is as expected.

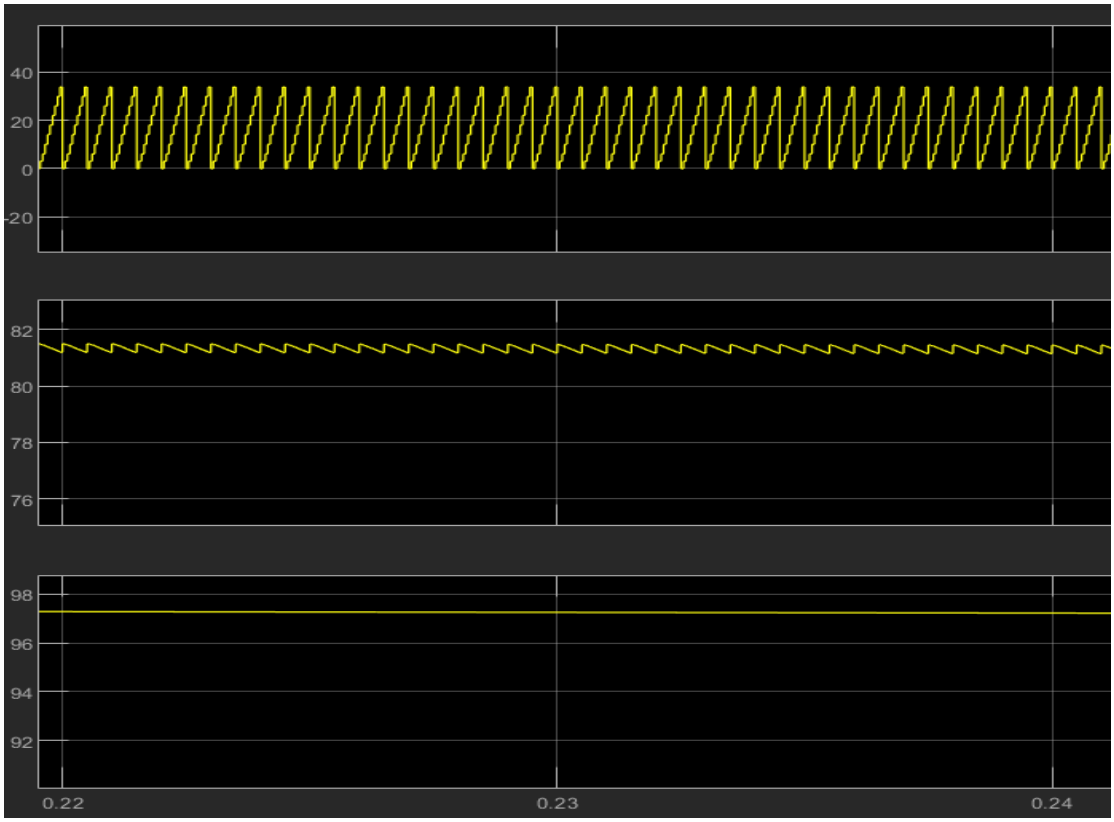

Figure 6.14 close-up of SC current, voltage and SOC.

Considering no imbalances were implemented into the HESS one submodule can represent them all. In a non-ideal case we would have to compare the difference between submodules to see the effects of different SOCs on output currents.

6.1.3 Inverter output with HESS contributing after the system has settled

In this simulation the HESS starts contributing after 0.5 seconds to see if the system handles the implementation of the HESS better once it has reached a stable state and the HESS does not contribute to increase transients.

This is essentially a test of how the ESS works in an already working state for the system, which is ultimately the state in which the ESS would be used.

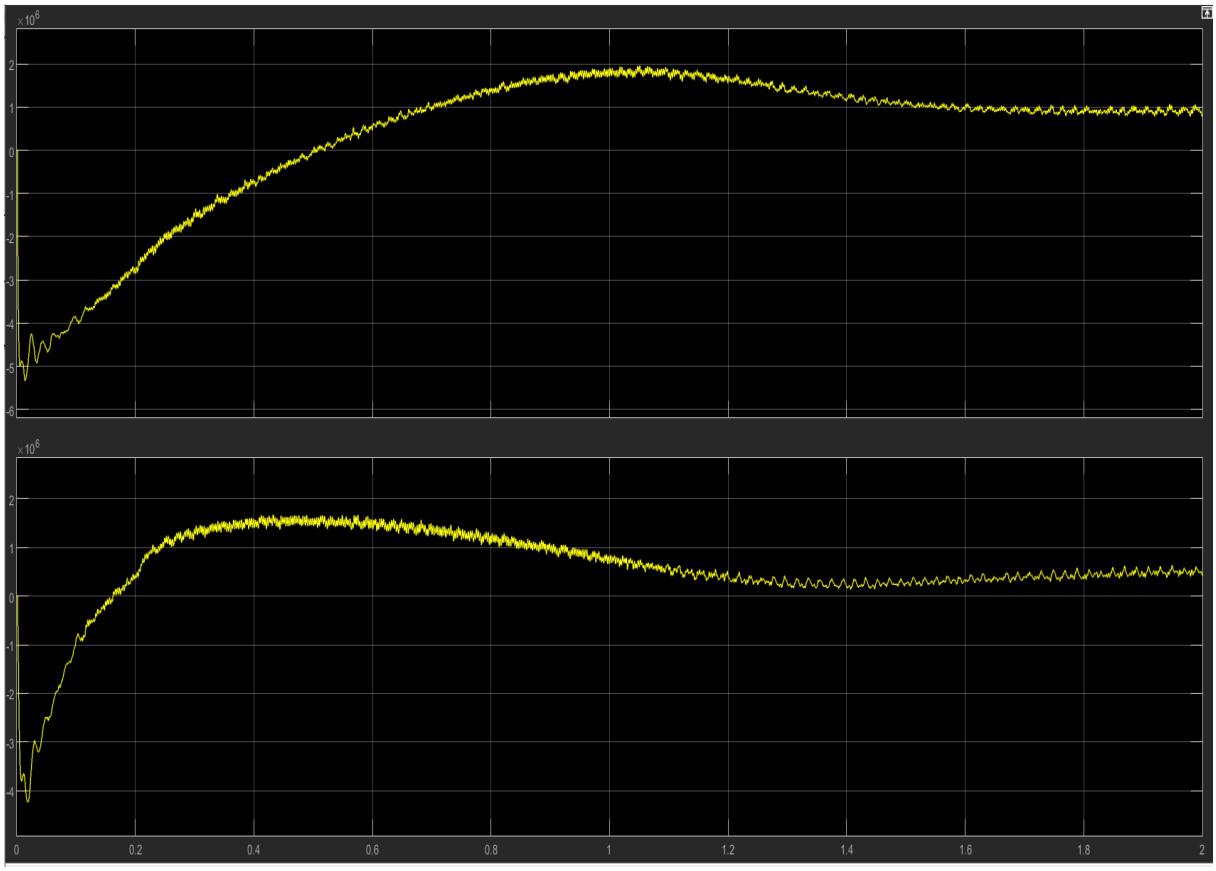

Figure 6.15 active and reactive power from the inverter.

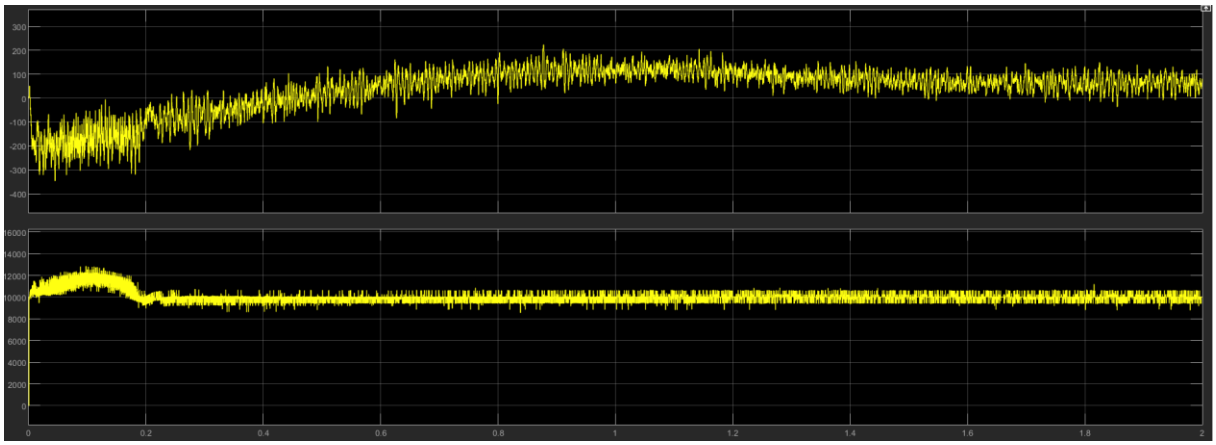

Figure 6.16 DC voltage and current.

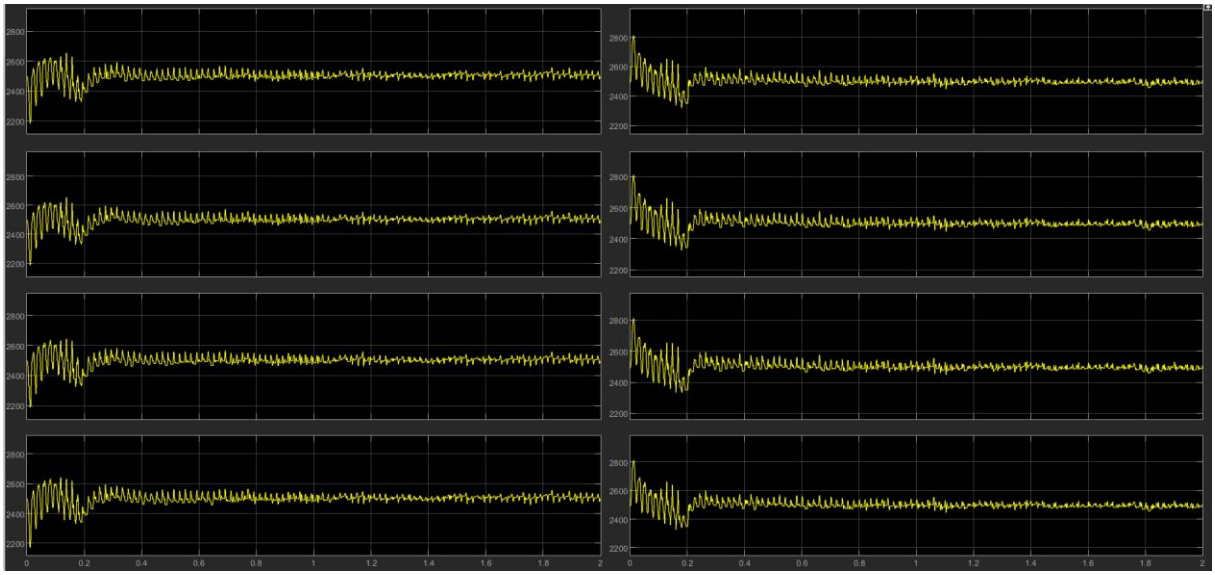

Figure 6.17. Capacitor voltages

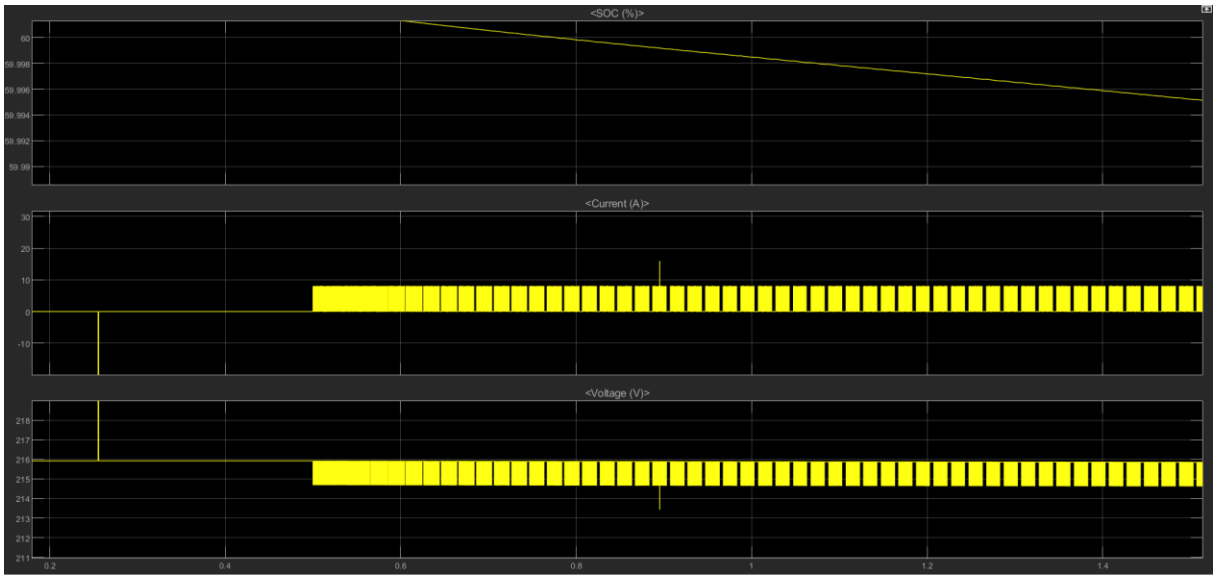

Figure 6.18. SC SOC, voltage and current.

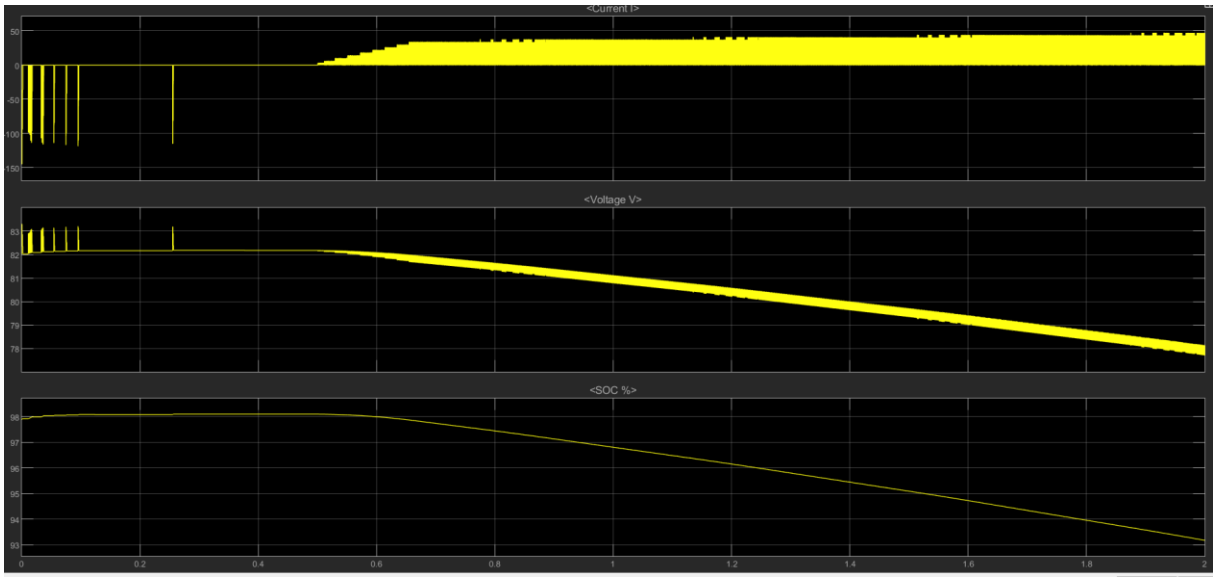

Figure 6.19. Battery current, voltage and SOC.

We see clearly that the delay worked. The battery and SC are mostly turned off during the delay, while quickly ramping up the contribution when the delay is over.

6.1.4 Surplus power to inverter, charging HESS.

Here the energy storage system will be charged. The generator will produce a surplus, while the power requested from the SMs will be negative. Here the effect on the power from the

inverter, the DC current and voltage and the SOC of batteries and SCs is of interest. This is to confirm that the HESS will recharge when instructed to.

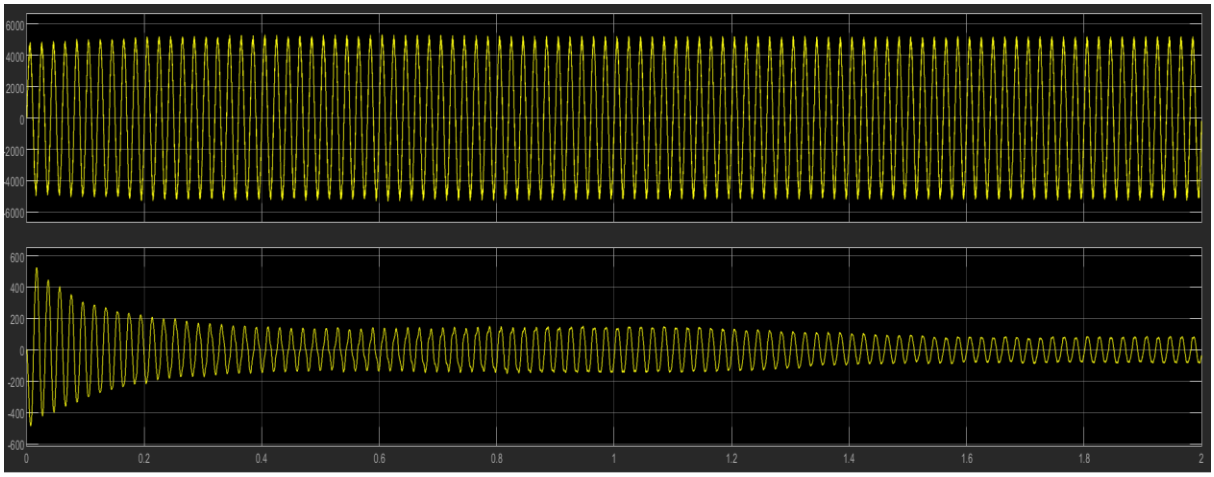

Figure 6.20 AC voltage and current

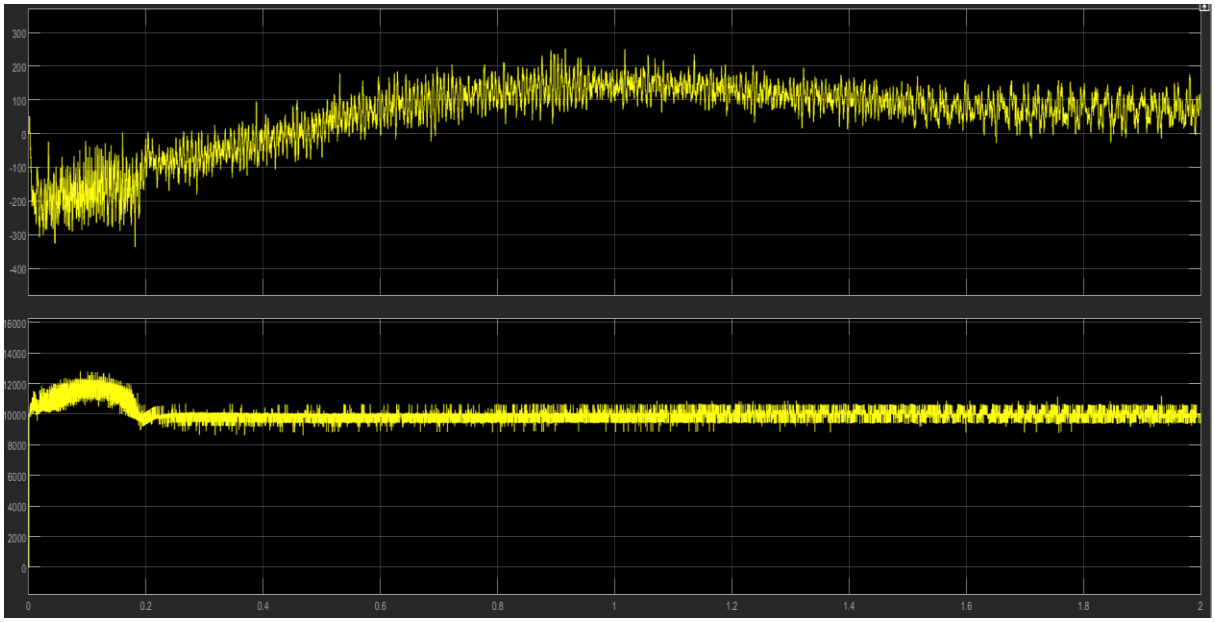

Figure 6.21 DC voltage and current

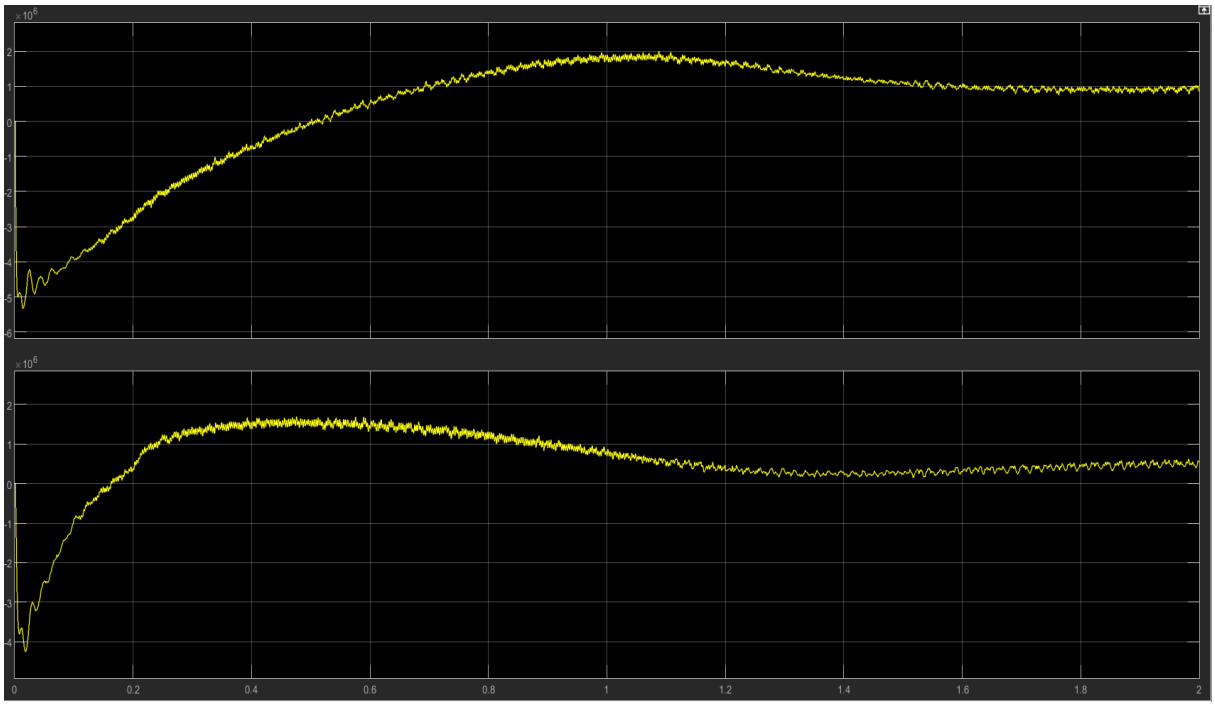

Figure 6.22 Active and reactive current

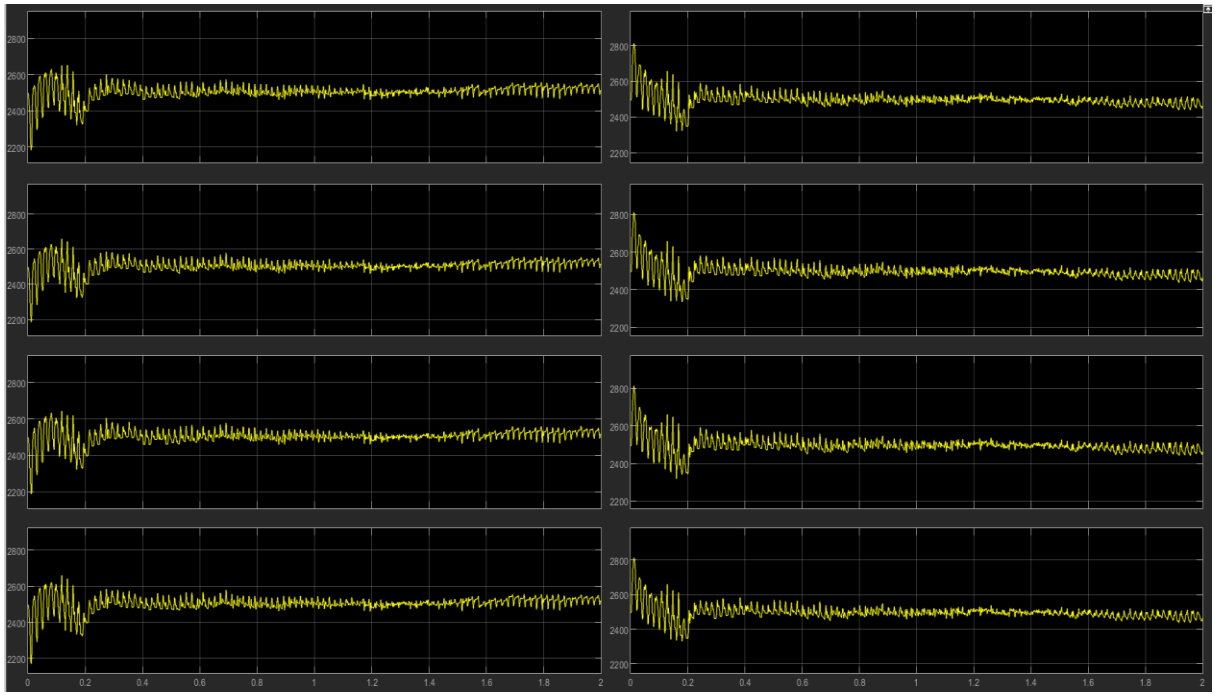

Figure 6.23 Capacitor voltages

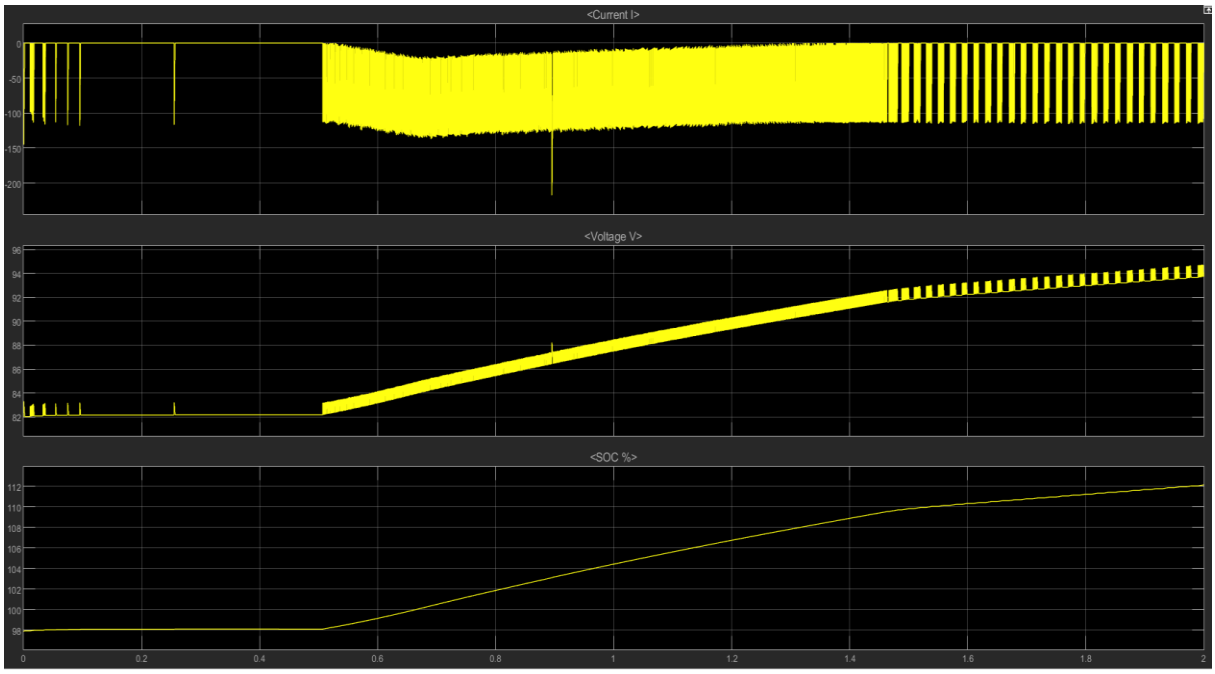

Figure 6.24 SC current, voltage and SOC

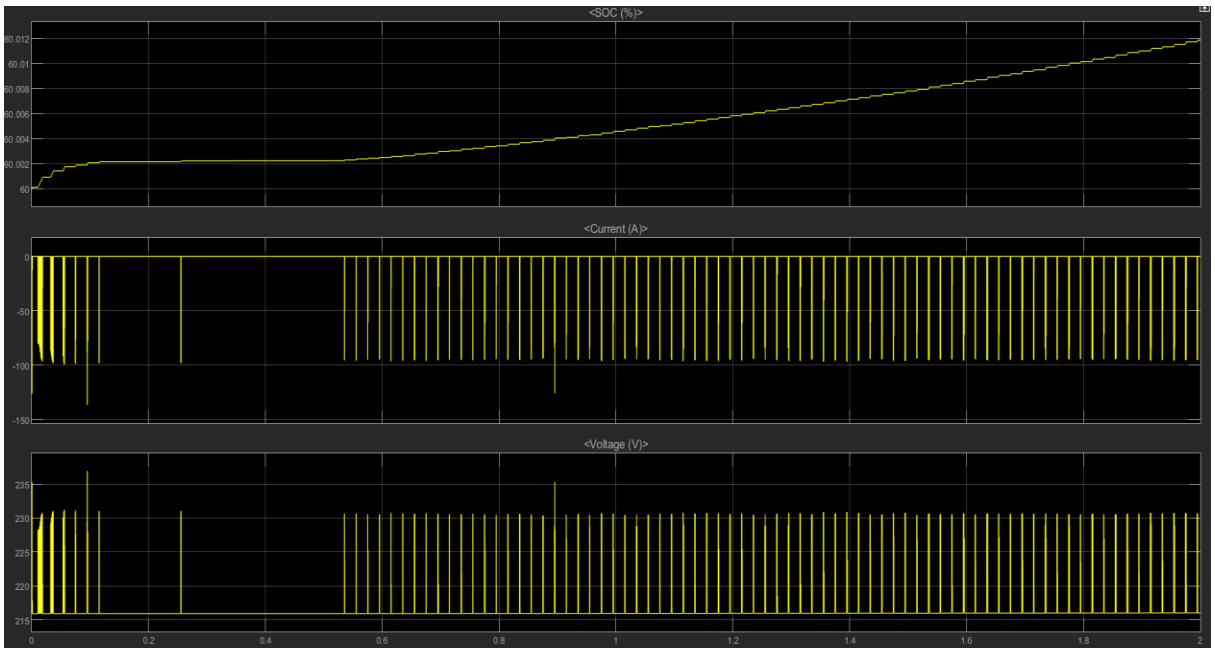

Figure 6.25 Battery SOC, current and voltage

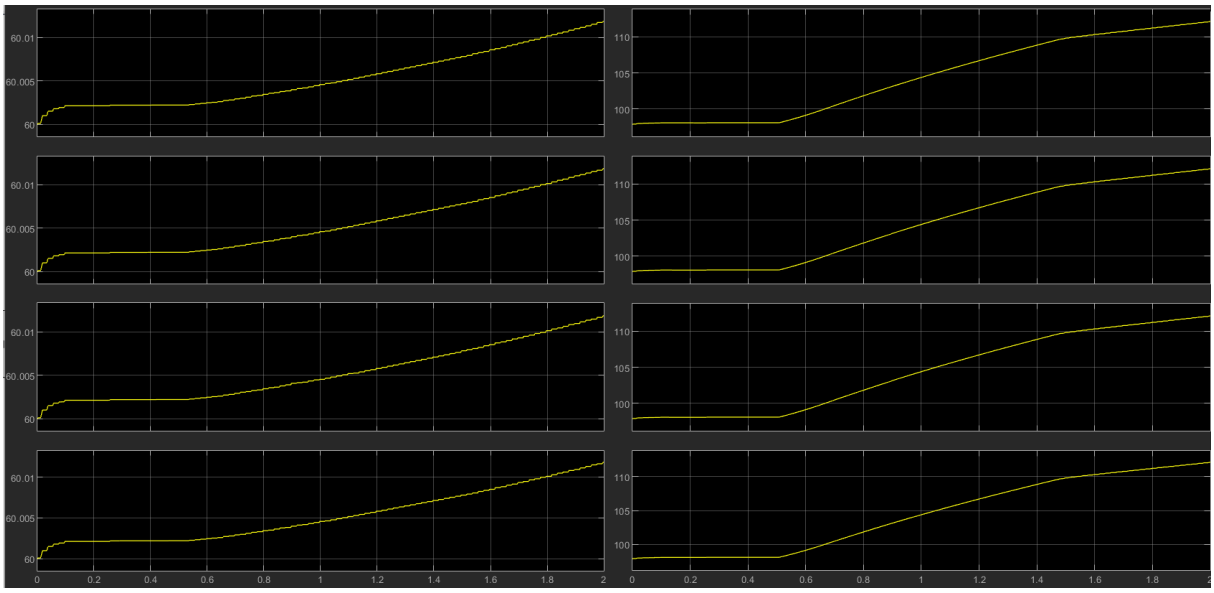

Figure 6. 26 HESS SOC

7 Discussion

7.1.1 Comparisons of the scenarios:

To draw a conclusion, it is vital to compare results to find the best solution or at least the effects the different scenarios have on the system.

7.1.1.1 DC voltage and currents.

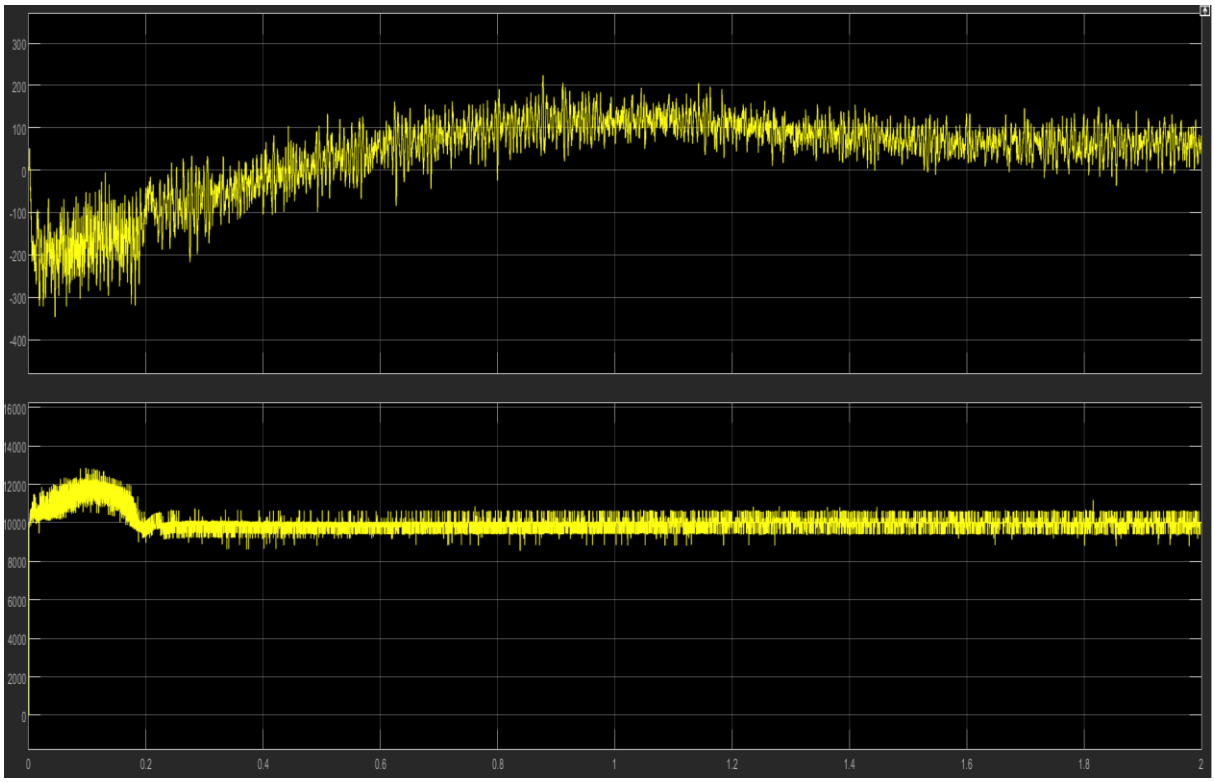

Delayed contribution

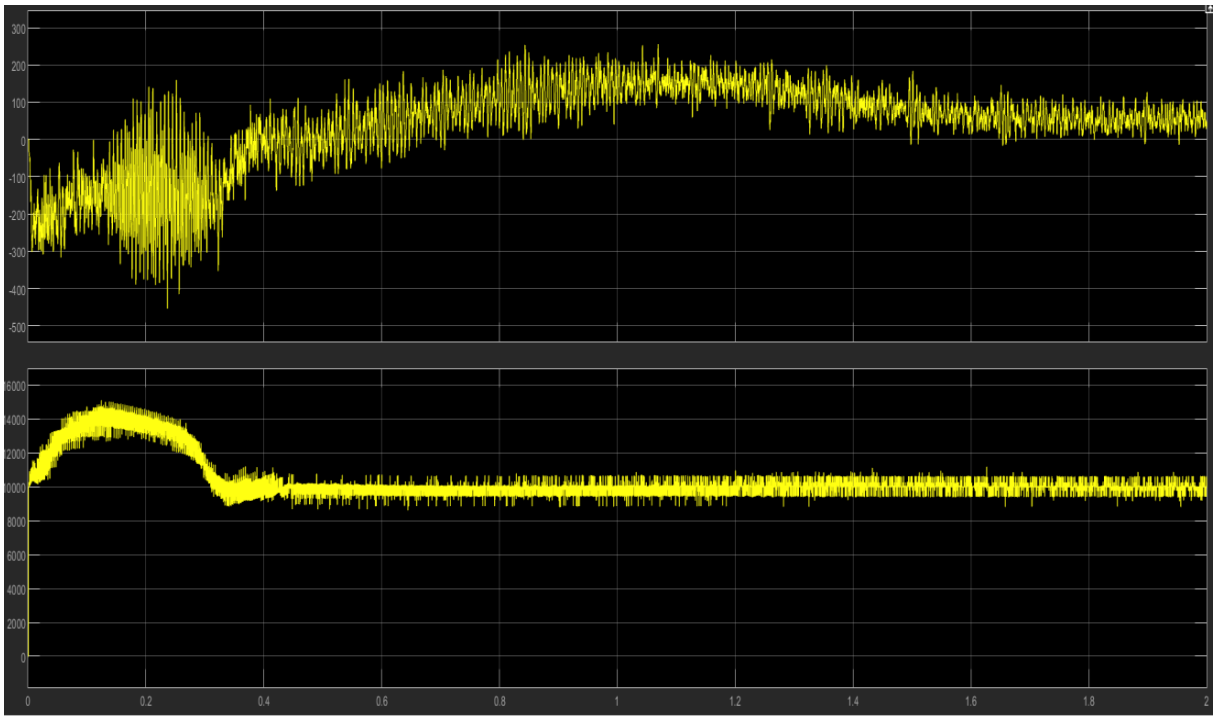

Constant contribution

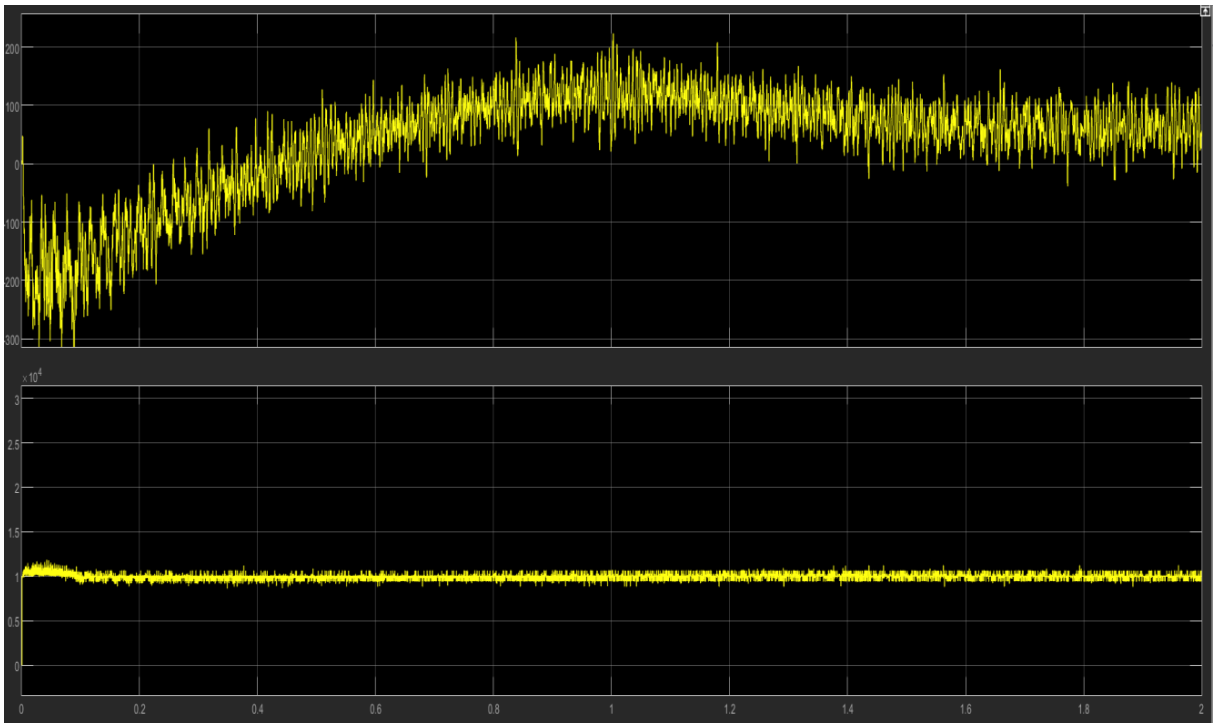

No contribution

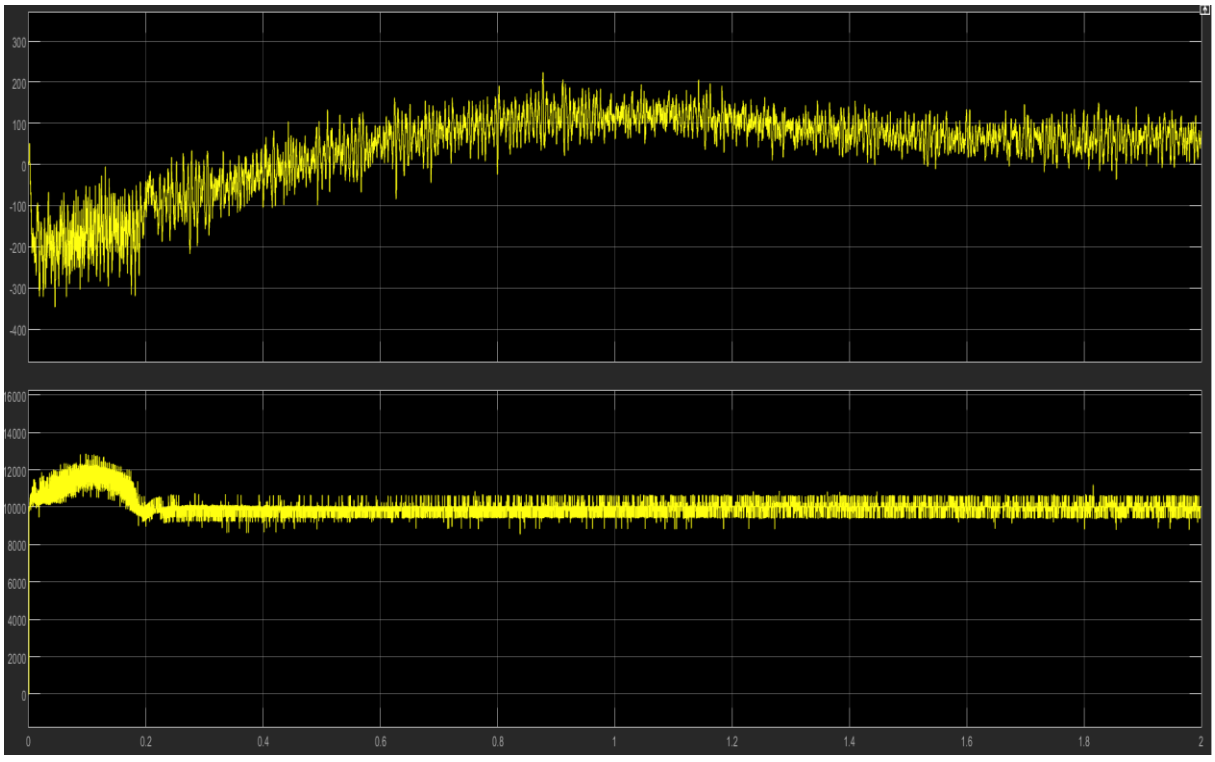

Absorption of power

The DC voltages all settle quickly. The difference between the scenarios is that the no contribution-scenario is faster than all the others, note that the measurement y-axis values are

different. The delayed contribution scenario is very similar to the no contribution-scenario, with a possibly slightly lower DC current at the end, which makes sense considering the HESS covers 5% of the power output.

With a higher percentage of HESS power coverage, the difference could be more noticeable.

The difference is slightly more noticeable between the absorbing scenario and the delayed contribution scenario.

With constant DC voltage the only variable for power transmission over the HVDC line would be the current, so a lower DC current means a lower amount of power is drawn from the rectifier.

7.1.1.2 Active and reactive power.

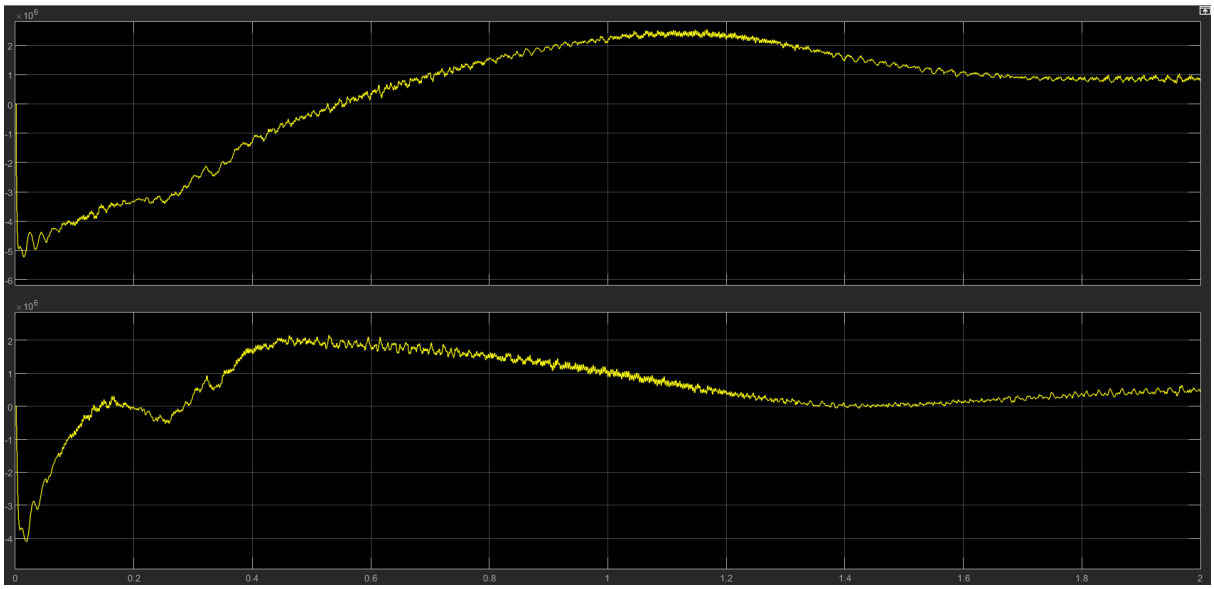

Instant contribution

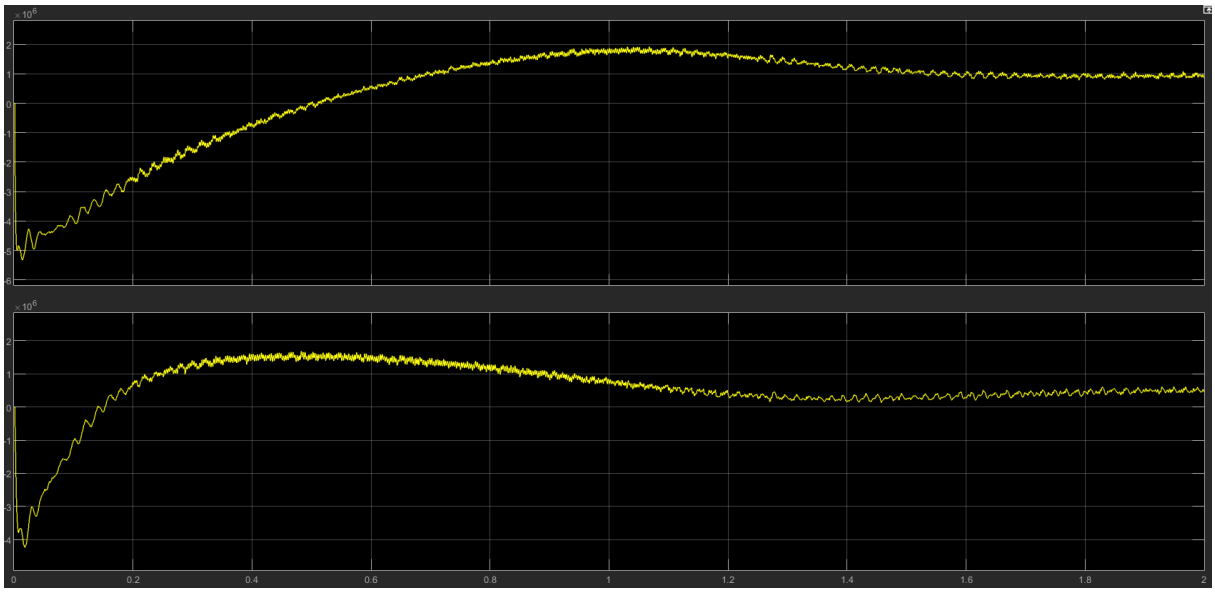

No contribution

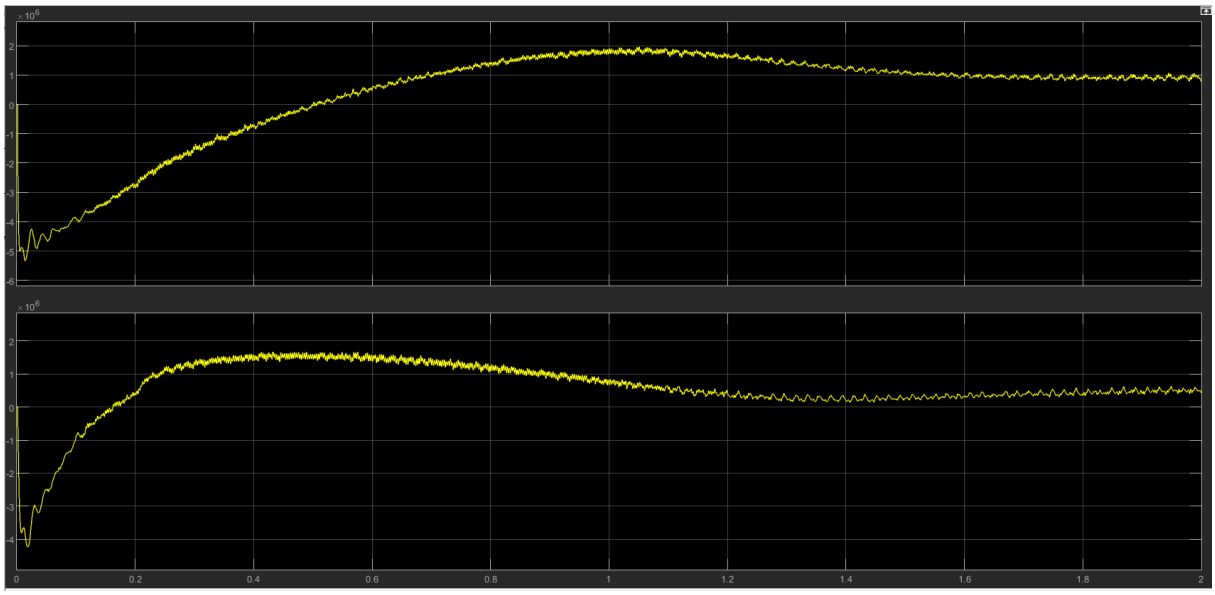

Delayed contribution

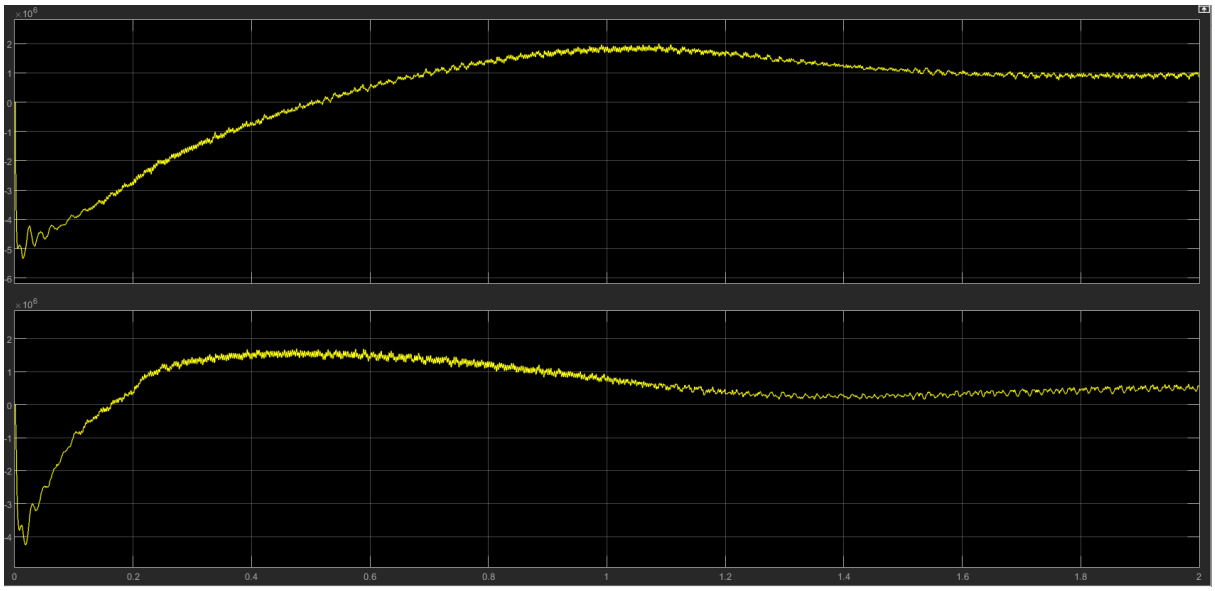

absorption

Here we clearly see the difference if the HESS is active from the beginning. The instant contribution curve is bent and slower to settle. The other 3 curves are very similar with little few differences between them. All scenarios end up at the correct output eventually, so the controllers are fully capable of correcting any added/missing power contributed by the HESS when the generator is not in a deficit/surplus situation.

7.1.2 Increased, delayed contribution and absorption from HESS

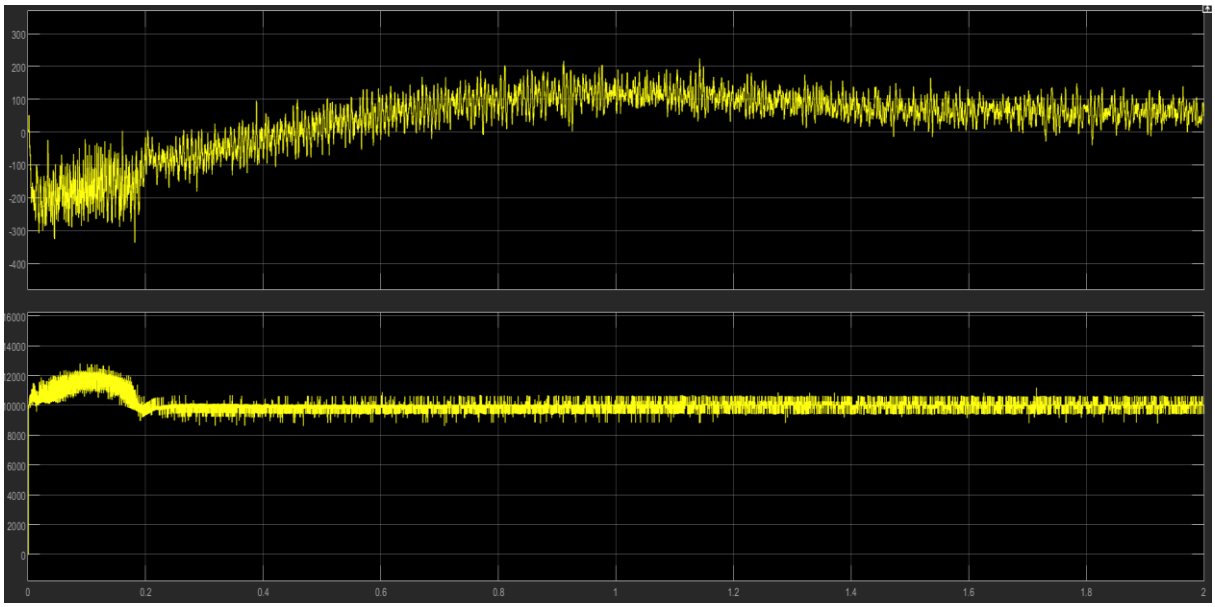

Figure 7.1 DC voltage and current at 120KW HESS contribution

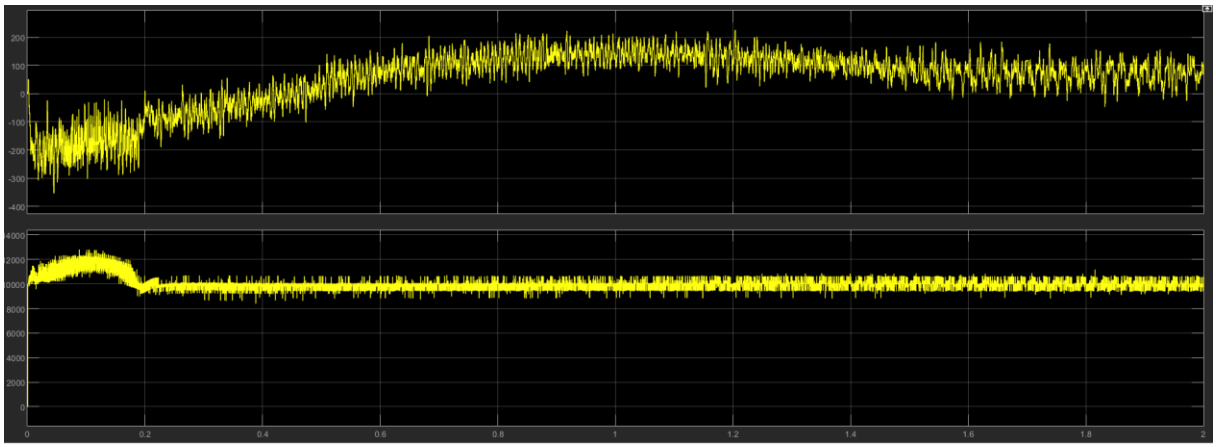

Figure 7.2 DC voltage and current from 120KW HESS absorption

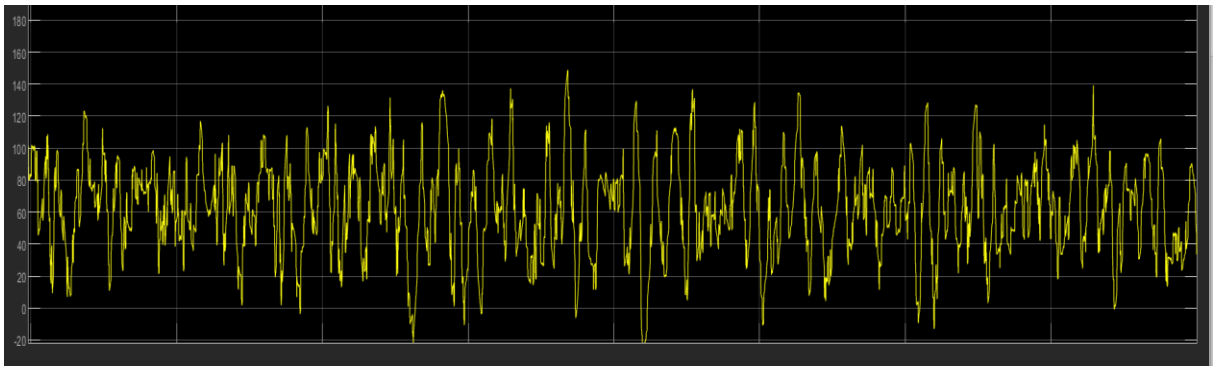

Figure 7.3 DC current close-up at 120KW HESS contribution

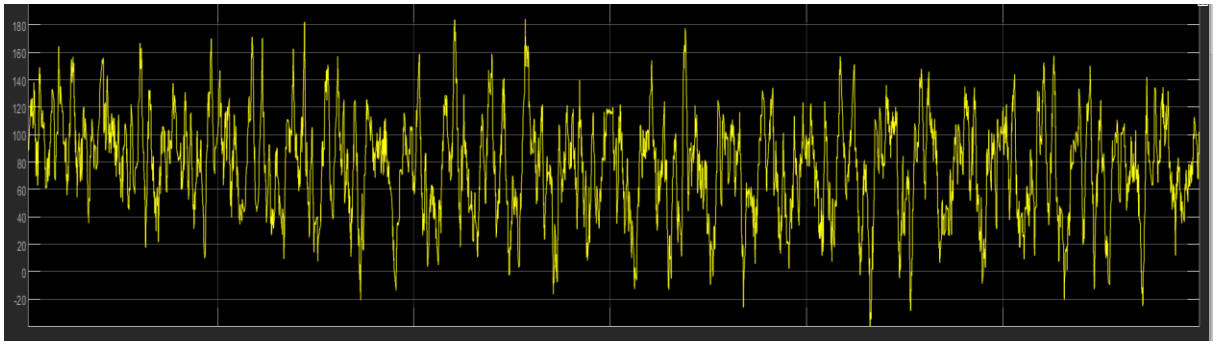

Figure 7.4 DC current close-up at 120KW HESS absorption

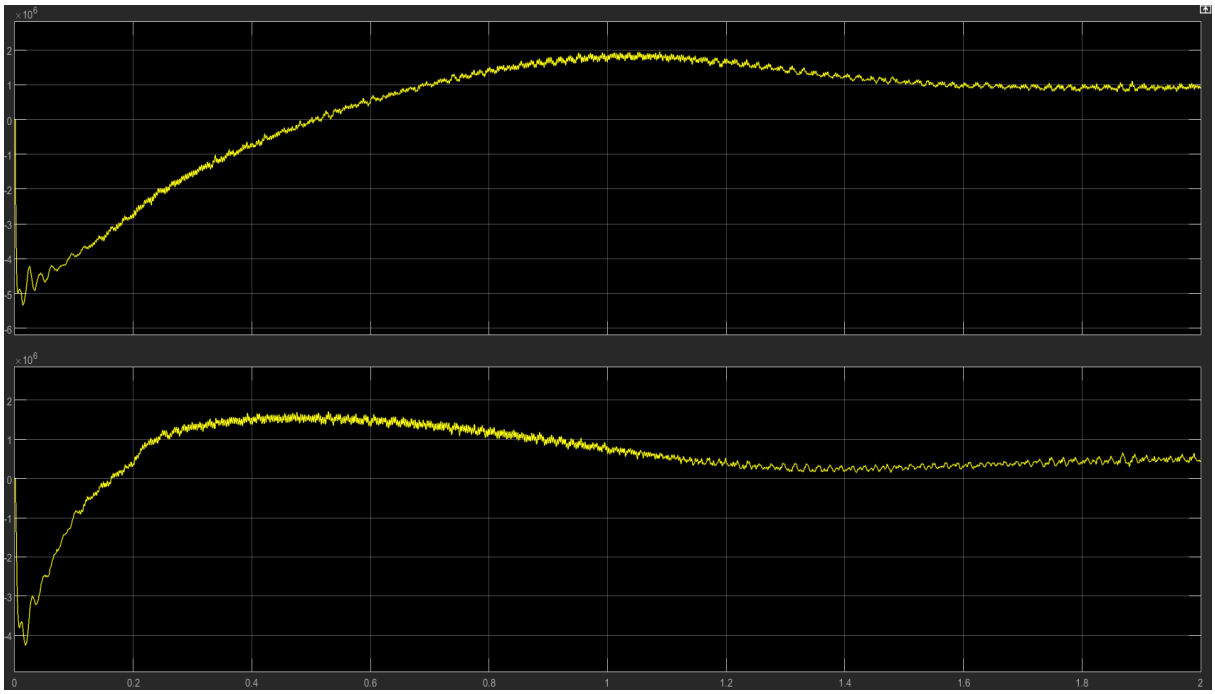

Figure 7.5 P-Q at 120KW HESS contribution

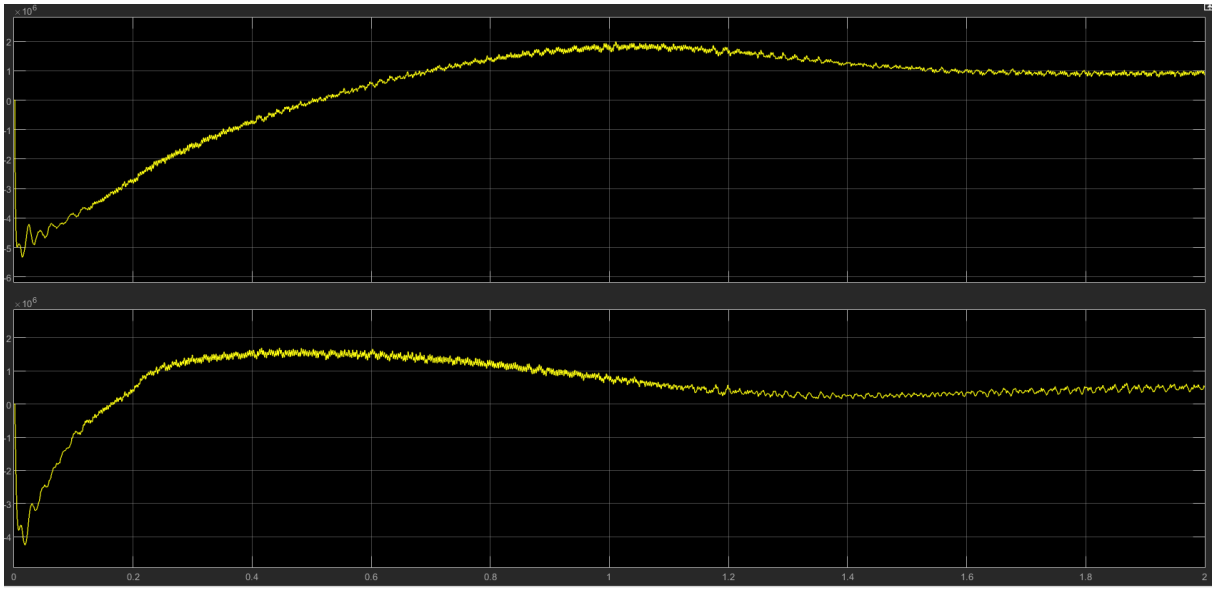

Figure 7.6 P-Q at 120KW HESS

The P-Q curves show little difference in output, which means that the inverter control system is successful in balancing the different impacts of the 120KW of HESS absorption/contribution, the close-up of the DC current show a clear difference in how much power is delivered to the inverter in contrast to the near identical power outputs of the inverter.

8 Conclusion

The hybrid energy storage system is working. The different scenarios have very similar results except for the constant contribution scenario, which was not a huge surprise since it disturbs the system when it is the most vulnerable. The reason for the lack of clear differences was probably that the scale of the HESS was too small.

The results from the original scenarios were inconclusive. But the scenarios with a higher in/output from the HESS show quite clearly that the HESS can contribute to the grid and reduce/increase the power taken from the HVDC line, which in this case comes in the form of reduced/increased HVDC currents.

The reduced need for current in the case of a contributing shows that the HESS can be used as a buffer for the intermittent nature of wind power, though the system of this thesis is too small to make a noticeable difference within nominal parameters. Considering physical MMCs tend to have over a 100 SMs the increase in storage capacity and power output for the HESS would not necessarily be costly in terms of more expensive storage devices, but rather in the number of devices needed. An MMC with a share of the submodules with energy storage capability is an alternative option if a 100% share of SMs with energy storage capabilities is unnecessary or too expensive for the benefits.

It is the authors belief that the submodule with energy storage system can make a positive impact on introducing a higher share of renewable energy sources like offshore wind parks without damaging grid stability due to the intermittent nature of wind power.

9 Authors contribution

Authors contribution in this simulation is modifying the MMC inverter submodules to incorporate the HESS and designing the HESS. The main connecting two different MMC converters together to form a complete HVDC line from the energy source to the grid.

Another contribution is the design and implementation of the HESS balancing scheme into the inverter arms to eliminate imbalances which could affect capacitor balancing if the HESS in a SM is unable to contribute.

Small modifications were needed on the inverter MMC to include it in the HVDC line instead of relying on an ideal voltage source.

10 Acknowledgements

The simulation and thesis would not have been possible without co-supervisor Umer Sohails contributing working MMC models with VSC and P-Q controls for use in the simulation as well as invaluable advice and direction.

I would also like to thank student Rolf Olaf Mikkelsen and Fredrik Vatshelle for all the help and motivation they have provided me. Hopefully they can say the same for me.

11 Future work

Suggestions for future work:

- The HESS is currently operating on a manual input for power in/output. Devising a way to automate this by comparing output power from the inverter and grid requirements would be highly beneficial.
- Physical small-scale tests of simulation.
- Rescaling for typical windfarm power scale and faster settling times.
- Implementation of the SOC limitation on the batteries.
- Test higher HESS power coverage.

Appendix

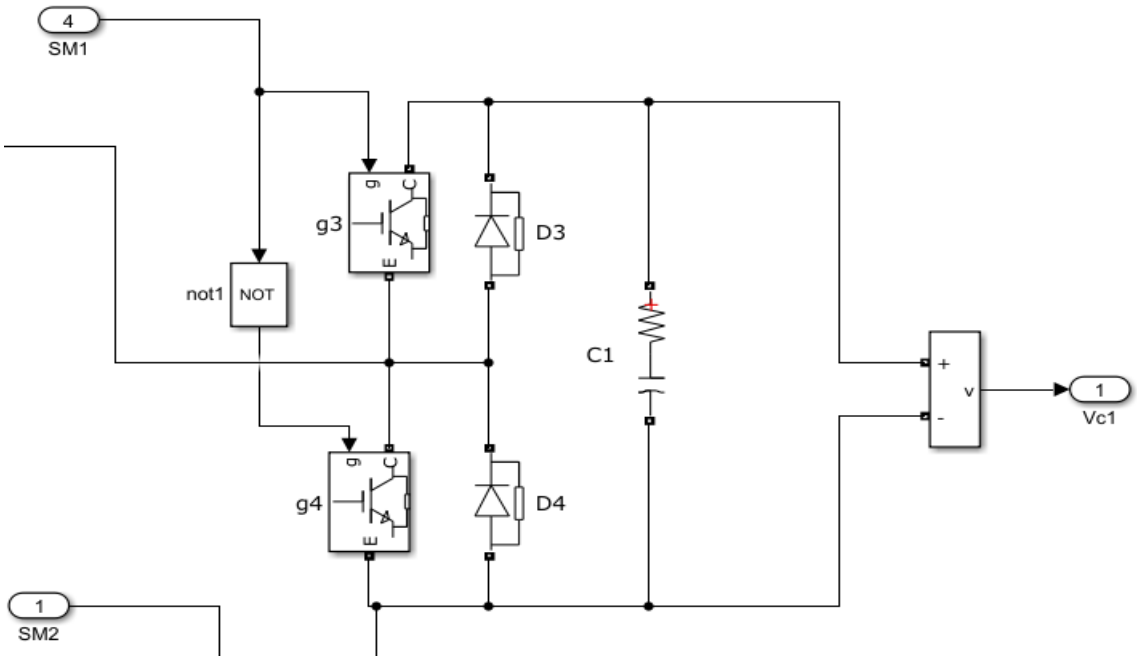

Rectifier submodule

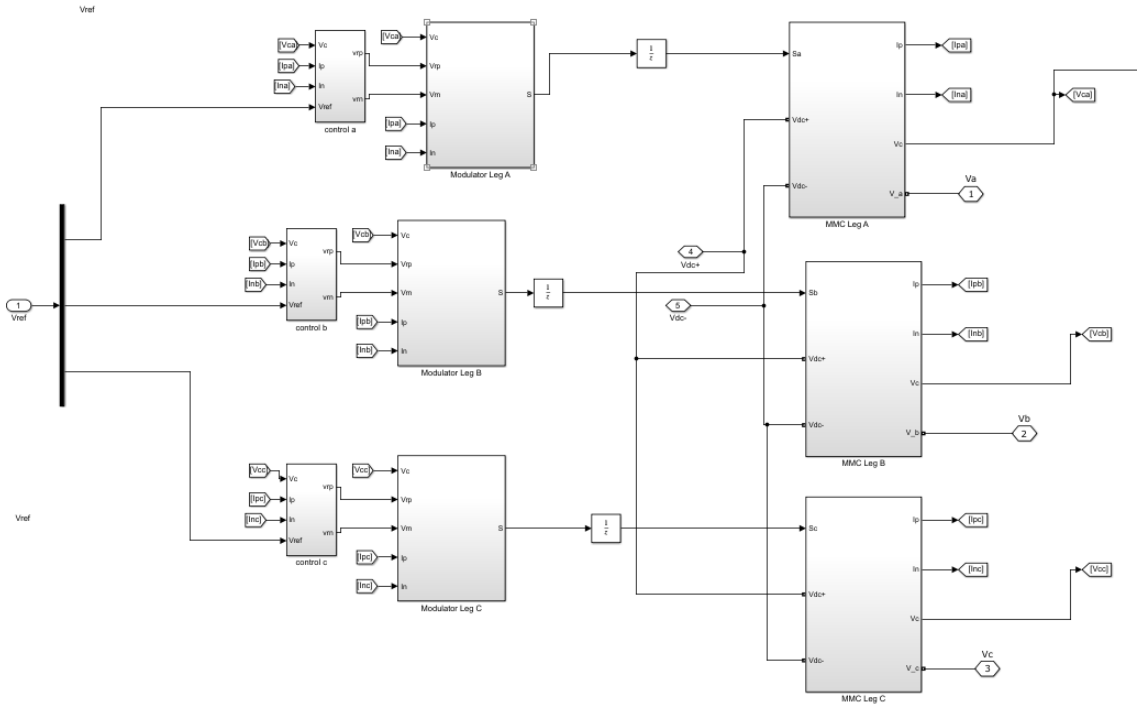

MMC simulation, rectifier

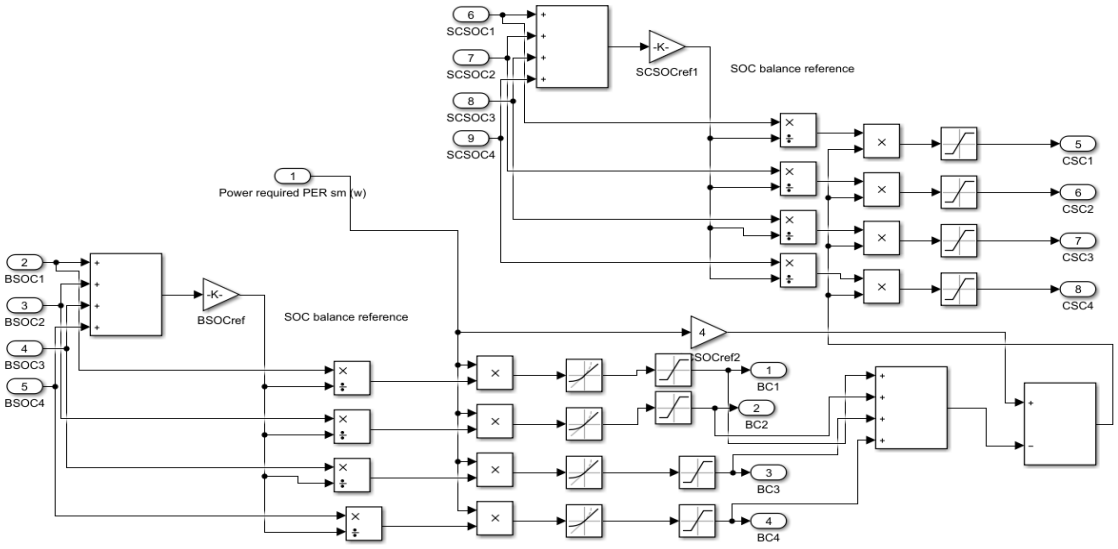

Battery and supercapacitor balancing system.

```
function y=sortvc(x)
i=x(1);
a(1)=x(2);
a(2)=x(3);
a(3)=x(4);
a(4)=x(5);
b=[1 a(1);2 a(2);3 a(3);4 a(4)];
c=sortrows(b,2);
if i>=0
y(c(1,1))=1;
y(c(2,1))=2;
y(c(3,1))=3;
y(c(4,1))=4;
else
y(c(4,1))=1;
y(c(3,1))=2;
y(c(2,1))=3;
y(c(1,1))=4;
end
end
```

Sorting function for capacitor voltages

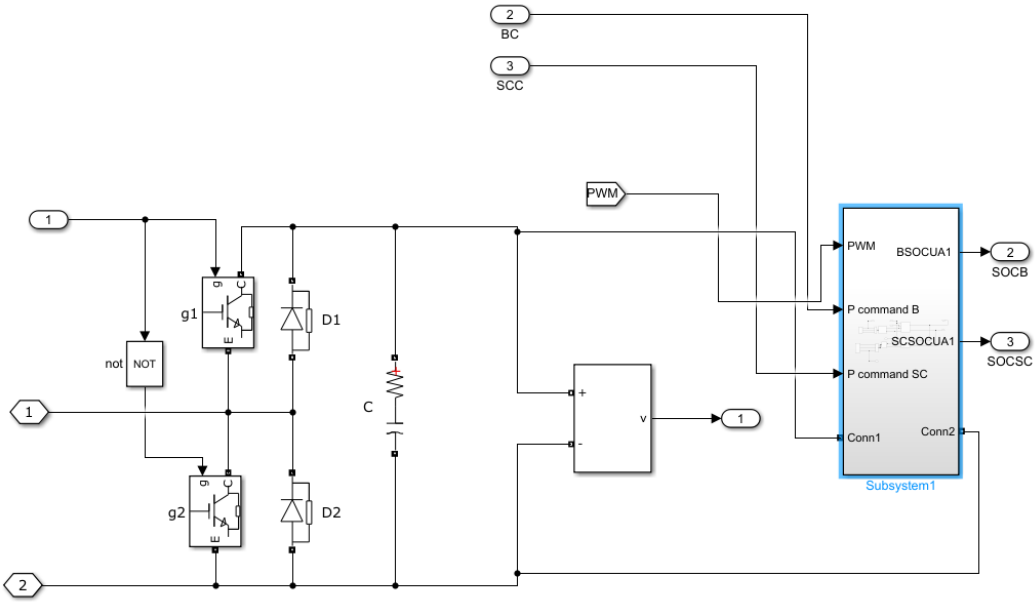

Inverter submodule with incorporated HESS.

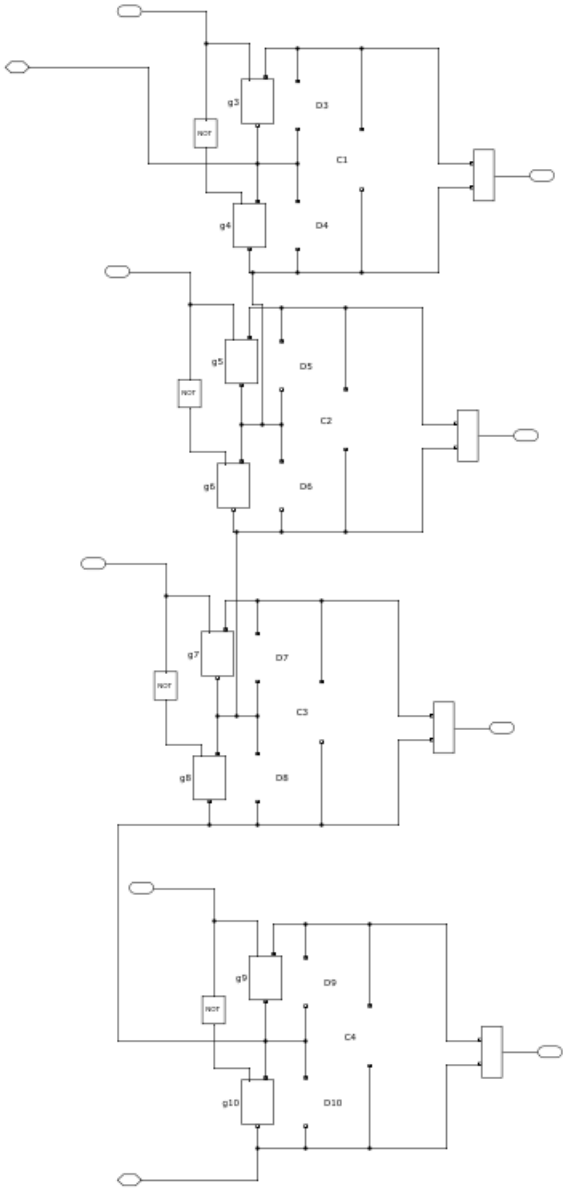

Rectifier phase arm

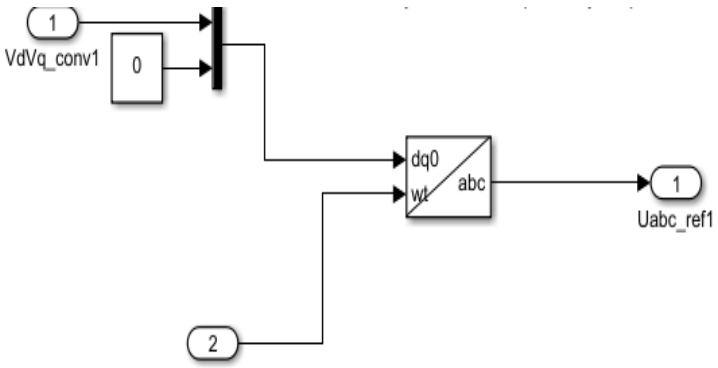

Dq0 to abc voltage reference transform VSC

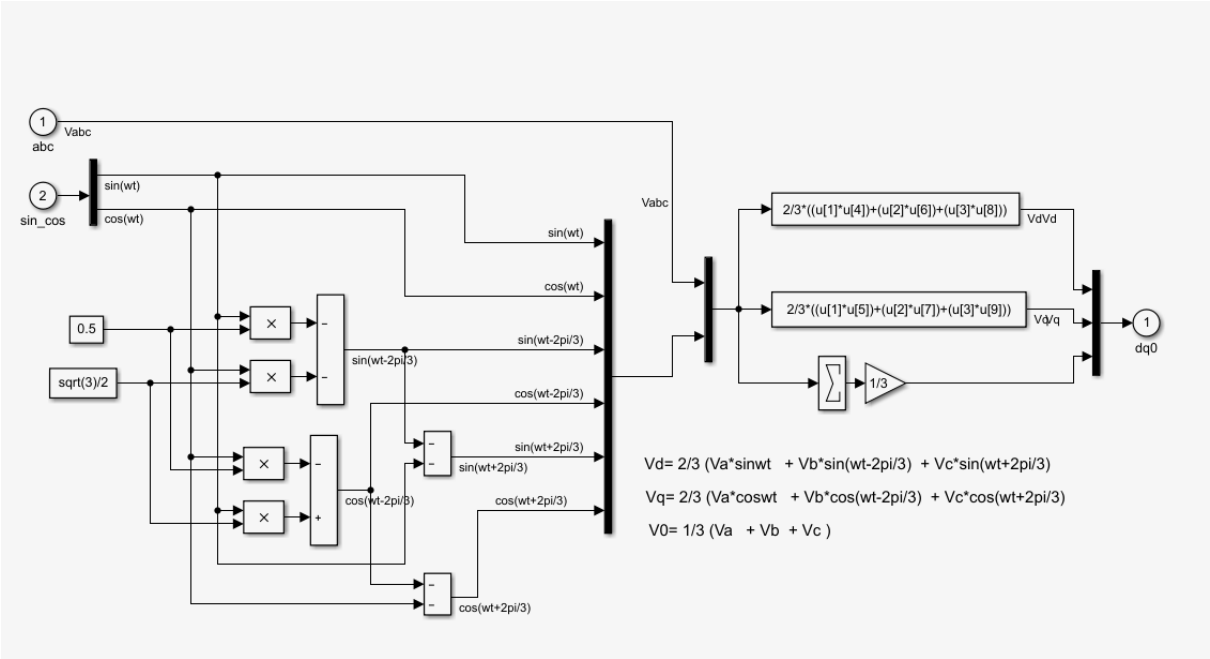

Voltage dq0 transformation

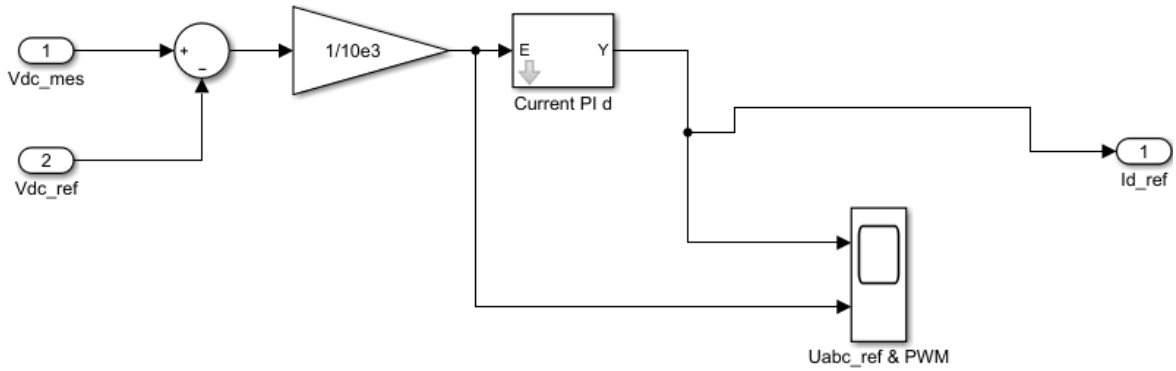

DC voltage regulator VSC

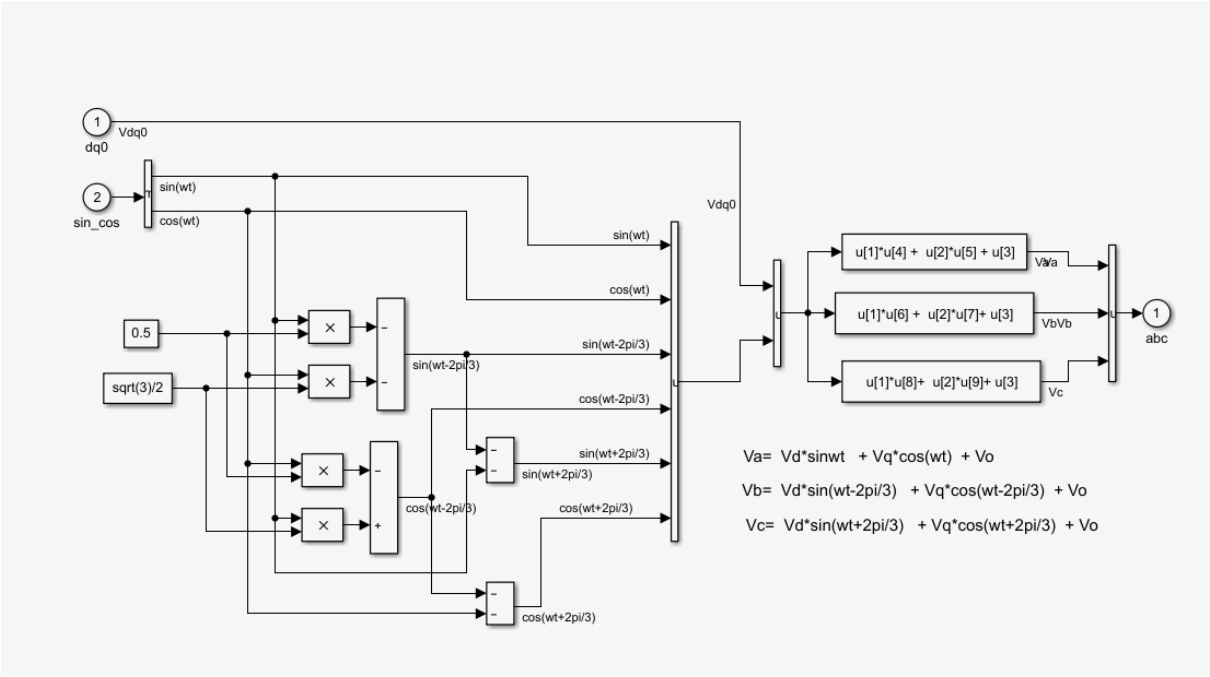

V_{dq0} to V_{ref} transform

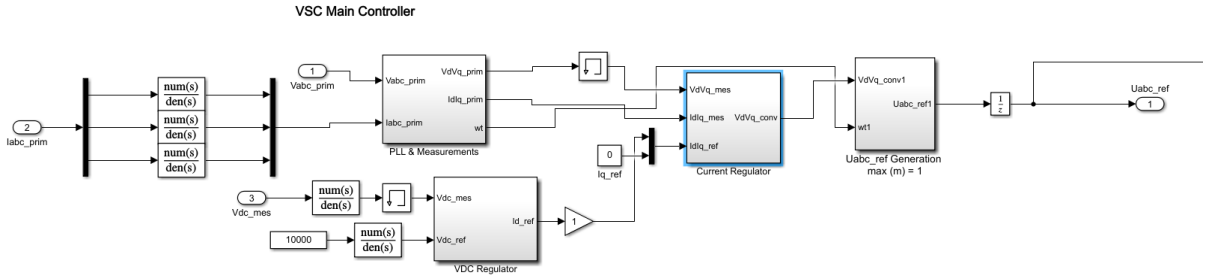

VSC controller

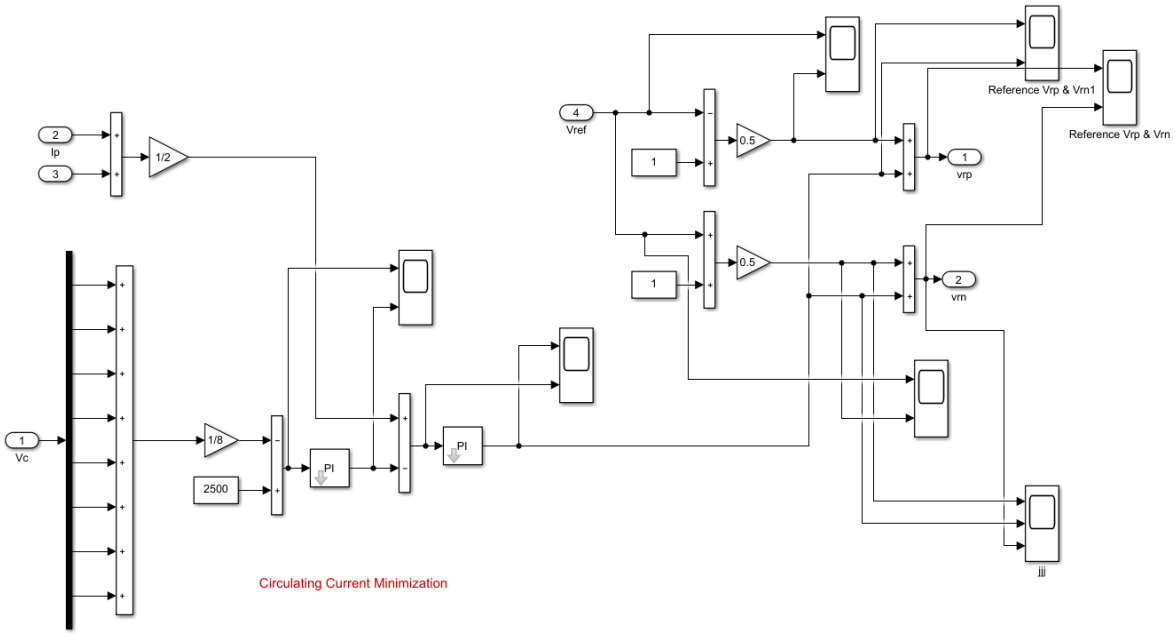

Circulating current minimization and Vref distribution between positive and negative arms

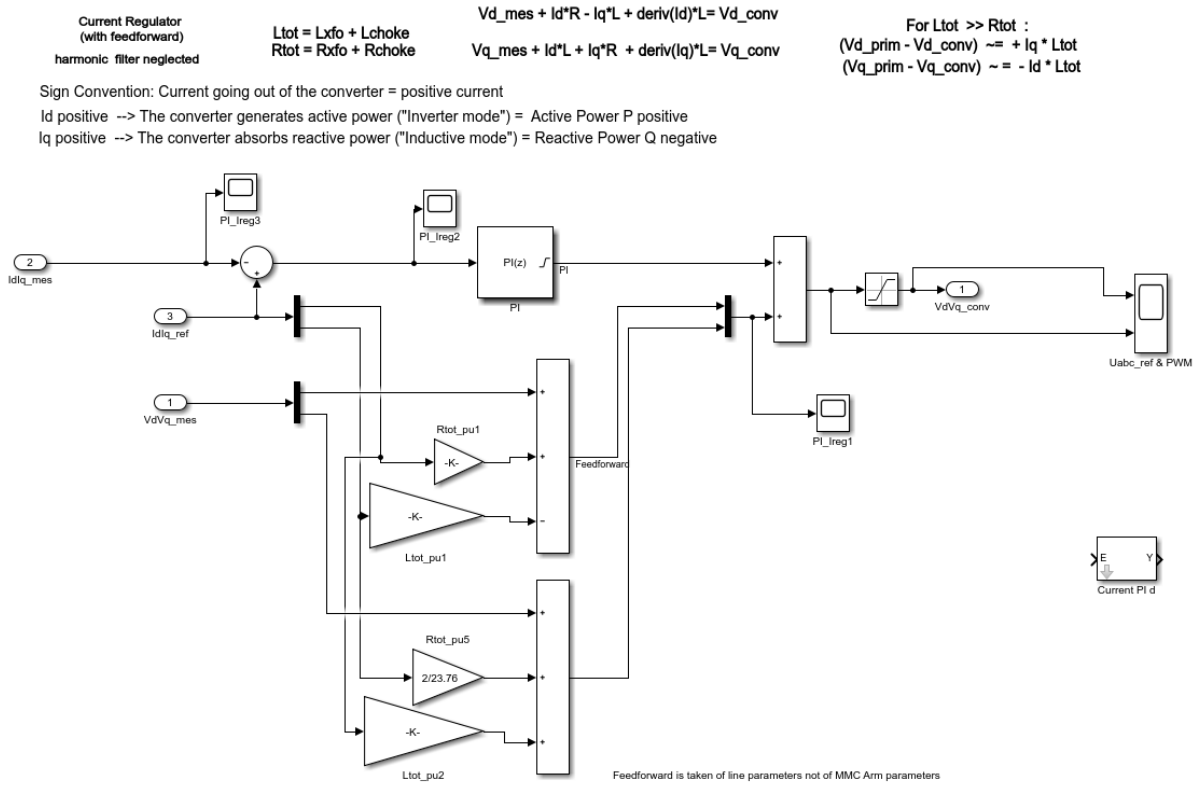

VSC current regulator

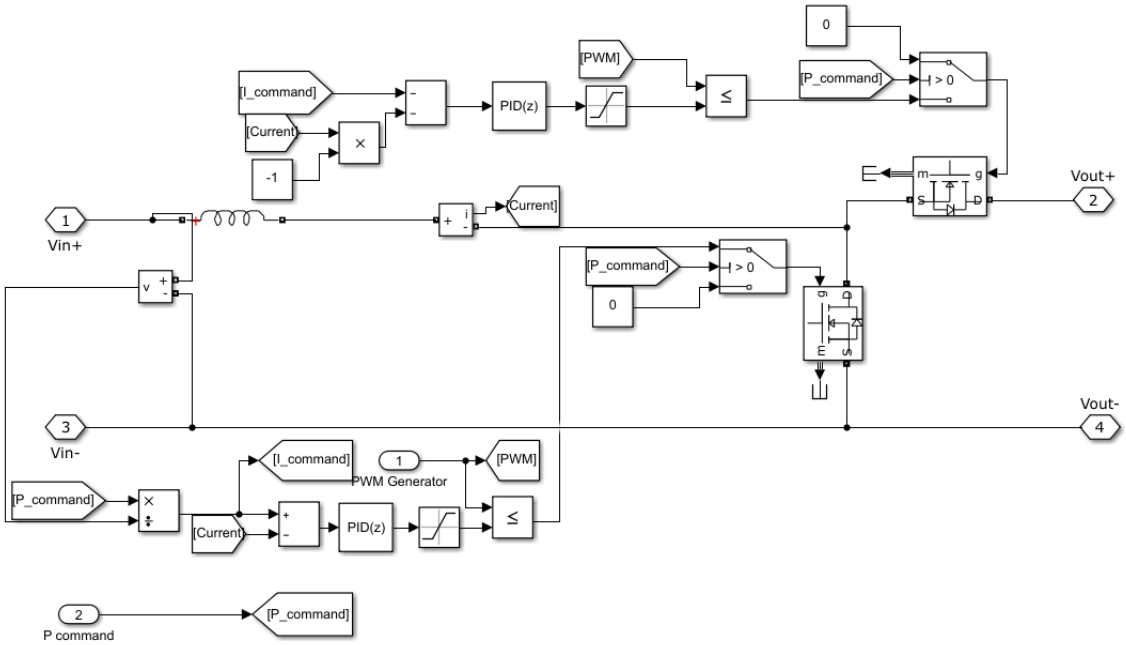

Buck/boost converter

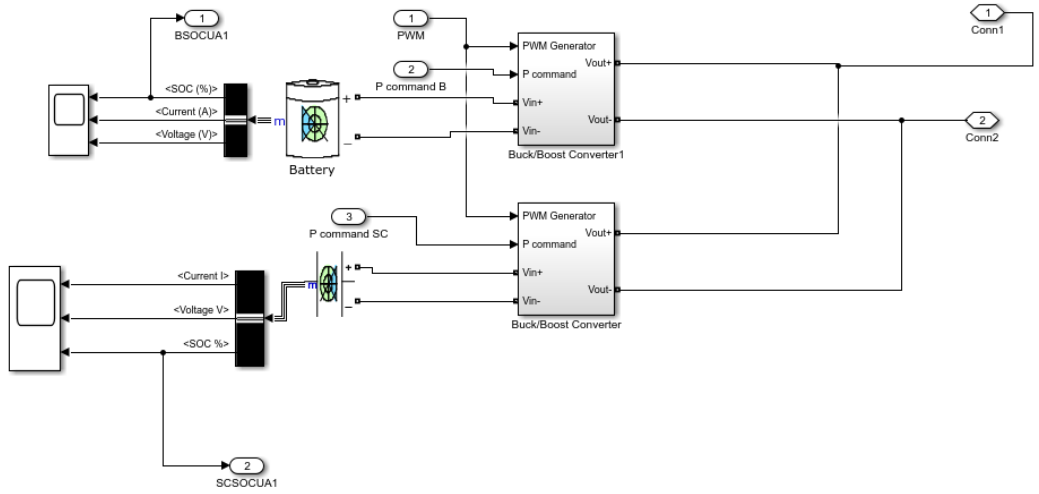

HESS

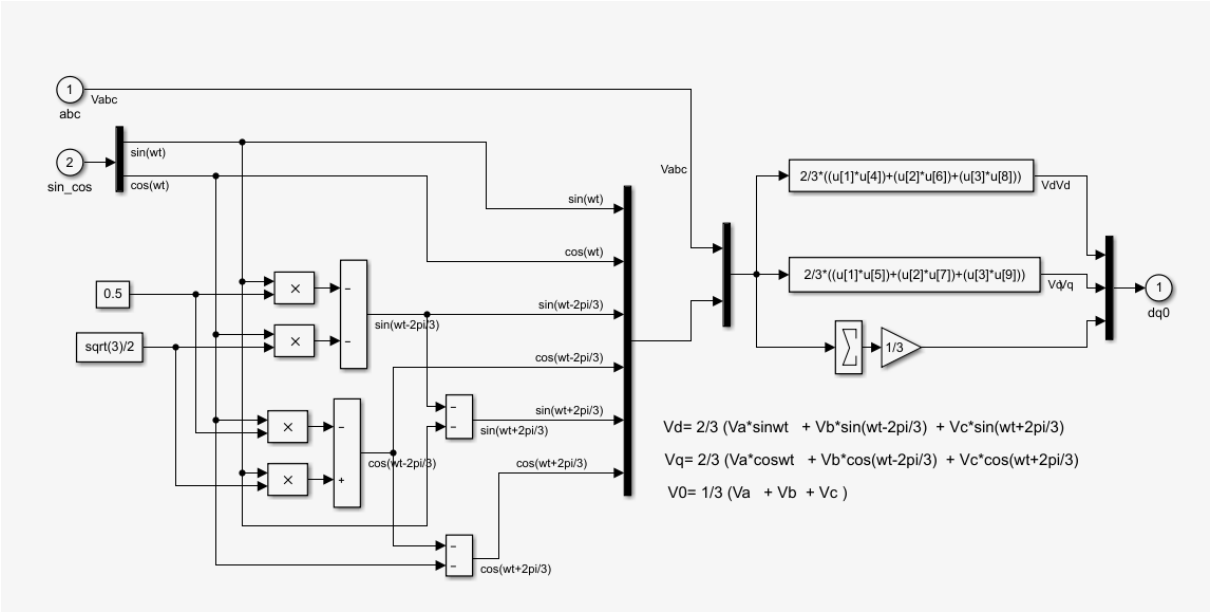

Iabc to Idq0 transformation (not voltage)

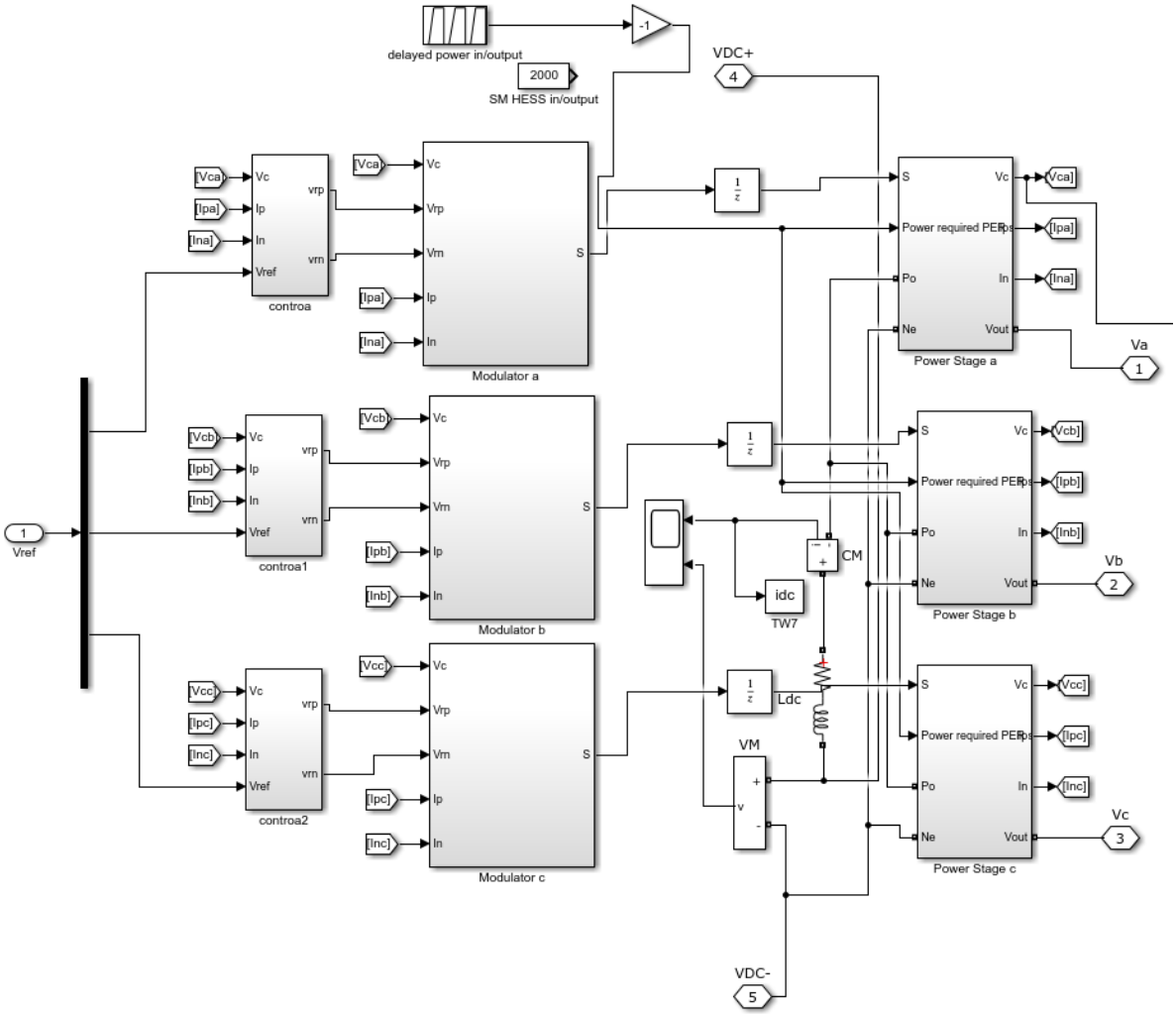

Inverter MMC. Notice the HESS power input per submodule

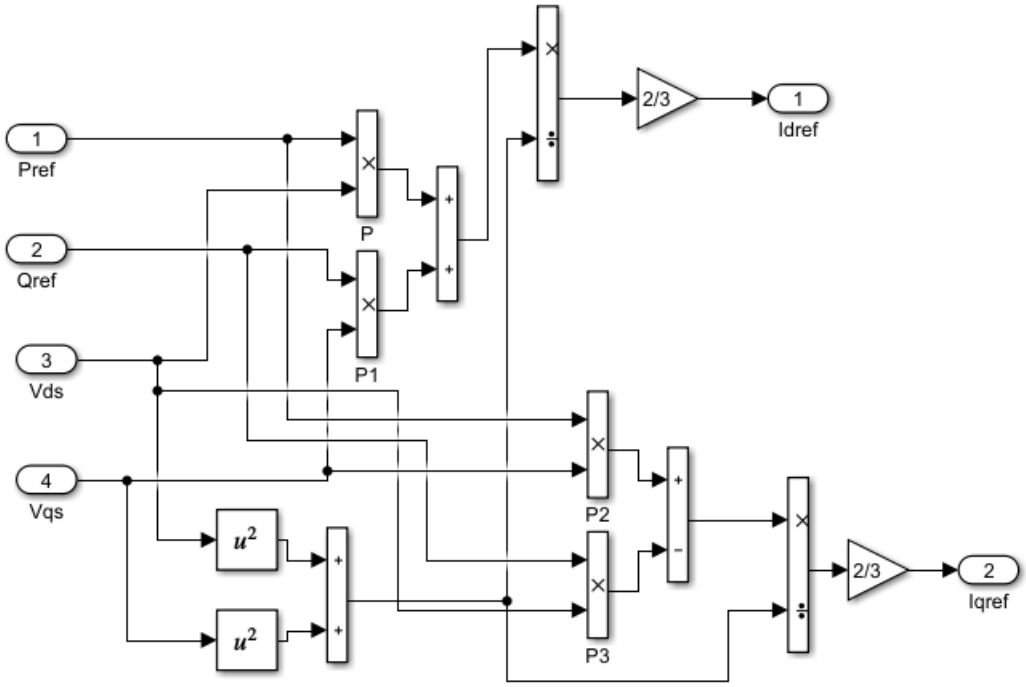

Ipqref calculation

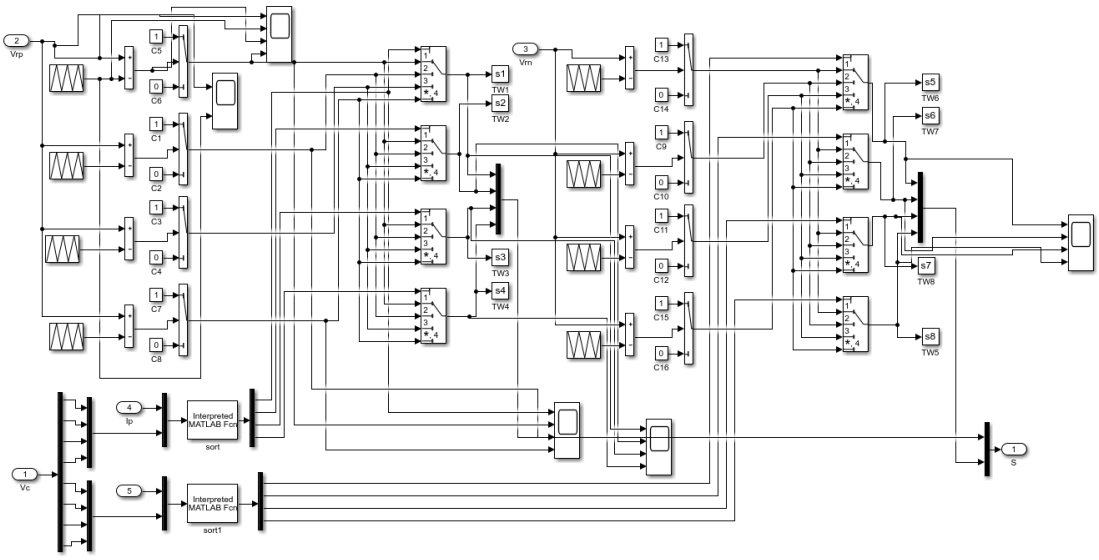

MMC modulator

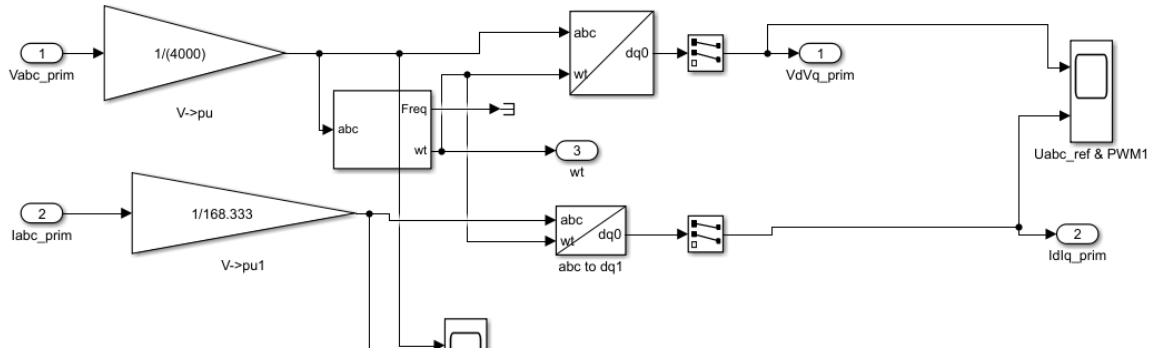

PLL measurements VSC

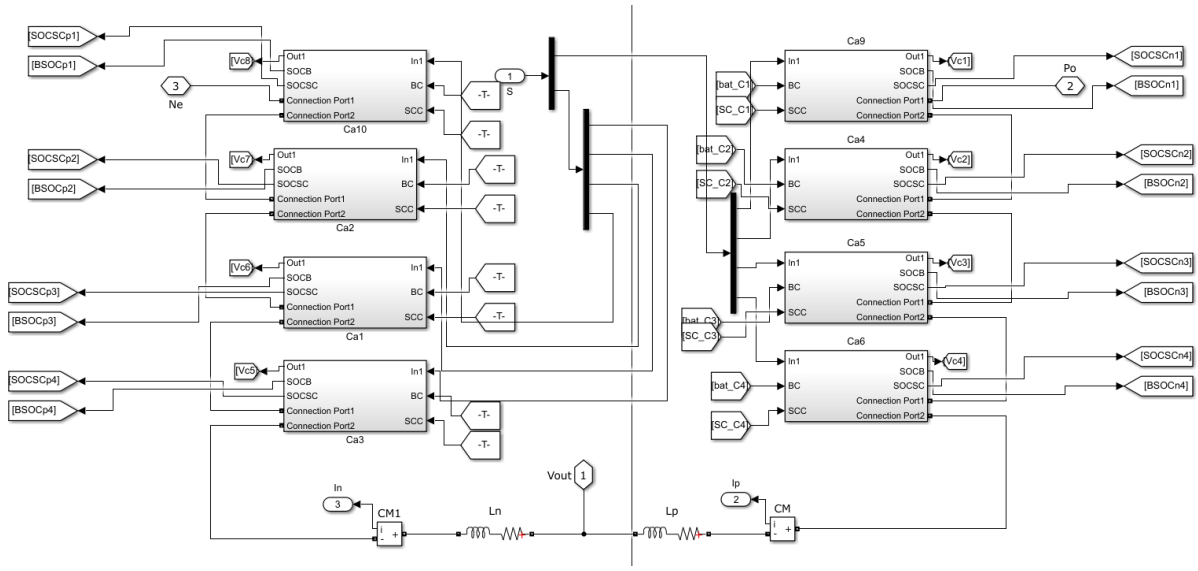

Inverter phase submodules. Positive SMs on the right

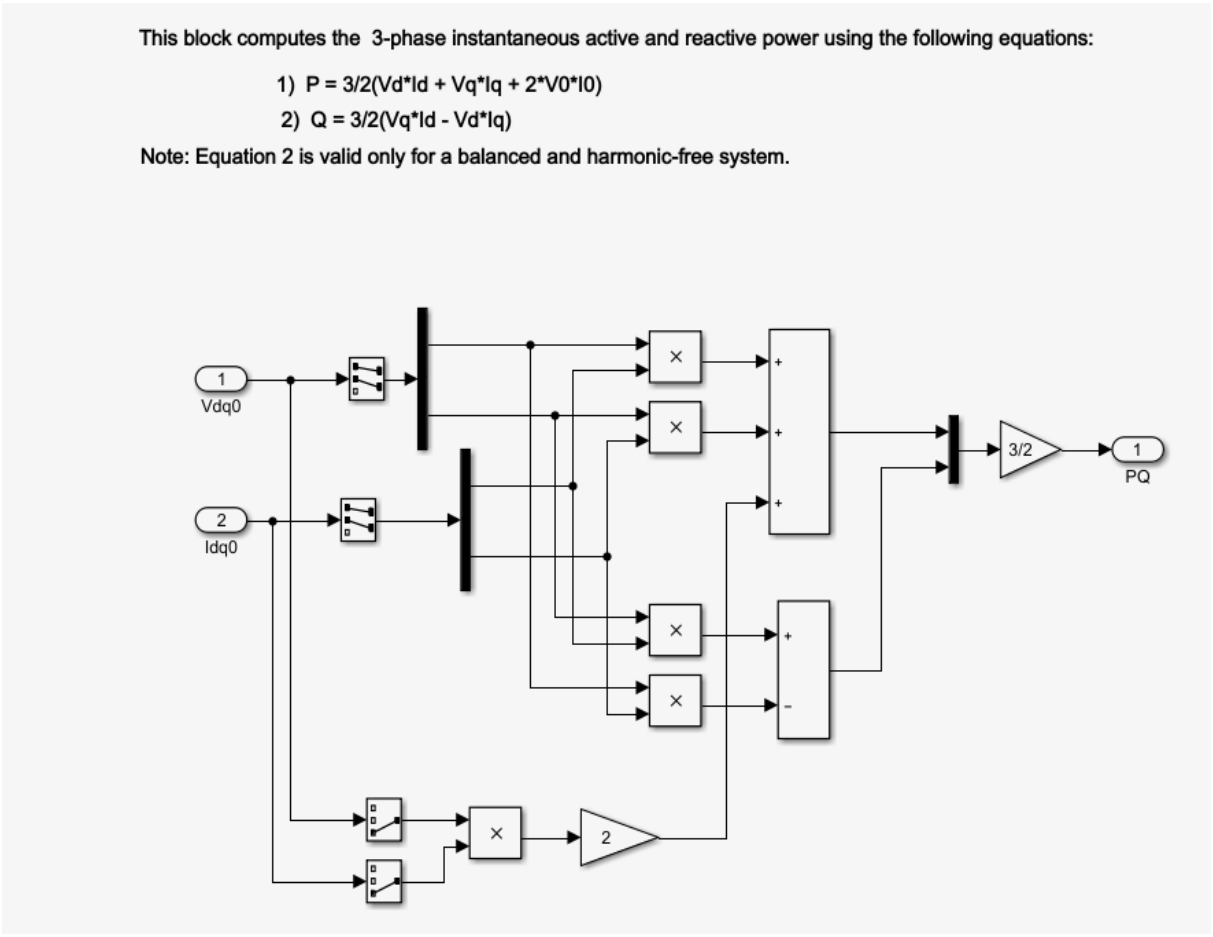

Active and reactive power computation.

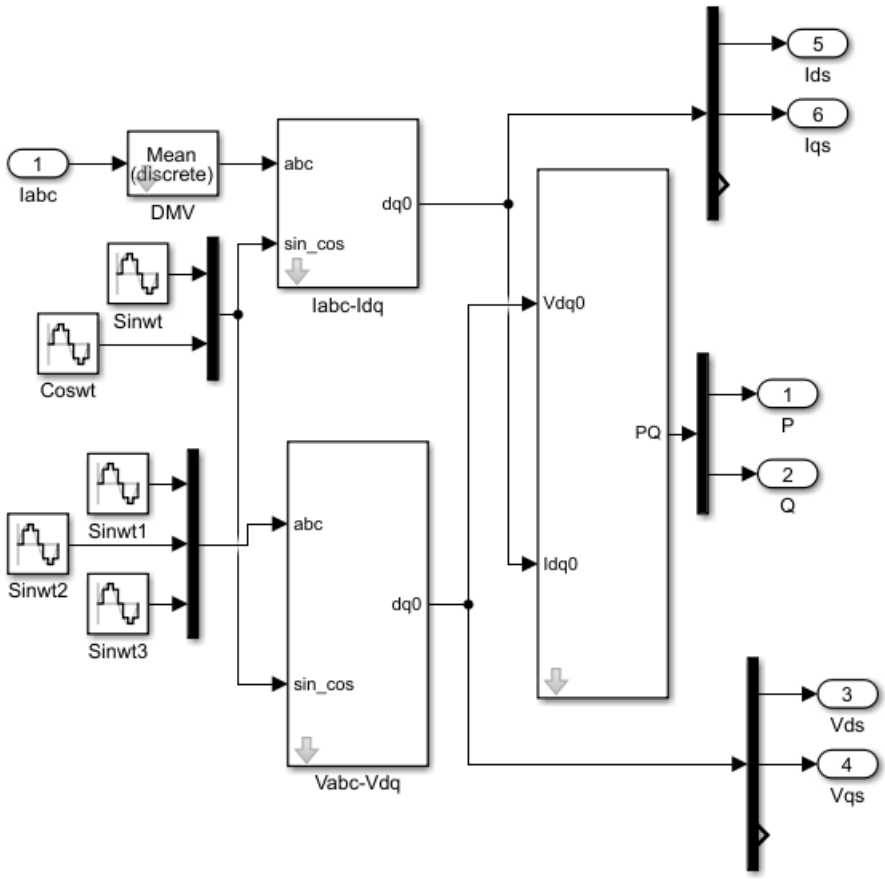

P-Q calculation

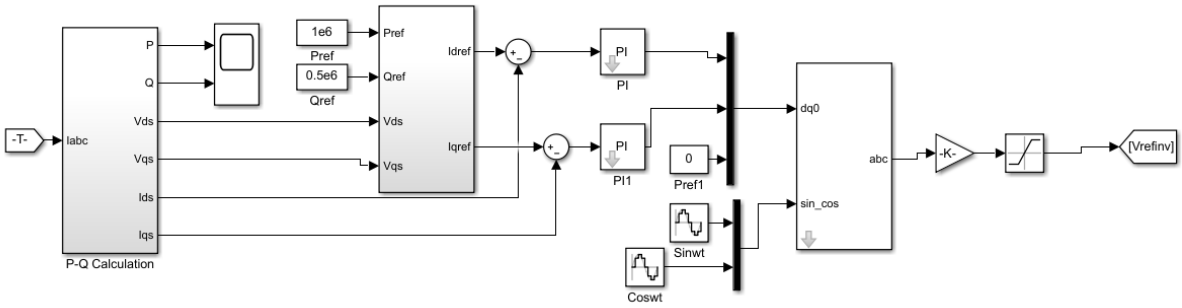

P-Q control

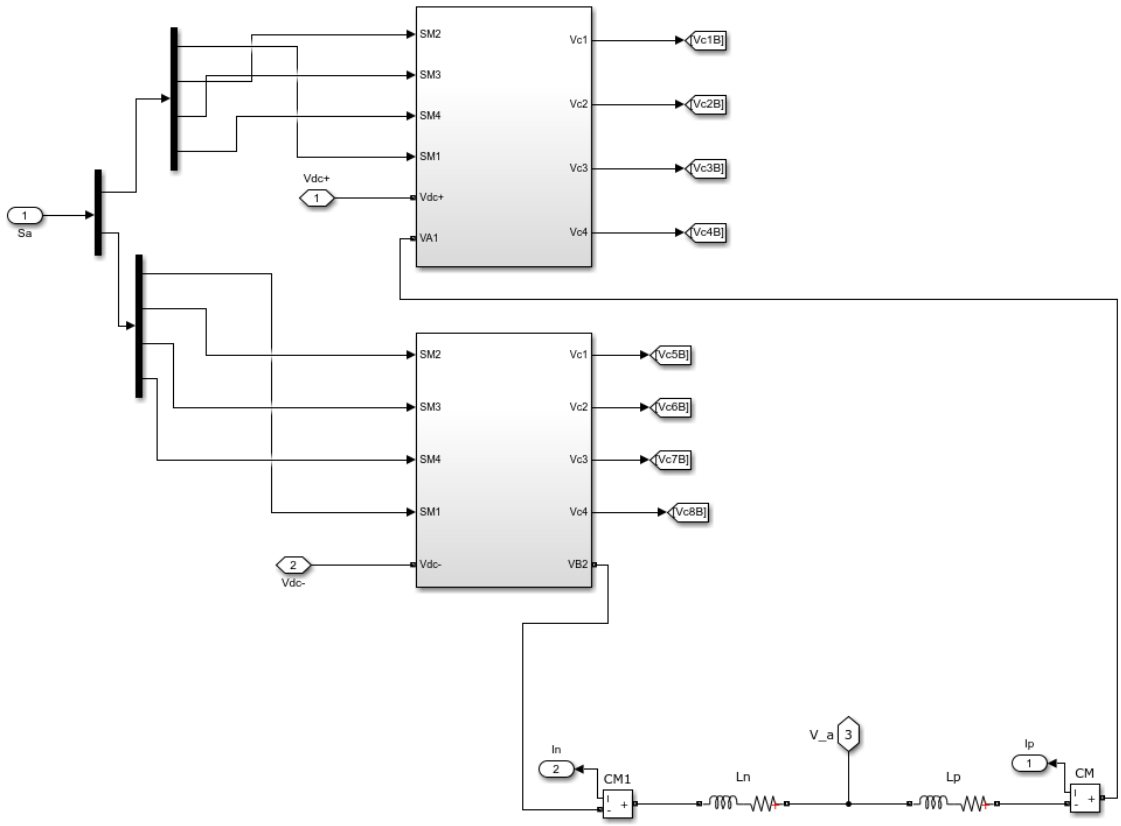

Rectifier phase submodules

References

1. Bartos, F.J. *Direct-drive Wind Turbines Flex Muscles*. 2011 [cited 2019 04.06]; Available from: https://www.controleng.com/articles/direct-drive-wind-turbines-flex-muscles/.
2. marquardt, A.l.R., *An innovative modular multilevel converter topology suitable for a wide power range.* 2003 IEEE Bologna Power Tech Conference Proceedings, 2003. **3**.
3. Salman Khan, E.T. *Modeling of MMC for Fast and Accurate Simulation of Electromagnetic Transients: A Review*. 2017 [cited 2019; Available from: https://www.researchgate.net/figure/MMC-submodule-a-half-bridge-b-full-bridge_fig2_318982818.
4. Sohail, U., *Modular multilevel power electronic converter for Photovoltaic energy conversion systems*, in *Electrical engineering*. 2018, UiT: Narvik.
5. Hamasaki, M.R.a.S.-i., *Control of Full Bridge type Modular Multilevel Converter for AC/AC Conversion with Grid Connection*, in *6th IEEE International Conference on Smart Grid*. 2018, IEEE: Nagasaki, JAPAN, December 4-6, 2018.
6. Ghazal, F., *Design, Modeling and Control of Modular Multilevel Converter based HVDC Systems.* 2015.
7. Falahi, G. *Modular multilevel converter MMC tutorial*. 2016.
8. . electronics weekly.
9. Paul D. Judge, M., IEEE, and Tim C. Green Senior Member, IEEE, *Modular Multilevel Converter with Partially Rated Integrated Energy Storage Suitable For Frequency Support and Ancillary Service Provision.* IEEE.
10. *How to Prolong Lithium-based Batteries*. 2019 Last updated 2019-02-08 [cited 2019 03-20].
11. Valle, M., *Ny oppdagelse kan gi elbilbatteri bedre ytelse og lengre levetid*. 2016, Teknisk Ukeblad: https://www.tu.no. p. https://www.tu.no/artikler/ny-oppdagelse-kan-gi-elbilbatteri-bedre-ytelse-og-lengre-levetid/350034.
12. *What Causes Li-ion to Die?* 2017 Last Updated 2017-08-31 [cited 2019 03-22].
13. Martin, J. *Why depth of discharge matters in solar battery storage system selection*. Batteries & Energy Storage 2016 [cited 2019 01-04].
14. *Battery*. [cited 2019 0406]; Available from: https://se.mathworks.com/help/physmod/sps/powersys/ref/battery.html?s_tid=srchtitle .
15. technologies, M., *Top 10 reasons for using Ultracapacitors in your system designs*.
16. *Battery VS Supercapacitor* 2016 [cited 2019 26/05].
17. *supercapacitor*. [cited 2019 04.06]; R2019a:[Available from: https://se.mathworks.com/help/physmod/sps/powersys/ref/supercapacitor.html?s_tid=doc_ta.
18. Yong-Gang Wang, Z.-D.W., Yong,Yao Xia, *An asymmetric supercapacitor using RuO2/TiO2 nanotube composite and activated carbon cartridges.* Science direct, 2005.
19. Wen Lu, L.D., *Carbon Nanotube Supercapacitors* Carbon Nanotubes ed. J.M. Marulanda. 2012: InTech.
20. Matin, A.M.S.A.-b.S.S.A.S.S.A.M., *A Comparative Design and Performance Study of a Non–Isolated DC–DC Buck Converter Based on Si–MOSFET/Si–Diode, SiC–JFET/SiC–Schottky Diode, and GaN–Transistor/SiC–Schottky Diode Power Devices.* IEEE, 2017.

21. M.S.Rajan, R.S., *Comparative Study of Multicarrier PWM Techniques for a Modular Multilevel Inverter.* International Journal of Engineering and Technology (IJET), 2013-2014. **5**(6).
22. Hirofumi Akagi, Y.K., Akira Nabae, *Instantaneous Reactive Power Compensators Comprising Switching Devices without Energy Storage Components.* IEEE, 1984. **IA-20**(3).
23. Suresh Mikkili, A.K.P., *PI Controller based Shunt Active Filter for Mitigation of Current Harmonics with p-q Control strategy using Simulation and RTDS Hardware*, in *2011 Annual IEEE India Conference*. 2011, IEEE.
24. Christopher Hendricks, N.W., Sony Mathew, Michael Pecht, *A failure modes, mechanisms, and effect analysis (FMMEA) of lithium.ion batteries.* Journal of power sources, 2015. **297**.
25. Damien F. Frost, D.A.H., *Novel MMC control for active balancing and minimum ripple current in series-connected battery strings.* IEEE, 2015.
26. Dolva, D.K., *Introduction of modular multilevel inverter for grid-connected Photovoltaic conversion plants*, in *department of electric power engineering*. 2016, NTNU: Trondheim.
27. Feng Gao, L.Z., Qi Zhou, Mengxing Chen, Shaogang Hu, *State-of-Charge Balancing Control Strategy of Battery Energy Storage System Based on Modular Multilevel Converter.* IEEE, 2014.
28. Feng Guo, Y.Y., and Ratnesh Sharma *A Modular Multilevel Converter Based BatteryUltraCapacitor Hybrid Energy Storage System for Photovoltaic Applications* IEEE, 2015.
29. Fengqi Chang, Z.Z., Yongdong Li, Ling Peng *A Two-level SOC Balance Strategy for a Novel Hybrid Energy Storage Topology*.
30. Fu-Sheng Pai, S.-J.H., Senior Member, IEEE, Chen-Wei Ku, Ying-Rong Chen, Bo-Ge Huang, and Yu-Chie Lin *Voltage Equalization of Lithium Iron Phosphate Batteries Cooperating with Supercapacitors.* IEEE, 2014.
31. Gean J. M. de Sousa, a.M.L.H., *Modular Multilevel Converter Based Unidirectional Medium/High Voltage Drive System.* IEEE, 2013. **13**.
32. Gean Jacques Maia de Sousa∗, A.d.S.D., Joable Andrade Alves †, and Marcelo Lobo Heldwein∗ *Modeling and Control of a Modular Multilevel Converter for Medium Voltage Drives Rectifier Applications.* IEEE, 2015. **15**.
33. Grain Philip Adam, S.F., Barry Williams, Innocent Ewean Davidson and Abdelaziz Yousif Mohammed Abbas, *Full-bridge Modular Multilevel Converter (FB-MMC) with Extended Control Range* IEEE, 2015. **15**.
34. Guo, F., *Real-time simulation of a modular multilevel converter based hybrid energy storage system*, N.l. America, Editor. 2015.
35. Görtz, S., *Battery energy storage for intermittent renewable electricity production. A review and demonstration of energy storage applications permitting higher penetration of renewables.* 2015, Umeå university: UMEÅ. p. 96.
36. Hellesnes, M.N., *Use of battery energy storage for power balancing in a large scale HVDC connected wind power plant*. 2017, NTNU: Trondheim, Norway. p. 234.
37. Josè R. Lebre, E.H.W., *Fullbridge MMC control for hybrid HVDC systems.* IEEE, 2017. **17**(978-1-5090-6248-5).
38. Lakshmikant M. Bopche, A.A.D., Muneeb Ahmad, *Combination of Parallel Connected Supercapacitor & Battery for Enhancing Battery Life* in *2016 International Conference on Automatic Control and Dynamic Optimization Techniques (ICACDOT) International Institute of Information Technology (I²IT)*. 2016, IEEE: Pune.

39. Li Bin, W.J., Li Mingshui, Ge Ang, *Research on elevator drive device for super capacitor energy storage.* 2009.
40. Liu Danqing, W.G., Ou Zhujian, Liu Jiaxing, *A control strategy of MMC battery energy storage system based on arm current control.* IEEJ, 2018.
41. Marcin Zygmanowski, B.G., Radosław Nalepa, *Capacitance and Inductance Selection of the Modular Multilevel Converter*
42. Nada Ahmed, A.M., *A Matlab/Simulink Model for Capacitor Voltages Balancing in Modular Multilevel Converters.*
43. Nan Li, F.G., Tianqu Hao, Zhan Ma, Changhui Zhang, *SOH Balancing Control Method for the MMC Battery Energy Storage System* IEEE, 2018. **65**(8).
44. Ning Zhihao, W.C., Zhang Bin, Zhang Keren, Zuo Jian, Xu Yonghai, *ResearchonApplicationofBatteryEnergyStorage SystemBasedonMMCinWindPowerIntegration.* IEEE, 2017.
45. Nobuo Satoh, A.K., Hiroshi Arai, and Masato Uchida, *Verification of charge and discharge system composed of multiple lithium ion batteries.* IEEE, 2017. **17**.
46. Ping Wang, S.M., IEEE, Tao Zhang, Rui Li1, Member, IEEE *A New Hybrid MMC with Integrated Energy Storage* IEEE, 2017.
47. Pou, J., *The Modular Multilevel Converter*. 2017.
48. Quansheng Wang, H.Y., Guomin Zhang, *ImprovedDynamic Phasor-based Modeling and Simulation of Modular Multilevel Converter* IEEE, 2017.
49. Rekdal, K., *Battery energy storage integration via DC/AC converter in grid connected wind turbines*, in *science and technology*. 2018, NTNU: Trondheim.
50. Ren Bin, X.Y., Lan Qiaoqian *A Control Method for Battery Energy Storage System Based on MMC.* IEEE, 2015.
51. Roy, S.S., *A Novel Approach of High Durable Super Battery* IEEE, 2015. **15**(978-1-4673-9223-5).
52. Saikot Baroi, S.I., Shawon Baroi, *Modeling and Simulation of a PV Power Generating System Using MMC Converter and High Frequency Magnetic Link* in *2nd International Conference on Electrical & Electronic Engineering (ICEEE), 19-21 December 2017*. 2017, IEEE: RUET, Rajshahi, Bangladesh
53. Sharma, F.G.a.R., *A Modular Multilevel Converter with Half-Bridge Submodules for Hybrid Energy Storage Systems Integrating Battery and UltraCapacitor* IEEE, 2015.
54. Siemens, *Siemens 6.0 MW offshore wind turbine*. 2012.
55. Sigurd Byrkjedal Wersland, A.B.A., Member, IEEE and Lars Einar Norum, Member, IEEE, *Integrating Battery into MMC Submodule Using Passive Technique.* IEEE, 2017. **17**.
56. Thilina. S. Ambagahawaththa and D. R. Nayanasiri, M.I.S.D.G.J., Senior Member IEEE *Ultra-high Step-up DC-DC Converter Family Based on Feed-forward Capacitor and Coupled Inductor.* IEEE, 2018.
57. Thomas Szalai, T.H., Ulf Schwalbe, Fabian Endert, Svetlozar D. Ivanov *Dimensioning of Ultra Capacitors used for Range Extension in Electric Vehicles*
58. Vahid Najmi, M.N.N., Rolando Burgos, *A New Modeling Approach for Modular Multilevel Converter (MMC) in D-Q Frame* IEEE, 2015.
59. Yang Chang, H.F., Sai Li , Yan Yan, *Prognostics for lithium-ion battery operating under different depth of discharge using hybrid method.* IEEE, 2018. **18**.
60. Yang Xu, T.Z., *A Hierarchical Structure Approach of Battery Balancing Based on SOC* IEEE, 2018.
61. Yingjie Wu, C.G., Xiangdong Liu, Zhen Chenand Xuefei Mao, *A Power Routerbased on Modular Multilevel Converter Integrating UltraCapacitorEnergy Storage System.* IEEE, 2017.

62. Yu Zhang, Z.J., Xunwei Yu *Control Strategies for Battery/Supercapacitor Hybrid Energy Storage Systems.* IEEE Energy2030, 2008.
63. Zhan Ma, T.H., Feng Gao, Nan Li, Xin gu, *Enhanced SOH Balancing Method of MMC Battery Energy Storage System with Cell Equalization Capability* IEEE, 2018.
64. Zhou Jianqiao, Z.J., Cai Xu, Wang Jiacheng, Zang Jiajie, *family of modular multilevel converter (MMC) based solid state transformer (SST) topologies for hybrid AC/DC distribution grid applications.* IEEE, 2018.

[2, 4, 7, 9, 15, 24-64]